ABSTRACT

Title of Dissertation: RESPONSE INHIBITION AND THE CORTICO-STRIATAL CIRCUIT

Daniel William Bryden, Doctor of Philosophy, 2015

Dissertation directed by: Assistant Professor Dr. Matthew Roesch
Department of Psychology

The ability to flexibly control or inhibit unwanted actions is critical for everyday behavior. Lack of this capacity is characteristic of numerous psychiatric diseases including attention deficit hyperactivity disorder (ADHD). My project is designed to study the neural underpinnings of response inhibition and to what extent these mechanisms are disrupted in animals with impaired impulse control. I therefore recorded single neurons from dorsal striatum, orbitofrontal cortex, and medial prefrontal cortex from rats performing a novel rodent variant of the classic "stop signal" task used in clinical settings. This task asks motivated rats to repeatedly produce simple actions to obtain rewards while needing to semi-occasionally inhibit an already initiated response. To take this a step further, I compared normal rats to rats prenatally exposed to nicotine

in order to better understand the mechanism underlying inhibitory control. Rats exposed to nicotine before birth show abnormal attention, poor inhibitory control, and brain deficits consistent with impairments seen in humans prenatally exposed to nicotine and those with ADHD.

I found that dorsal striatum neurons tend to encode the direction of a response and the motor refinement necessary to guide behaviors within the task rather than playing a causal role in response inhibition. However the orbitofrontal cortex, a direct afferent of dorsal striatum, possesses the capacity to inform the striatum of the correct action during response inhibition within the critical time window required to flexibly alter an initiated movement. On the other hand, medial prefrontal cortex functions as a conflict "monitor" to broadly increase preparedness for flexible response inhibition by aggregating current and past conflict history. Lastly, rat pups exposed to nicotine during gestation exhibit faster movement speeds and reduced capacity for inhibitory behavior. Physiologically, prenatal nicotine exposure manifests in a hypoactive prefrontal cortex, diminished encoding of task parameters, and reduced capacity to maintain conflict information.

RESPONSE INHIBITION AND THE CORTICO-STRIATAL CIRCUIT

by

Daniel William Bryden

Dissertation submitted to the Faculty of Graduate School of the
University of Maryland, College Park in partial fulfillment
of the requirements for the degree of
Doctor of Philosophy
2015

Advisory Committee:

Professor Matthew Roesch, Chair
Professor Ricardo Araneda
Professor Jens Herberholz
Professor Alex Shackman
Professor Donald Bolger

Acknowledgement

This PhD thesis would not exist without the help of many people. I would first like to thank my wife Stephanie for all of her support and love while helping me to cope through the most stressful times. You always know the right things to say to me. I would also like to thank my parents Wayne and Noel for moral and financial support. I love you guys.

This thesis would not be possible without multiple supportive colleagues. I want to thank my first advisor Dr. Maggie McDevitt for transforming my unguided interests into meaningful scientific goals. I also want to thank Dr. Madeline Rhodes for directing me into the fascinating world of neuroscience. An unbridled thank you to Dr. Matthew Roesch, my PhD advisor, for allowing me to pursue a project I am passionate about and for being patient with me through my incessant theories and analyses. It is an absolute pleasure to work with and learn from you.

An additional thank you to the entire Roesch lab in alphabetical order: Gregory Bissonette, Amanda Burton, Ronny Gentry, Vadim Kashtelyan, Brian Lee, and Nina Lichtenburg.

Table of Contents

Acknowledgement ii
Chapter 1: Introduction 1
Chapter 2: Response inhibition and how it is investigated 6
Chapter 3: My stop signal task and its behavioral measurements 8
Chapter 4: Analyzing neuronal stop signal task data 14
Characterizing "increasing-" and "decreasing-" type cells: 20
Population Activity: 20
Stop Index: 20
Directional Index: 21
Sliding t-test analysis: 21
Multiple regression analysis: 21
Modulation of conflict by identity of previous trial: 22
Chapter 5: Medial dorsal striatal neurons represent direction-based response conflict 24
Published as: Bryden, DW et al. Front Integr Neurosci (2012) 6, 69. (1)
Increasing-type cells 26
Population activity: 26
Stop Index: 31
Directional Index: 31
Multiple regression analysis: 33
Modulation of conflict by identity of previous trial: 35
Summary: 39
Decreasing-type cells 40
Population activity: 40
Stop Index: 43
Directional Index: 43
Multiple regression analysis: 44
Modulation of conflict by identity of the previous trial: 46
Summary: 49
Disparate waveform characteristics as a means to define increasing- and decreasing populations 50

Chapter Discussion 52
Functions of mDS 52
Miscoding of direction and inhibition failure 53
Inhibition of movement 55
Control of behavior 56
Chapter 6: An inhibitory hypothesis for lateral orbitofrontal neurons 58
Published as: Bryden, DW et al. J Neurosci (2015) 35, 3903-3914. (2)
Increasing-type Cells 60
Population Activity: 60
Stop index: 63
Directional index: 63
Multiple regression analysis: 64
Modulation of conflict by identity of the previous trial: 66
Summary: 70
Decreasing-type cells 70
Population Activity: 70
Multiple regression analysis: 73
Modulation of conflict by identity of the previous trial: 76
Summary: 79
Disparate waveform characteristics as a means to define increasing- and decreasing populations in lOFC 79
Chapter Discussion 82
Chapter 7: Medial prefrontal cortex and its role in conflict monitoring 85
Increasing-type Cells 86
Population Activity: 86
Stop index: 89
Directional index: 89
Multiple regression analysis: 90
Modulation of conflict by identity of previous trial: 93
Decreasing-type Cells 97
Population activity: 97

Multiple regression analysis: 100
Modulation of conflict by identity of previous trial: 102
Disparate waveform characteristics as a means to define increasing- and decreasing populations: 105
Chapter Discussion 107
Chapter 8: The prenatal nicotine exposure model of rodent impulsivity suggests that normal firing in medial prefrontal cortex is necessary for inhibitory control 109
Accepted as: Bryden, DW et al. J Neuropsychopharm (2015). (in press).
Prenatal nicotine exposure impairs inhibitory control 110
Impact of prenatal nicotine exposure on population activity in mPFC 116
Multiple regression analysis of single-unit activity in mPFC 117
Activity in mPFC is correlated with behavioral performance 122
Previous trial encoding and the ability to resolve conflict 124
Disparate waveform characteristics as a means to define increasing- and decreasing populations in mPFC 129
Chapter Discussion 131
Chapter 9: Comparison of areas and broad discussion 135
The comparative roles of mDS, lOFC, and mPFC in the stop signal task: Increasing-type 137
The comparative roles of mDS, lOFC, and mPFC in the stop signal task: Decreasing-type 148
Summary: Placing the explored brain regions in functional context 158
Chapter 10: Detailed methodology 161
Subjects: 161
Surgical procedures and histology: 161
Behavioral task: 161
Single-unit recording: 162
Data analysis: 163
Prenatal nicotine exposure: 165
References 167

Chapter 1: Introduction

The ability to flexibly control or inhibit unwanted actions is critical for everyday behavior. Walking down a busy street is a dynamic process of constant action initiation and inhibition where individual actions are only loosely tied to the ultimate goal of reaching the end of the street. Lack of inhibitory adaptability is characteristic of numerous psychiatric disorders including attention deficit hyperactivity disorder (ADHD), substance abuse, Tourette syndrome, pathological gambling, and obsessive-compulsive disorder (*3-21*). The current project is designed to study the neural underpinnings of how animals are able to suppress or inhibit a behavioral response and to what extent these mechanisms are disrupted in those with impaired impulse control. With a preponderance of ADHD diagnoses in today's society, characterizing the underlying circuitry behind this and other disorders characterized by poor impulse control is paramount.

The worldwide prevalence of ADHD has been estimated at 5.3% (*22*) and the disease has been associated with poor school performance, anxiety, aggression, and substance abuse as well as other impulsive disorders. It has been suggested that suboptimal inhibitory capacity is a central tenet of various psychiatric symptoms including compulsivity, perseveration, obsessions, and attention deficits (*23, 24*). In addition, those with marked behavioral disinhibition tend to possess poor cognitive control whereby conflicting circumstances do not lead to greater control over subsequent responses in the immediate future (*25-28*). It is therefore critical to systematically

measure response inhibition behaviorally in order to infer the brain regions responsible for this behavior and whether/to what extent they are affected by disease states.

Research has reported that within the brain, the striatum works as an input structure to the basal ganglia, a conglomerate of regions thought to arbitrate between initiating and inhibiting motor actions. In order for the striatum to swiftly gather information on which action to proceed with, functioning upstream signals from the frontal cortex are necessary to flexibly inform the striatum (*29, 30*) whether a given behavioral response is applicable. In fact, prefrontal regions have shown common BOLD activations across multiple tasks that measure impulsivity differently (*31*).

The functions of the brain areas involved in response inhibition have been inferred using inactivation/pharmacological techniques, but the neural signals underlying inhibitory functions have yet to be fully characterized. From studies using recording and imaging techniques, it is clear that orbitofrontal cortex (OFC), medial prefrontal cortex (mPFC), and medial dorsal striatum (mDS) are critical for executive control and response inhibition (Fig 1.1). Though OFC and mPFC are neighboring structures, the literature shows distinct roles for these areas relating to reward and value processing. As it pertains to response inhibition, the distinctions between mPFC and OFC are less clear. Both of these frontal regions have been shown to be important for sufficient behavior in inhibitory tasks (although contradicting results have also been found) and both regions directly synapse onto dorsal striatum (*32-34*) and with each other (*35, 36*) with a presumed role of informing the brain of appropriate versus inappropriate action. Further, damage to the dorsal striatum has been shown to diminish inhibitory control in reaction

time tasks as defined by greater premature responding (*5, 37, 38*) although replications of this result have proven elusive (*39, 40*).

To gain an appreciation for the cortical and striatal nodes within the context of response inhibition, it is important to place them in context of both structure and function relative to their afferents and efferents. Figure 1.1 depicts the established structural framework of the cortico-basal ganglia loops that comprise the majority of the regions currently thought to be important for active motor suppression. The medial dorsal striatum (mDS) is the primary input structure to the basal ganglia, a collection of areas shown to be able to promote actions via monosynaptic connections ("the direct pathway") from mDS to substantia nigra pars reticulata (SNr), or suppress actions via globus pallidus (GPe) to (subthalamic nucleus) STN to SNr ("the indirect pathway")(*41*). Importantly, decreases in activity in the output structure of the basal ganglia (SNr) via direct inhibitory mDS to SNr connections removes the tonic inhibition SNr sends to motor outputs and promotes a movement. In contrast, direct excitatory STN to SNr connections increases the tonic inhibition in SNr and pauses or refines movements (*42, 43*). It is because of this control that mDS has over the basal ganglia (and by extension, the motor system) that it has been implicated in response inhibition (*5*). However, it has been known since the studies of Phineas Gage that inhibitory control can be diminished even with a healthy, intact basal ganglia system (*44*). Therefore, cortical regions including lOFC (lateral orbitofrontal cortex) and mPFC have been hypothesized to "alert" the mDS via their independent afferents of a prompt change in external context in order for the basal ganglia to inhibit or redirect behavior. Naturally, after a decision has been made and an action produced, portions of the motor outputs (particularly motor thalamus)

synapse back onto mDS and the cortex presumably to update these upstream regions regarding the action that was commenced. This overall organization forms what are known as the cortico-basal ganglia-thalamo-cortical loops.

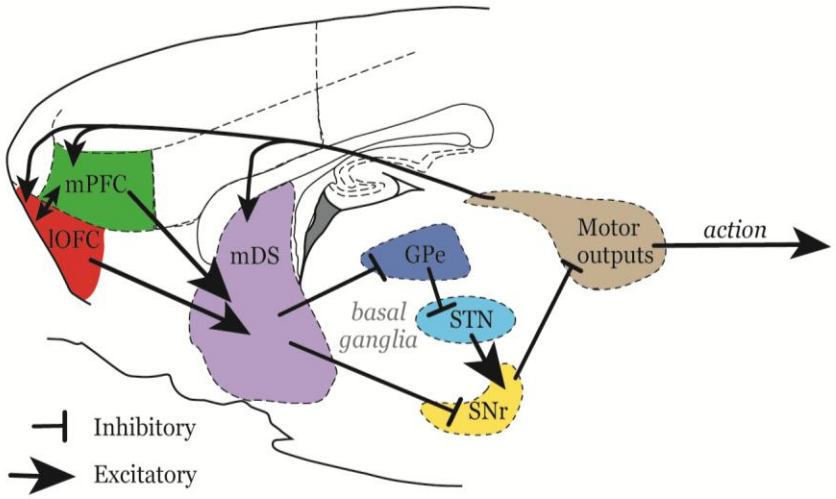

Figure 1.1: **Cortico-striatal circuitry overview.** A schematic of the rodent cortex, basal ganglia, and motor outputs necessary for response control. Among other cortical regions, the mPFC and lOFC project directly to mDS via excitatory projection neurons with the presumed role of providing top-down control to the motor circuitry within the basal ganglia. mDS has the ability to functionally arbitrate between promoting and suppressing actions via its control over SNr. Direct projections to SNr via striatal GABAergic medium spiny neurons inhibits the tonic inhibition (disinhibition) from SNr to motor outputs and promotes movement. Alternatively, indirect projections to SNr from mDS via GPe and STN excite SNr neurons via glutamatergic STN afferents. This "indirect pathway" increases the inhibition that SNr sends to motor outputs and suppresses or finely tunes behaviors. Outputs of the basal ganglia form a "loop" back on to cortical regions (termed "cortico-striatal-thalamo-cortical loops") with the supposed functional role of updating action history. Abbreviations: mPFC = medial prefrontal cortex; lOFC = lateral orbito-frontal cortex; mDS = medial dorsal striatum; GPe = globus pallidus external; STN = subthalamic nucleus; SNr = substantia nigra pars reticulata and parts of globus pallidus internal; motor outputs = motor thalamus, superior colliculus, and cerebellum.

The first objective of my research was to resolve the role of single dorsal striatal cells in response inhibition via recording from these neurons while rats perform a novel rodent variant of the classic "stop signal" task typically used in clinical settings. This task asks motivated rats to repeatedly produce simple actions to obtain fluid rewards while needing to semi-occasionally inhibit these responses. A second goal of this research is to discriminate the functions of lOFC and mPFC by recording single cell data from each brain area during performance of the stop signal task. Use of this task will allow me to address the void in cortico-striatal literature and propose a specific locus in the brain that may be impacted by diseases characterized by reduced response inhibition ability, such as addiction. The cortico-basal ganglia-thalamo-cortical circuitry has been nicely mapped structurally (Fig. 1.1), but the functions and interactions of these brains regions pertaining to response inhibition have yet to be agreed upon. To take this one step further, this work offers an opportunity to compare healthy control rats to rats prenatally exposed to nicotine in order to better understand the mechanism underlying impulse control. Rats exposed to nicotine before birth show abnormal attention, poor inhibitory control, and brain deficits consistent with impairments seen in humans prenatally exposed to nicotine and those with ADHD. I will test if inhibitory signaling in mPFC is affected by the exposure to nicotine by recording from the mPFC of these animals in the same stop signal task.

Chapter 2: Response inhibition and how it is investigated

Response inhibition refers to the capacity to swiftly and flexibly suppress or alter behavior when new information suggests that an initiated action is no longer ideal. Uncovering the neurological basis underlying response inhibition deficits has been a goal of a subset of neuroscientists for years. Approaches to this topic have included electroencephalographic recordings (*45*), fMRI scanning (*46*), clinical pre-existing brain lesion experiments (*47, 48*), and behavioral/drug testing (*49, 50*). These methods have yielded overwhelming advances in the treatment of patients suffering from these disorders including the (generally) successful administration of pharmacological agents such as Ritalin, Adderall, and Prozac. Despite these developments, the neural circuitry regulating behavioral inhibitory proficiency is understudied and not fully established.

Due to inherent limitations of human neuroscience techniques, much of the basic research studying neural connections at the systems level is done in animals. The use of animals in discerning the biological processes behind response inhibition deficits has supplied the field with invaluable data. For decades, research groups have worked to establish the functions of numerous brain regions in inhibitory behavior using reversal tasks (*51, 52*) designed to test the flexibility of goal directed behavior, delay discounting tasks (*53*) used to measure impulsive decision making, and Go/NoGo tasks (*54*) thought to directly assess response suppression. Additionally, establishing the role of individual basal ganglia regions in movement generating (Huntington's) and movement suppressing (Parkinson's) diseases (*55*) provided a subcortical framework that led to further exploration of the roles of striatal and cortical brain areas in response inhibition via *in vivo* neural recordings in monkeys performing a countermanding task (*56, 57*).

The aforementioned tasks have fundamental strengths but few of these paradigms address the rapid suppression of initiated actions while concurrently accounting for interactive effects of expected outcomes. For example, inadequate reversal ability can be explained by the failure to update cue-outcome expectancies rather than a specific deficit in inhibiting an initially correct response. To overcome this obstacle, researchers have used the "stop signal task" where subjects are asked to make speeded motor responses to simple cues in order to obtain rewards. These speeded movements, referred to as "go" responses, are designed to be uncomplicated and completed with high accuracy. On a minority of trials, the instructions are identical and "go" actions are commenced, but a "stop" cue, introduced after movement initiation, instructs the subject to inhibit the response in order to complete the trial successfully. The ability of the subject to resist completing responses on these "stop" trials is a measure of flexible inhibitory capacity that cannot be evaluated using tasks where subjects are asked to simply refrain from action *prior* to initiation (e.g. Go/NoGo, 5-choice-serial-reaction-time task).

To date, few of the experiments that have specifically tested behavioral restraint after action commencement (i.e. stop signal task) have done so while recording single cells from the brains of rodents. The intention of my research was to create a response inhibition task suitable for *in vivo* recording in rats and to explore the contributions of a number of brain regions to this behavior; notably medial dorsal striatum (mDS), lateral OFC (lOFC), and medial prefrontal cortex (mPFC).

Chapter 3: My stop signal task and its behavioral measurements

There are many challenges associated with creating a response inhibition task suitable for *in vivo* single unit recording. First, rats need to be trained to respond to a simple cue stimulus for reward while maintaining the ability to semi-accurately (>50%) inhibit that response. This can be trying for a water deprived rat who is motivated to respond rapidly to obtain fluid. Additionally, single neurons in the cortex and striatum tend to bias firing to one direction over another (see Fig. 1.4A and below). Therefore, it is necessary for responses toward both directions (contra- and ipsilateral to the recording electrode) be required in each session so that a neuron's firing pattern is fully characterized. Despite these difficulties, I found it appropriate to remain steadfast in these task necessities due to previously used paradigms in the literature not accounting for these variables. After several arduous failed attempts at designing this task, the behavior on its final iteration was sufficient for measuring response inhibition. The details of that task are as follows:

Experimental subjects are male Long Evans rats acquired from Charles River Labs at weights between 175 and 200g. Training and behavior was conducted in aluminum chambers approximately 18" on each side with downward sloping walls narrowing to an area of 12" x 12" at the bottom. On one wall, a central nose port was located above two adjacent fluid wells. Directional lights were located next to the fluid wells. House lights were located above the panel. Task control was implemented via computer. Port entry and licking were monitored by disruption of photobeams (Fig. 1.2A).

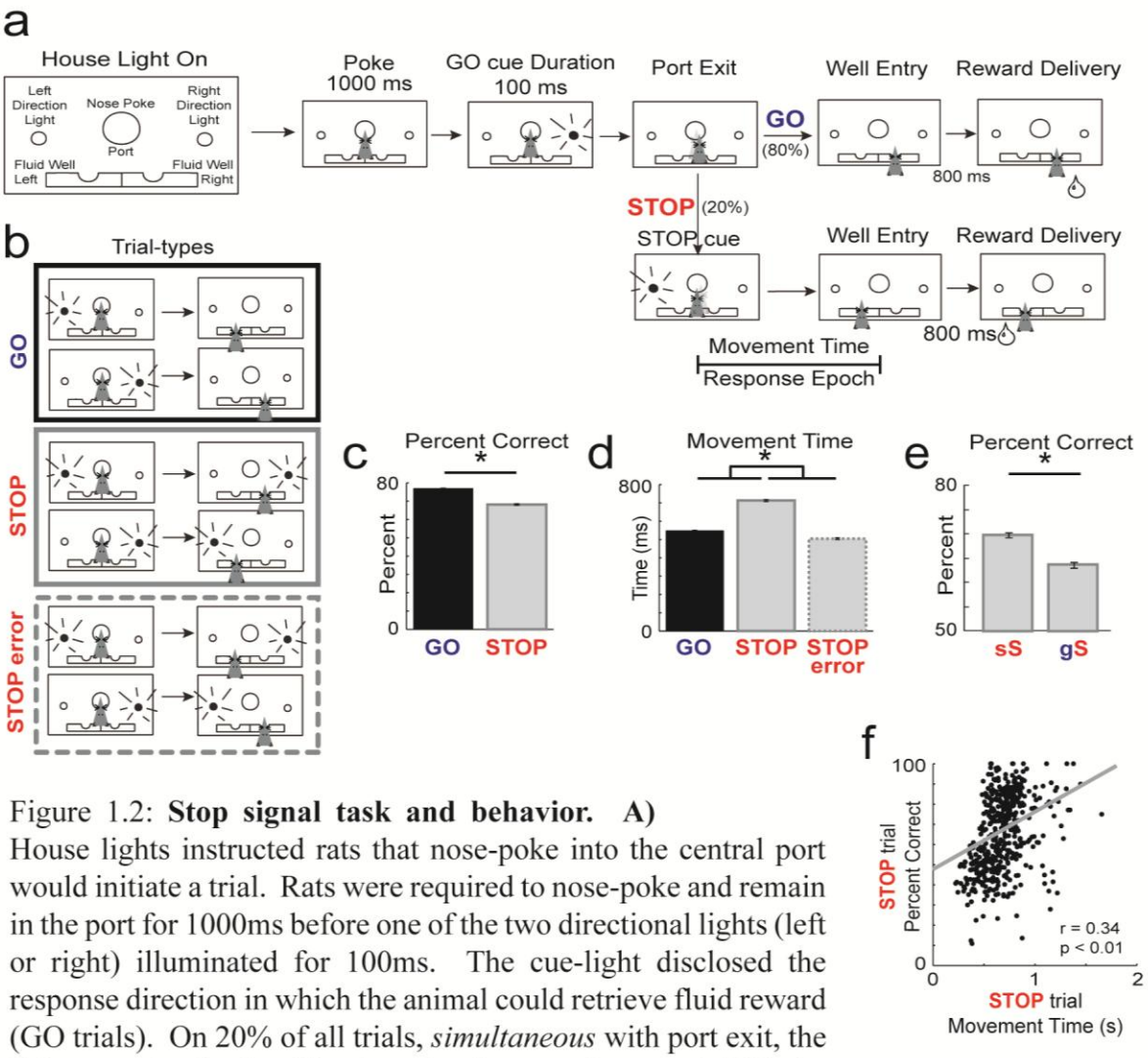

Figure 1.2: **Stop signal task and behavior. A)** House lights instructed rats that nose-poke into the central port would initiate a trial. Rats were required to nose-poke and remain in the port for 1000ms before one of the two directional lights (left or right) illuminated for 100ms. The cue-light disclosed the response direction in which the animal could retrieve fluid reward (GO trials). On 20% of all trials, *simultaneous* with port exit, the light opposite the first illuminated to instruct the rat to inhibit the current action and redirect behavior to the corresponding well under the second light (STOP trials). With the selection of the correct fluid well, reward was delivered after an 800-1000ms delay. **B)** Two conditions by two directions yields four possible trial types (GO and STOP). Errors are unrewarded. **C)** Average percent of correct trials (±SEM) for GO and STOP trials. **D)** Average movement time in ms (±SEM) for GO trials, STOP trials, and STOP errors defined as the latency from port exit to fluid well entry (see A). **E)** Average percent of correct STOP trials (±SEM) when the immediately preceding trial was a STOP trial (sS) or a GO trial (gS). All behavior was taken from neural recording sessions of all control animals. Asterisks indicate planned comparisons revealing statistically significant differences (t-test, $p < 0.05$). **F)** Speed/accuracy tradeoff. Percent correct on STOP trials for every session plotted against average movement time (port exit to well

The basic design of a trial is illustrated in figure 1.2A. Each trial began by illumination of house lights that instructed the rat to nose poke into the central port. Nose poking began a 1000ms pre-cue delay period during which the animal was required to fixate. At the end of this delay, a directional light to the animal's left or right was flashed for 100ms. The trial was aborted if the rat exited the port at any time prior to offset of the directional cue light. On 80% of trials, presentation of either the left or right light signaled the direction in which the fluid-deprived animal could respond in order to obtain sucrose reward in the fluid well below (GO trials). The remaining 20% of trials began in the same manner, but *simultaneous with the rat exiting the nose port*, the light opposite to the location of the originally cued direction turned on and remained on until the behavioral response was made (STOP trials). On these STOP trials, rats were required to inhibit the movement signaled by the first light and respond in the direction of the second light which was illuminated *concurrently* with port exit. STOP trials were randomly interleaved with GO trials. After correct responses on each type of trial, rats were required to remain in the well for 800ms (pre-fluid delay) before reward delivery (10% sucrose solution). Trials were presented in a pseudorandom sequence such that left and right trials were presented in equal numbers (+/- 1 over 250 trials). The trial types are represented in figure 1.2B. The value of the reward after each correct response, regardless of the trial type, was always the same (one drop of sucrose solution; ~75µl). All behavior is taken from sessions during which at least one cell was recorded. Unless otherwise stated, all subsequent behavioral analyses will be taken from the sessions (n = 468) performed by control rats (n = 24).

The low proportion of STOP trials relative to GO trials (20/80) induced a prepotency to respond swiftly to the first directional (light) cue. Predictably, rats were more accurate on GO trials compared to STOP trials (Fig. 1.2C; t-test; $p < 0.01$) presumably due to the difficulty in inhibiting initiated responses. In addition, rats were faster on GO trials (measured as latency between port exit and well entry) than STOP trials suggesting that they were not using a "wait-and-see" tactic to distinguish between STOP and GO trial types prior to responding (Fig. 1.2D; t-test; $p < 0.01$). Slower latencies resulted in STOP trial performance consistent with a speed accuracy trade off. This is illustrated in figure 1.2F which plots average movement times (well entry minus port exit) on STOP trials against percentage of correct STOP trials for all recording sessions. During sessions in which rats were slower, performance was better ($r = 0.34$; $p < 0.01$). Compatible with this finding, movement times on STOP error trials were significantly faster than movement times on correctly performed STOP trials (Fig. 1.2D; t-test; $p < 0.01$).

Combined, these results demonstrate that there is high conflict between two competing responses during STOP trials. That is, rats were planning and generating a movement prior to illumination of the STOP cue in response to the first cue light, and inhibition and redirection of the behavioral response was necessary to correctly perform STOP trials. Intriguingly, the directional conflict induced by STOP trials was somewhat mitigated when the previous trial was also a STOP trial. That is, rats were more accurate on STOP trials when the immediately preceding trial was a STOP trial ("sS" trial) rather than a GO trial ("gS" trial; Fig. 1.2E). This suggests that when animals were less prepared for the upcoming conflict induced by a STOP trial (i.e. on gS trials), behavior

suffers. Throughout the remainder of the document, the identity of the previous trial will be denoted in lowercase ('g' for GO; 's' for STOP) while the identity of the current trial is represented by a capital letter ('G' for GO; 'S' for STOP).

Prior research into the neural basis of inhibitory control of non-human subjects has utilized stop signal tasks with subtle variations. The stop signal task that I piloted has a number of advantages over tasks used in the past. For example, counter-balanced directions (Fig. 1.2B) in my task allow me to decipher the neuronal and behavioral differences between commencing/inhibiting responses to directions either contralateral or ipsilateral to the recording electrode which cannot be done in other tasks (*58-60*). Additionally, other tasks instruct animals to inhibit *all* responding (i.e. "freeze") for a short period during stop trials (*41, 60*) which is both unnatural and further confounded with a delay to the ultimate reward, as well as effortful stagnation, upon correct stopping. Lastly, some tasks exhibit a lack of response homogeneity such that the speed and/or ultimate movement trajectory differs dramatically between stop and go trial types. This forces these researchers to estimate the time necessary for an animal to inhibit a response (termed "stop signal reaction time"). In theory, the estimation of the stop signal reaction time allows for the analysis of neuronal firing around a hypothetical behavioral threshold in order to determine whether a brain area can successfully encode response inhibition prior to behavioral stopping (*57*). Due to the very similar response movements on GO and STOP trials in my task (e.g. a rightward response can result from either trial type, correct or incorrect), I am able calculate a more accurate measure of the time-point by which response inhibition in the brain needs to be recruited. Specifically, I subtracted the movement latency on correct GO trials from the movement latency on correct STOP

trials, the remainder of which is the time the animal needs to engage any/all necessary neural machinery to successfully refrain from responding to the initial GO cue.

In general rats have difficulty inhibiting responses, particularly when asked to rapidly arbitrate between conflicting decisions. The behavioral results demonstrate that rats were planning and generating a movement prior to illumination of the STOP cue in response to the first directional light, and that inhibition and redirection of the behavioral response was necessary to correctly perform STOP trials. Neural activity elicited on trials during which the movement had to be stopped and redirected will be compared to activity elicited on responses made in the same ultimate direction, which cannot be accomplished with more typical stop signal tasks that require subjects to either pause all movement (*41*) or redirect toward a centralized food cup (*61*). This is important because the activity of neurons in many rodent brain areas including lOFC and mDS have been shown to fire more highly for one response direction over the other (i.e. "directionally selective") (*62-65*). Additionally, I will determine whether activity in single cells changes prior to, or after, my behavioral measure of time needed to inhibit responding on a STOP trial; SCRT (stop change reaction time). In order to calculate these neuronal measures and compare them across brain regions, it was necessary to analyze each region identically. These methodological details are presented below.

Chapter 4: Analyzing neuronal stop signal task data

I collected neuronal data from three brain regions in separate groups of rats using the stop signal task described above. To compare these regions in an unbiased way, I will analyze each region using the same calculations and organize them in individual chapters below. Within each chapter, the results of the various analysis routines will be arranged in sub-headings. These common analyses are detailed below but the intricate statistical methodologies are located in Chapter 10: Detailed methodology.

In recording from single neurons while rats perform the stop signal task, I intend to analyze neuronal data by comparing firing patterns in both response directions (contralateral or ipsilateral relative to the recorded hemisphere) during both trial types (STOP vs. GO) at the time point in which the animal is making or inhibiting/redirecting its response (i.e. port exit to well entry; "response epoch"; Fig. 1.2A). I hypothesize that neurons within individual brain regions will fit into one of three rigid possibilities, but I accept that cells will likely fire in a combination of patterns. These three hypothetical firing characteristics are outlined in figure 1.3A-C where the larger diameter of a representative circle indicates higher firing.

Figure 1.3: **Hypothesized firing characteristics.** Firing of single neurons within each brain region will be analyzed primarily during the response epoch (port exit to well entry) to capture any inhibition/redirection of movement. The size of the circle represents greater firing (spikes/s) during this period. **A)** "Directional signal" patterns will appear as either greater firing in the response direction contralateral to the recording electrode (*left*) or greater firing ipsilateral to the recording electrode (*middle*) with no dissociable firing differences between GO and STOP trials. **B)** Firing patterns consistent with a "conflicted directional signal" will emerge as either greater firing during contralateral movements (*left*) or ipsilateral movements (*middle*) on GO trials. STOP trial activity will remain unchanged based on direction. This lack of directional effect on STOP trials will reflect conflicted response information. **C)** Firing consistent with the an "inhibitory signal" will manifest as greater firing on STOP trials compared with GO trials (*left*) or lower firing on STOP trials compared with GO trials (*middle*), without regard to response direction. Since activity in each of the investigated brain areas have been shown to be modulated by response direction - but not always the same direction - I segregated population activity into each individual cell's preferred and nonpreferred response directions. Preferred direction is defined as the response direction that elicited the strongest firing during the response epoch, averaged over correct STOP and GO trials (always referred to the ultimate response direction performed, *not* the successfully inhibited direction). Therefore, the three hypothesized categories under which cells could fall would be better interpreted using a directional preference precept (A-C *right*).

a

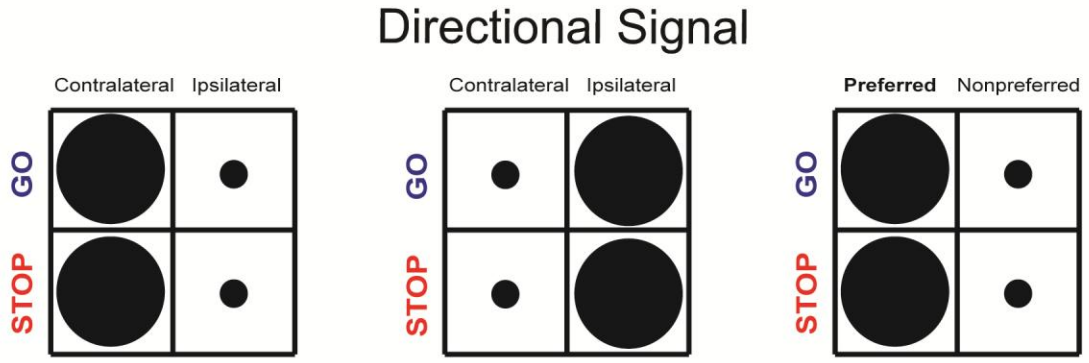
Directional Signal
Contralateral
Ipsilateral
GO
STOP
Contralateral
Ipsilateral
GO
STOP
Preferred
Nonpreferred
GO
STOP

b

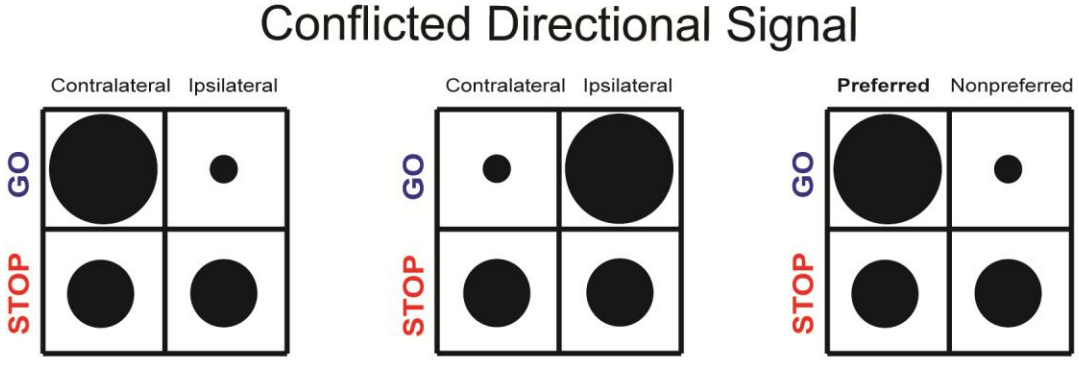
Conflicted Directional Signal
Contralateral
Ipsilateral
GO
STOP
Contralateral
Ipsilateral
GO
STOP
Preferred
Nonpreferred
GO
STOP

c

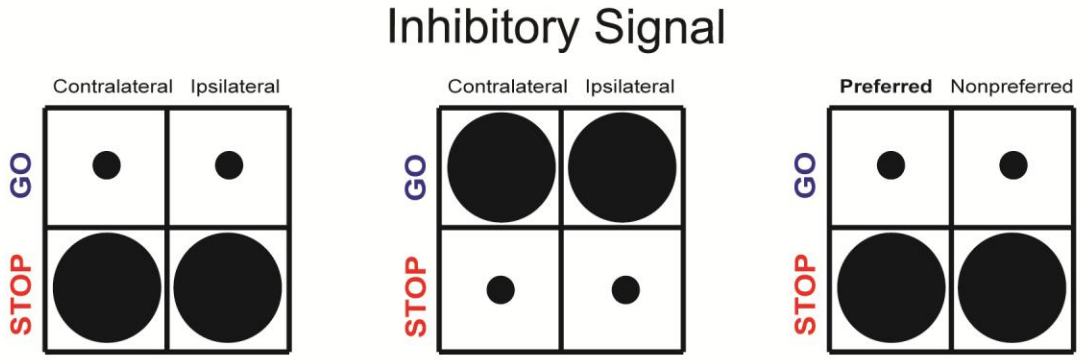
Inhibitory Signal
Contralateral
Ipsilateral
GO
STOP
Contralateral
Ipsilateral
GO
STOP
Preferred
Nonpreferred
GO
STOP

If a group of neurons strictly follows the "directional signal" hypothesis (Fig. 1.3A), firing should not discriminate between STOP and GO trial types, but would vary by direction via firing more highly in either the contralateral direction (Fig. 1.3A *left*) or ipsilateral direction (Fig. 1.3A *middle*). These firing attributes would suggest that a brain region is simply responsible for encoding response direction and not differences pertaining to response inhibition and/or redirection of an action. If a group of neurons adheres to the "conflicted directional signal" hypothesis (Fig. 1.3B); activity should appear higher in the contralateral (Fig. 1.3B *left*) or ipsilateral direction (Fig. 1.3B *middle*) on GO trials whereas activity on STOP trials should not vary by direction. This pattern would indicate that neurons are sensitive to the direction of responding on GO trials, but this firing would be "conflicted" as to the correct direction on STOP trials because one direction is initiated (in response to the GO cue) and the opposite direction needs to be programmed in a sufficiently swift manner (in response to the STOP cue). The last type of firing I would expect is an "inhibitory signal" (Fig. 1.3C). This pattern is marked by a difference in firing between STOP and GO trials that does not vary by direction. Neurons that fit this hypothesis would presumably communicate to downstream structures that inhibition is necessary during STOP trials regardless of direction, particularly if this trial type distinction in firing was apparent prior to the SCRT time-point. Importantly, a single neuron may encode this "inhibitory signal" after the SCRT time-point. Although this encoding may not be helpful for inhibiting the ongoing response on the current trial, the tracking or "monitoring" of the response just made can be useful for guiding subsequent behavior.

Since activity in each of the investigated brain areas has been shown to be modulated by response direction - but not always the same direction – below, I will segregate population activity into each cell's preferred and nonpreferred response directions. Preferred direction is defined as the movement direction that elicited the strongest firing during the response epoch, averaged over correct STOP and GO trials (always referred to the ultimate response direction performed, *not* the successfully inhibited direction). Therefore, the three hypothesized categories under which cells could fall would be better interpreted using a directional preference precept (Fig. 1.3A-C *right*) where firing preference is determined individually for every cell.

Figure 1.4 includes three single cells which exemplify the hypothesized patterns originally defined in figure 1.3. Specifically, the "directional signal" pattern is reflected in the neuron depicted in figure 1.4A where activity is greater during the response in the contralateral direction but does not vary by the type of trial (STOP or GO). Importantly, the contralateral direction would be defined as this individual cell's "preferred" direction where responses to the ipsilateral direction would be the "nonpreferred" direction. In the neuron presented in figure 1.4B, activity is substantially greater under GO trials in the contralateral direction relative to the ipsilateral direction. However, activity on STOP trials does not vary by direction due to the nature of the task inducing a "conflicted directional signal" when one direction needs to be inhibited while the other commenced. Lastly, a cell providing an "inhibitory signal" fires at greater frequencies under STOP trials relative to activity on GO trials. In this neuron, activity does not vary by the direction of the response.

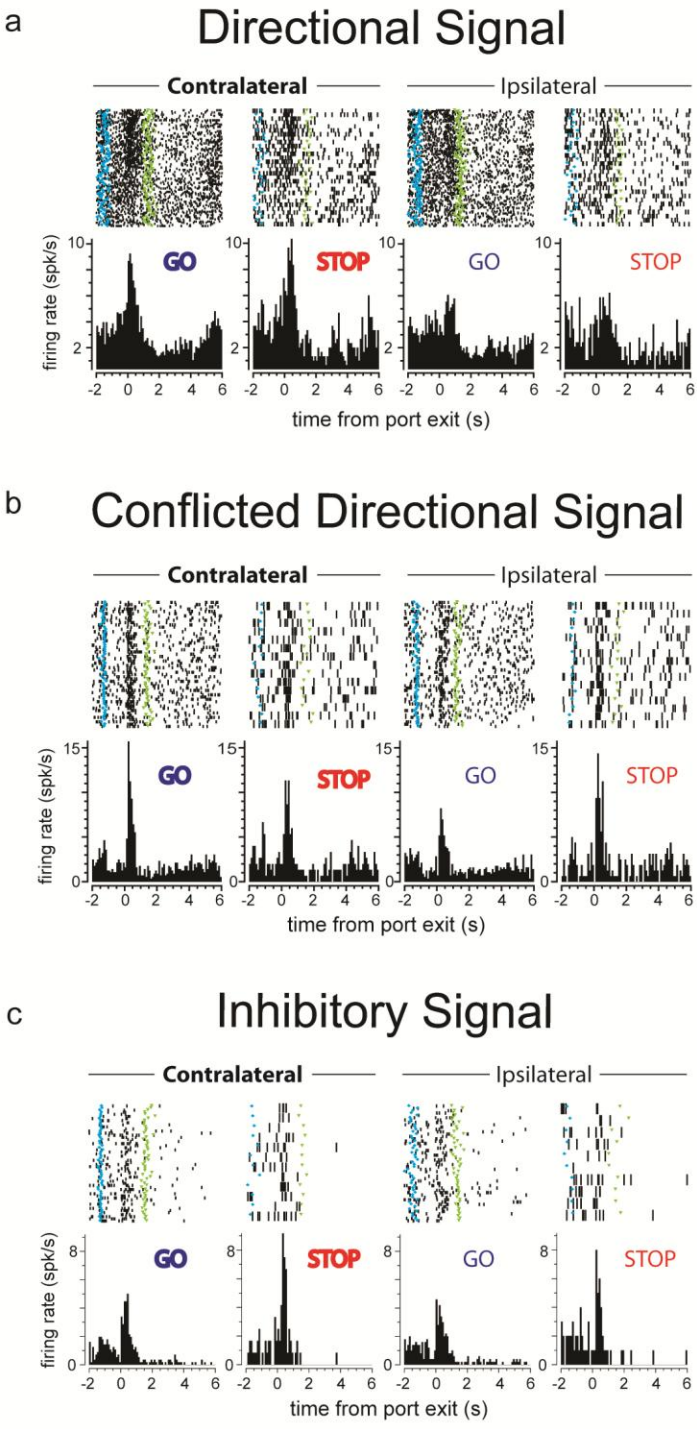

Figure 1.4: **Characteristic single neuron examples.** Raster plots depict firing on individual trials where every row is a trial, and each tick mark represents an action potential. Peri-event time histograms are presented below marking the average firing rate across all iterations of that trial type during the session. All raster plots and histograms are aligned to port exit. **A)** This neuron is selective for the direction of the response where activity was stronger when the animal responded contralateral to the recording electrode but activity by the type of trial did not vary. **B)** This neuron shows differential modulation by the direction of the response on GO trials, but not STOP trials. Therefore, on STOP trials, the correct direction is "conflicted" in the neural activity. **C)** This neuron is selective for trial type in that activity was stronger under STOP trials relative to GO trials regardless of the response direction. In raster plots, blue diamonds and green triangles represent time of nose-poke at trial start and fluid well entry, respectively.

Characterizing "increasing-" and "decreasing-" type cells: For all analyses I will first divide neurons into whether they increased or decreased firing during the response epoch (port exit to well entry) relative to baseline (1s before trial onset; t-test; $p < 0.05$). All subsequent analyses will be done on these individual populations.

Population Activity: I will quantify activity for both increasing- and decreasing-type neurons by examining population activity. For each chapter, I display population histograms that plot the average activity (spikes/s) over all neurons within a sub-population (e.g. increasing-type neurons) aligned to an individual task event. I am interested in discerning if/how a brain region is impacted by response inhibition, thus I will align population activity to port exit. On GO trials, port exit is the beginning of the movement toward the fluid well and on STOP trials, this time-point is *simultaneous* with the onset of the STOP cue. Average activity will be plotted individually for both directions (preferred and nonpreferred) on GO trials, STOP trials, and STOP errors.

Stop Index: For each population of neurons I will compute a "stop index", which quantifies the counts of neurons that fire differently on STOP versus GO trials. The stop index is defined as the difference between firing on STOP trials and GO trials in the same direction during the "response epoch" (port exit to well entry) normalized by the sum of these firing rates ((STOP-GO)/(STOP+GO)). Thus values above and below zero indicate higher and lower firing, respectively, on STOP trials versus GO trials. This will be computed for every neuron and displayed as individual distributions for the preferred and nonpreferred directions.

Directional Index: For each population of neurons I will compute a "directional index", which quantifies the strength of directional tuning for both GO and STOP trials. This "directional index" takes the difference in firing rates between the preferred direction and nonpreferred direction normalized by the sum of these firing rates ((preferred-nonpreferred)/(preferred+nonpreferred)). This will be computed for every neuron and displayed as individual distributions for GO trials, STOP trials, and STOP errors.

Sliding t-test analysis: Although the directional index is a powerful statistic that can determine the difference in responding between two spatially opposite locations during the entirety of a response, it does not have the temporal precision to determine at which time point a brain region distinguishes between two directions. I therefore calculated the difference between the preferred and nonpreferred directions in 100ms epochs that slide every 10ms and added "tick marks" to the population histograms where this comparison was significantly different (t-test; $p < 0.01$). Importantly, if the correct direction on STOP trials is significantly encoded prior to the SCRT in a population of neurons, these neurons may possess the temporal capacity to "fix" a conflicted directional signal in time to guide response inhibition behavior.

Multiple regression analysis: It is well-documented that single neurons within a brain region are sensitive to different task parameters. The beauty of the single cell recording technique is that this sensitivity can be analyzed at the level of individual neurons. Therefore, I analyzed each neuron using a multiple regression analysis (equation in Chapter 10: Detailed methodology) that determines how many neurons were sensitive to the direction of the response, the speed of the response, or whether it was a

STOP or GO trial when variance in firing rate of the other two parameters was accounted for (partial r^2).

Modulation of conflict by identity of previous trial: The final analysis that will be completed across multiple brain regions is designed to test for sensitivity of firing patterns to the past and present conflict induced by the trial sequence. Behaviorally, using multiple tasks, it has been shown that efficient performance on the current trial is dependent on the degree of conflict on the previous trial (*66*). The theory suggests that on a non-conflict trial preceded by a conflict trial, the subject should exhibit slower response times and higher control than in situations where the non-conflict trial is preceded by a non-conflict trial. Additionally, on a conflict trial preceded by a non-conflict trial, the competing irrelevant response should have a larger impact on the ultimate response and therefore increase response latencies relative to when a conflict trial is preceded by a conflict trial. These behavioral findings have been referred to as "conflict adaptation" or "Gratton effect" (*67-70*).

My task is specifically designed to study the role of response inhibition on single cells via the presentation of a conflicting stimulus after initiation of a response. However, the swift and continuous manner in which rats completed trials in addition to the pseudo-random sequence of the trial types allows me to investigate the impact of immediate prior conflict on activity. That is, the presence of a conflict trial (STOP trial) immediately preceding a STOP trial (sS trial) can impact preparation and accuracy relative to when a STOP trial is preceded by a simple GO trial (gS trial).

In my task, animals exhibit behavior consistent with conflict adaptation such that a conflicting trial (in this task; STOP trial) is performed more accurately when the

preceding trial is also a conflict trial. For instance, rats are more successful at STOP trials when they are preceded by STOP trials than GO trials (Fig. 1.2E). This observed behavioral effect suggests that neurons may respond differently to STOP trials depending on the previous trial. Therefore, population histograms will be reconstructed to dissociate STOP trials after GO trials ('gS') from STOP trials after STOP trials ('sS'). I will compare these trial types directly by taking the firing rate during the response epoch and calculating a "stop index" that subtracts firing on sS trials from firing on gS trials (gS-sS). Additionally, I will compare each of these STOP trial "types" to the average of all GO trials (gS-GO) and (sS-GO). Since the previous trial may also have an effect on the strength of the directional signal, I also plan to recreate "directional indices" that subtract firing in the preferred direction from firing in the nonpreferred direction individually for GO trials, gS trials, and sS trials. Lastly, to determine if the previous trial impacts firing on GO trials, I will replicate the previous analyses for current GO trials by comparing gG to sG trials.

Chapter 5: Medial dorsal striatal neurons represent direction-based response conflict

As mentioned Chapter 3, my task is specifically designed to induce an inhibitory mechanism by invoking directional conflict (i.e. the second light is spatially opposite the first). I therefore chose to record single neurons from the medial dorsal striatum (mDS), a region known to be tightly correlated with response encoding. As the major input structure to the basal ganglia mDS has been implicated in habitual, over-learned, and automatic responding (*71-78*), but recent work has also pointed to the mDS as being involved in executive functioning (*79*) including response inhibition (*5, 37, 38*).

Pharmacological and anatomical studies have demonstrated that mDS is involved in response inhibition (*5*), but its exact role in this critical function remains elusive. For example, during performance of a stop signal task in which rats had to suppress an ongoing movement in the minority of trials, rats showed reduced ability to inhibit responding after mDS lesions (*5, 58*). In this task, rats were required in the large majority of trials (80%) to respond quickly to an instrumental stimulus (light). On 20% of trials, rats were signaled by a tone to "stop" sometime between the initiation of the response and its final execution. Stopping was easier when the stop cue (tone) sounded earlier as opposed to immediately before the instrumental response (lever press). Rats with mDS lesions needed earlier warnings to be able to adequately inhibit movement as compared to controls suggesting a deficit in response inhibition. Unfortunately, this result was tainted by the finding that rats were also slower on non-stop trials (i.e. "go" trials), making the pure response inhibition interpretation a difficult one.

Similarly intriguing results have been found in other tasks. For example, in the 5-choice-serial-reaction-time task, rats responded to a brief visual stimulus after a fixed or variable interval (e.g. ~5s). Rats with dorsal striatum lesions were unable to refrain from action before the appropriate time (*5, 37, 38*). Responses made prior to the end the delay period were considered premature errors and were more common in rats with dorsal striatum lesions. Although this result suggests that response inhibition is dependent on dorsal striatum, others have failed to report premature responding after dorsal striatum interference during performance of similar tasks (*39, 40*).

These variable results likely reflect distinct populations of neurons in mDS are performing different functions or that mDS is responsible for unrelated operations that happen to coincide with response inhibition on the tasks that have been implemented. Therefore, global destruction or non-specific inactivation of mDS is not a sufficient technique to understand the role of mDS in response inhibition. This points to the need for a single unit recording study that examines the neural mechanism by which mDS promotes and suppresses behavior to determine what information is being encoded during performance of a stop signal task. I therefore recorded from 437 individual mDS neurons (recording locations in figure 2.7C) from seven rats performing the stop signal task.

In the following chapter, I will describe the mDS as a brain region that robustly encodes the direction of the intended response including the initial miscoding of direction during the early portion of STOP trials. I will also expand on the relative insensitivity of mDS neurons to encode a pure "inhibitory signal" (Fig. 1.3C) and the strong occurrence of "direction signal" and "response conflict" firing. Lastly, I will detail how firing in

mDS is largely impartial to prior conflict where firing tends to follow the mechanics of the response, not the conflict associated with it.

In order to directly compare neural activity on GO trials and STOP trials, I first asked how many neurons increased or decreased firing during the movement toward the fluid well. To do this I determined how many neurons fired more or less frequently (i.e. task responsive) during the "response epoch" (port exit to well entry) compared to baseline (1s epoch starting 2s prior to the trial initiation nose poke). This response epoch captures any inhibitory/directional encoding while accounting for response time variability. Of these 437 neurons, 122 (28%) and 164 (38%) significantly increased and decreased firing during the response epoch, respectively.

Since most mDS cells were modulated by response direction - but not always the same direction - I segregated population activity into each cell's preferred and nonpreferred response directions. Preferred direction is defined as the movement direction that elicited the strongest firing during the response epoch, averaged over correct STOP and GO trials. An example of such a cell is illustrated in figure 1.4A where activity increases after port exit and fired more strongly for one direction (Fig. 1.4A; contralateral) over the other (Fig. 1.4A; ipsilateral).

Increasing-type cells

Population activity: Figure 2.1A and B illustrate the average activity over all 122 increasing-type mDS cells over time (aligned to port exit, A, and reward well entry, B). Critically, on STOP trials, port exit is *simultaneous* with STOP cue onset. The direction

specified by thick and thin lines *always* refers to the direction the animal responded to. Animals made responses on every trial shown. For example, "go pref" trials (**thick** blue), "stop nonpref went pref" trials (**thick** red), and "stop pref went pref" trials (**thick** dashed red) all refer to trials where the animal ultimately responded to the preferred direction even though the cues were not identical (pref = preferred direction; nonpref = nonpreferred direction). Notable time-points are indicated by vertical dashed lines; "GO cue" represents the average time the GO cue illuminated prior to port exit and "SCRT" represents the average stop change reaction time as described above. Additionally, average movement times (port exit to well entry) for correct GO and STOP trials are marked as downward facing arrows (blue and red, respectively). GO cue onset, SCRT, and movement times are variable and are therefore specific to the sessions during which the analyzed cells were taken.

Figure 2.1: **Direction and trial type encoding of increasing-type mDS neurons. A-B)** Average firing rate (spikes/s) over time aligned on port exit (A) and well entry (B) for all mDS neurons that fired more strongly during the 'response epoch' (port exit to well entry) relative to baseline (1s epoch beginning 2s prior to trial initiation). The time necessary to inhibit a response (stop change reaction time; SCRT) is defined as the difference between STOP trial movement time and GO trial movement time. SCRT is marked as the vertical dotted line labeled 'SCRT' at 133ms. 'GO cue' and its associated vertical dashed line indicates the average onset of the GO cue as measured by the latency from port exit (-358ms). Blue lines refer to GO trials, red lines refer to STOP trials, and dashed lines refer to errant trials (incorrect direction). Due to the heterogeneous direction specificity of individual cells, each cell was characterized as having a preferred direction and a nonpreferred direction. This preference was determined by asking which direction (contra- or ipsilateral to the recorded hemisphere) elicited the highest firing rate during the response epoch for each cell. Therefore, as defined by the analysis, preferred direction (thick lines) is always higher than the nonpreferred direction (thin lines) during the response epoch. Tick marks represent significant p-values in temporal space after preferred direction was compared to nonpreferred direction in the population for GO trials (blue ticks) and STOP trials (red ticks) in 100ms epochs that slid by 10ms after each iteration (t-test; $p < 0.01$). Pink ticks refer to the temporally short period where the incorrect direction was significantly encoded (t-test; $p < 0.01$) on STOP trials. Although each tick mark signifies statistical difference for a 100ms epoch, tick width is 10ms for the purpose of presentational detail. Arrowheads denote the average movement time (well entry) during GO trials (blue arrowhead = 472ms) and STOP trials (red arrowhead = 605ms). GO cue, SCRT, and movement times (arrowheads) are variable values based on the behavior of the animals in the analyzed sessions. These values (except SCRT) are estimates with variance and cannot be treated as constants relative to port exit. **C)** Stop indices for preferred (*left*) and nonpreferred (*right*) directions. Stop indices are calculated by taking the activity during the response epoch from STOP trials, subtracting activity during the response epoch on GO trials, and dividing it by the sum of the two ((STOP-GO/(STOP+GO)) in each direction for every cell. Significant shifts from zero (as calculated by Wilcoxon) denote that neuronal activity is significantly different between STOP and GO trials in a given direction. **D)** Directional index distributions defined as activity during the response epoch in the preferred direction minus activity during the response epoch in the nonpreferred direction divided by the sum ((preferred-nonpreferred)/(preferred+nonpreferred)) in every cell. These calculations are specific to GO trials (*left*), STOP trials (*middle*), and STOP errors (*right*). Significant shifts from zero (as calculated by Wilcoxon) signify that activity is greater in one direction than the other at the neuronal level. Asterisks in C and D indicate that two distributions are significantly different via Wilcoxon.

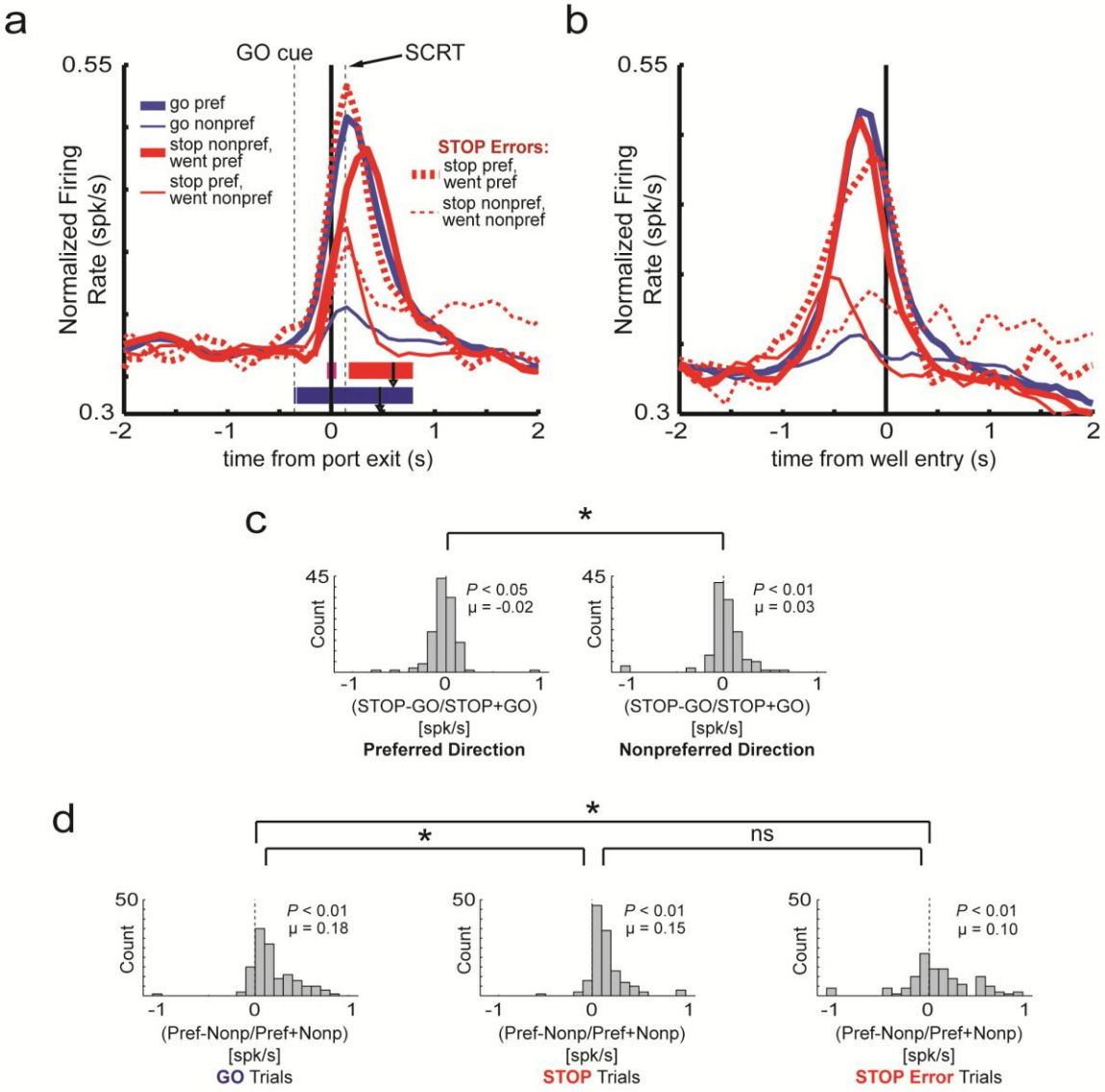
a
GO cue
SCRT
0.55
0.3
Normalized Firing Rate (spk/s)
go pref
go nonpref
stop nonpref, went pref
stop pref, went nonpref
STOP Errors:
stop pref, went pref
stop nonpref, went nonpref
-2
-1
0
1
2
time from port exit (s)
b
0.55
0.3
Normalized Firing Rate (spk/s)
time from well entry (s)
c
*
45
Count
P < 0.05
μ = -0.02
(STOP-GO/STOP+GO)
[spk/s]
Preferred Direction
P < 0.01
μ = 0.03
Nonpreferred Direction
d
*
*
ns
50
P < 0.01
μ = 0.18
(Pref-Nonp/Pref+Nonp)
[spk/s]
GO Trials
P < 0.01
μ = 0.15
STOP Trials
P < 0.01
μ = 0.10
STOP Error Trials

As defined by the analysis, activity in the preferred direction (Fig. 2.1A-B; thick lines) was stronger than activity in the nonpreferred direction (Fig. 2.1A-B; thin lines) during the response epoch. On correct GO trials (blue), activity differentiated between the preferred (thick) and nonpreferred (thin) directions promptly as is shown by the blue ticks marks that represent significant differences between preferred and nonpreferred directional responses after comparing activity in 100ms that slid every 10ms (t-test; $p < 0.01$). Early differentiation of firing during responses in opposing directions is necessary to make speeded movements toward the correct fluid well. In fact, this directionality on correct GO trials occurred shortly after average GO cue onset (Fig. 2.1; blue ticks). On successful STOP trials (solid red lines), significant direction differentiation occurred later than GO trials (Fig. 2.1; red ticks). Critically, the initial encoding of STOP direction was the *incorrect* direction (i.e. "direction miscoding") as the neurons were beginning to bifurcate into the directions indicated by the GO cue. This is shown explicitly in figure 2.1A by the pink tick marks around the time of port exit. It was not until after the SCRT where the correct direction was encoded on successful STOP trials. This is critical because it suggests that even though activity on correct STOP trials rectified itself after encoding the wrong direction, the correct direction was not encoded until after the time-point necessary for the system to recruit any inhibitory mechanisms. Therefore, this brain region alone cannot be responsible for the prompt correction of behavior necessary for this task.

When rats made errors on STOP trials (dashed red lines), neurons did not change activity patterns after port exit in response to the STOP cue and proceeded to more closely mirror correct GO trials (blue) than STOP trials (red) suggesting that revising the

direction trajectory on STOP trials is both necessary for the task and an important function of mDS. Lastly, it is notable that the encoding of direction differed very little between GO and STOP trials once the response was completed. This is shown in figure 1.1B where activity is aligned to well entry. Reward administration is not a confounding factor here as reward is delivered >800ms after well entry.

Stop Index: To quantify trial type differences, I created an index that compares STOP trial activity to GO trial activity termed "stop index." This index is calculated by subtracting firing during GO trials from firing during STOP trials and dividing by the sum of the two ((STOP-GO)/(STOP+GO)) independently for each direction. Average firing for each neuron in each type of trial is taken during the response epoch. The distribution of stop indices in the preferred direction (Fig. 2.1C *left*) is significantly shifted in the negative direction (Wilcoxon; $p < 0.05$) which indicates that, at the population level, activity tends to be greater on GO trials than STOP trials. The opposite is true in the nonpreferred direction (Fig. 2.1C *right*) where activity tends to be greater during STOP trials (Wilcoxon; $p < 0.05$). These distributions are significantly different from one another (Wilcoxon; $p < 0.01$) which quantitatively demonstrates that mDS neurons encode similar movements differently depending on whether it was a STOP or GO trial.

Directional Index: In order to further quantify the degree to which direction is encoded in mDS neurons for both STOP and GO trials I computed a directional index defined as the difference between firing in the preferred direction and firing in the nonpreferred direction (((preferred-nonpreferred) / (preferred+nonpreferred)); Fig. 2.1D) for both trial types during the response epoch. This analysis allows me to ask if the

distribution of directional indices, and therefore the strength of the directional signal during the response, is different between the two trial types across the population of increasing-type neurons. Although both correct GO and STOP trial direction indices were significantly shifted from zero (Fig. 2.1D *left*, *middle*; Wilcoxon; ps < 0.01), the directional index under GO trials was significantly greater than under STOP trials (Fig. 2.1 *left* vs. *middle*; Wilcoxon; $p < 0.01$), demonstrating that direction encoding was attenuated under STOP trials. This fits nicely with the "conflicted directional signal" hypothesis (Fig. 1.3B) as mDS neurons are modulated by response direction on GO trials, but this directional firing pattern is conflicted during STOP trials, thus the reduced directional index on STOP trials (Fig. 2.1D). Lastly, although the directional index on STOP error trials (Fig. 2.1D *right*) is significantly shifted in the positive direction (Wilcoxon; $p < 0.01$) and is not statistically different from the directional index on correct STOP trials (Fig. 2.1D *middle* vs. *right*; Wilcoxon; $p = 0.58$), neurons are largely encoding the incorrect direction on STOP errors.

This collection of mDS results support the "conflicted directional signal" hypothesis laid out in figure 1.3B, not the "inhibitory signal." One would expect that if mDS has a specialized role in response suppression as suggested by previous research (*5*), firing during STOP trials would emerge as a direction agnostic increase or decrease relative to GO trial firing as depicted in figures 1.3C and 1.4C. Despite previous research implying a specific inhibitory role for mDS neurons, my neural data does not support this proclamation. Instead, the firing features I have described signify a direction-based generation and redirection role for mDS that occurs under conflict (Fig. 1.3B).

Multiple regression analysis: From the previous results I conclude that average population activity of increasing-type mDS neurons is modulated during performance of the stop signal task but, of course, this analysis was done on the population as a whole and there may be a smaller population of single neurons that encode purely for response inhibition. To assess task correlates at the single cell level I performed a multiple regression analysis (see Chapter 10: Detailed methodology). This was done to determine the contribution of single cells to a specific portion of the task after variance for other portions was accounted for. For example, the size of the top circle in figure 2.2 indicates the proportion of increasing-type mDS neurons that showed a significant partial r^2 statistic for the direction parameter (Fig 2.2; direction). Sixty-five percent of increasing-type mDS neurons (n = 79) exhibited a significant partial r^2 for direction and of these 79 neurons, 59 β-values were positive (greater firing for the contralateral direction) whereas 20 β-values were negative (binomial sign test; $p < 0.01$) showing that firing in more mDS neurons favor the contralateral direction. These neurons individually would more closely resemble the "directional signal" hypothesis laid out in figure 1.3A. For the movement time parameter, 28% (n = 34) of neurons are significantly modulated (Fig. 2.2; movement time) where a higher proportion of β-values were negative (6 vs. 28; binomial sign test; $p < 0.01$). Lastly, only 14 neurons (11%) are significantly modulated by trial type (Fig. 2.2; trial type), the β-values of which were not proportionally different (9 vs. 5; binomial sign test; $p = 0.21$). Therefore, when variance for movement speed and direction were parsed out, only 11% of mDS increasing-type neurons could fall into the "inhibitory signal" category.

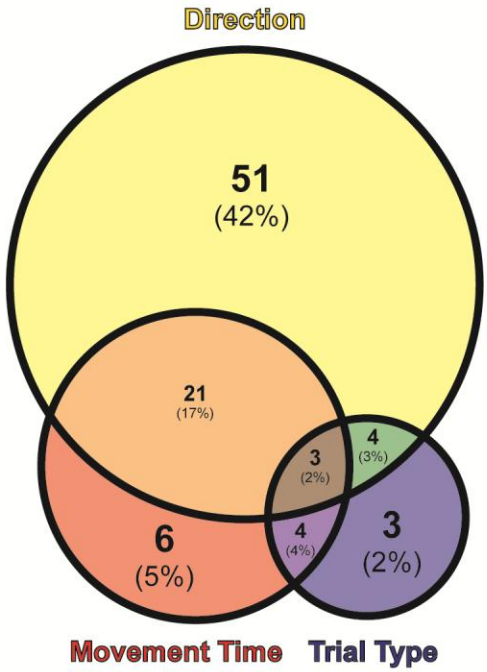

	Direction		Movement Time		Trial Type	
β-valence	+	-	+	-	+	-
	59*	20	6	***28****	9	5

Figure 2.2: **Multiple regression results for increasing-type mDS neurons.** Circle sizes represent the relative proportions of neurons showing significant partial r^2 values for the individual task parameters. Top circle encompasses the proportion of neurons that show significant partial r^2 values for the direction parameter. Conventions as above for the movement time (red circle) and trial type (blue circle) parameters. Non-overlapping portions represent the counts (and percentages) of neurons with significant partial r^2 values for one parameter. Overlapping portions denote the counts (and percentages) of single cells that exhibited significant partial r^2 values for two (orange, green, purple) or all three (brown) parameters. The table specifies the counts of neurons significant within a variable that have associated positive ("+") or negative ("-") β-values. As specified by the model, positive β-values indicate greater firing for the contralateral direction (direction), greater firing for slower movement times (movement time), and greater firing for STOP over GO trials (trial type). Asterisks indicate significantly more β-values for one valence within a parameter (binomial sign test; $p < 0.05$).

Modulation of conflict by identity of previous trial: In figure 2.3A, I replotted the population histogram originally in figure 2.1A to now include correct STOP trials preceded by GO trials (Fig. 2.3A; red lines; 'gS') and correct STOP trials preceded by STOP trials (Fig. 2.3A; orange lines; 'sS') relative to all correct GO trials. All other conventions remain unchanged. Consistent with behavioral conflict adaptation, rats in my task were faster on correct STOP trials following STOP (i.e. conflict) trials relative to those that followed GO (i.e. no conflict) trials (Fig. 2.3A; orange vs. red arrowheads). Put simply, animals are faster and more accurate on STOP trials preceded by STOP trials because they have prepared for upcoming conflict and can more swiftly resolve it.

Figure 2.3: **Impact on neuronal encoding based on conflict induced by the previous trial in increasing-type mDS neurons. A)** Population histogram of mDS neurons that increased significantly above baseline. Activity is aligned to port exit. Blue lines refer to all GO trials. Red lines represent STOP trials preceded by GO trials ('gS'). Orange lines indicate trials where a STOP trial is preceded by a STOP trial ('sS'). Calculation of direction preference remained unchanged from figure 2.1. Tick marks represent 100ms epochs where the preferred direction was significantly different from the nonpreferred direction (t-test; $p < 0.01$) for GO trials (blue), gS trials (red), and sS trials (orange). Pink ticks represent windows where activity was significantly greater in the nonpreferred direction (t-test; $p < 0.01$). Although each tick mark signifies statistical difference for a 100ms epoch, tick width is 10ms for the purpose of presentational detail. Arrowheads indicate average movement times (port exit to well entry) for GO trials (blue; 471ms), gS trials (red; 626ms), and sS trials (598ms). Note the longer movement times for gS trials relative to sS trials consistent with reduced preparation for conflict. Vertical dashed lines mark the times of the stop change reaction time (SCRT; 133ms) and the average GO cue onset as measured as the latency from port exit (GO cue; -358ms) for the analyzed sessions. **B)** Indices compare the difference in firing between the three trial types presented in A. Leftmost distribution calculates the differences between gS and GO trials for each cell. The middle distribution marks the difference between sS and GO trials. Rightmost distribution computes the difference between gS and sS trials. **C)** Directional index distributions calculate the difference between the preferred and nonpreferred direction in each neuron during GO trials (*left*), gS trials (*middle*), and sS trials (*right*). **D)** Population histogram of increasing-type mDS neurons is aligned to port exit. All lines represent accurate GO trials that either followed a GO trial ('gG'; dark blue) or followed a STOP trial ('sG'; light blue). Thick lines refer to the preferred direction and thin lines refer to the nonpreferred direction. Tick marks denote the 100ms epochs where the preferred direction significantly differed from the nonpreferred direction (t-test; $p < 0.01$) during gG trials (dark blue) and sG trials (light blue). Arrowheads mark the average movement times for gG trials (dark blue; 470ms) and sG trials (light blue; 471ms). **E)** Distribution calculates the difference between firing on gG versus sG trials. **F)** Directional index distributions calculate the difference between the preferred and nonpreferred direction in each neuron during gG trials (*left*) and sG trials (*right*). Activity for all distributions was taken during the response epoch and significant shifts from zero are determined via Wilcoxon ($p < 0.05$). Asterisks indicate a direct comparison between two distributions is significant (Wilcoxon; $p < 0.05$ corrected for multiple comparisons).

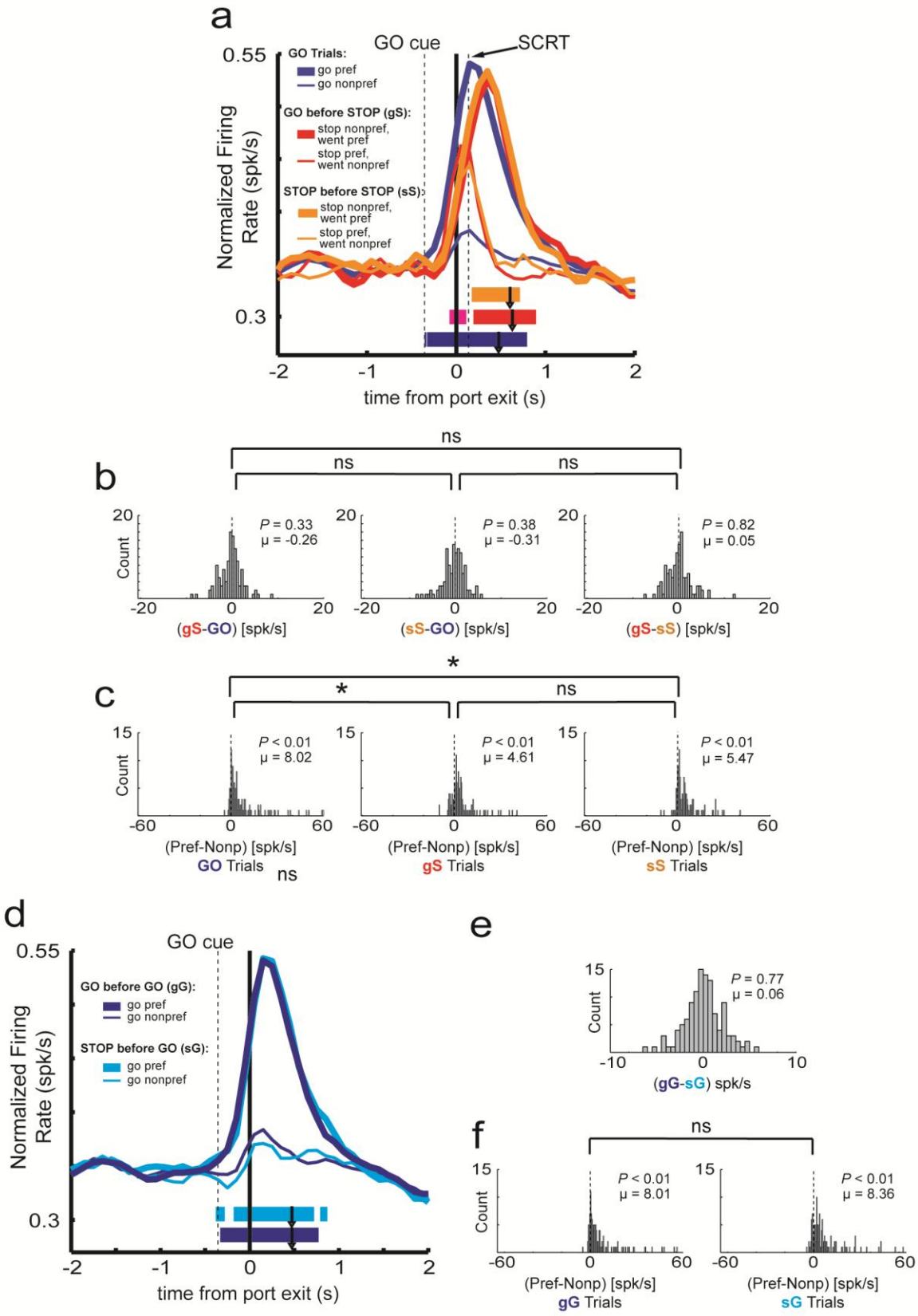
a
GO cue
SCRT
0.55
0.3
GO Trials:
go pref
go nonpref
GO before STOP (gS):
stop nonpref, went pref
stop pref, went nonpref
STOP before STOP (sS):
stop nonpref, went pref
stop pref, went nonpref
Normalized Firing Rate (spk/s)
-2
-1
0
1
2
time from port exit (s)
b
ns
ns
ns
20
Count
P = 0.33
μ = -0.26
P = 0.38
μ = -0.31
P = 0.82
μ = 0.05
-20
0
20
(gS-GO) [spk/s]
(sS-GO) [spk/s]
(gS-sS) [spk/s]
c
*
*
ns
15
P < 0.01
μ = 8.02
P < 0.01
μ = 4.61
P < 0.01
μ = 5.47
-60
0
60
(Pref-Nonp) [spk/s]
GO Trials
gS Trials
sS Trials
ns
d
GO cue
0.55
0.3
GO before GO (gG):
go pref
go nonpref
STOP before GO (sG):
go pref
go nonpref
Normalized Firing Rate (spk/s)
-2
-1
0
1
2
time from port exit (s)
e
15
Count
P = 0.77
μ = 0.06
-10
0
10
(gG-sG) spk/s
f
ns
15
Count
P < 0.01
μ = 8.01
P < 0.01
μ = 8.36
-60
0
60
(Pref-Nonp) [spk/s]
gG Trials
sG Trials

If one considers that inhibition/redirection on STOP trials is a conflicting response relative to a non-conflicting GO trial, it is possible to parse out the function of mDS neurons when preparation for response inhibition is high (after STOP trials; sS) versus when this preparation is low (after GO trials; gS). The striking result is that on sS trials (Fig.2.3A; orange ticks), when preparation for stopping is highest, direction is not miscoded whereas direction *is* miscoded on gS trials (Fig. 2.3A; pink ticks). Additionally, the *correct* direction is encoded ~20ms later in gS trials relative to sS trials. However, significant directionality on both of these types of STOP trials occurred after the SCRT.

In order to quantify differences between gS, sS, and GO trials, I calculated "stop" and directional indices similarly to previous figures. Specifically for "stop indices", I took firing during the response epoch for each trial averaged over the preferred and nonpreferred directions and calculated gS minus GO trials (Fig. 2.3B *left*), sS minus GO trials (Fig. 2.3B *middle*), and gS minus sS trials (Fig. 2.3B *right*). None of these comparisons yielded significant results (Fig. 2.3B *left*, *middle*, *right*; Wilcoxon; ps > 0.33). However, when direction indices were calculated for GO, gS, and sS trials, each were significantly shifted positively (Fig. 2.3C *left*, *middle*, *right*; Wilcoxon; ps < 0.01). Interestingly, the directional index on GO trials differed from both gS trials (Fig. 2.3C *left* vs. *middle*; Wilcoxon; $p < 0.01$) and sS trials (Fig. 2.3C *left* vs. *right*; Wilcoxon; $p < 0.05$) but direction indices between gS and sS trials did not differ (Fig. 2.3C *middle* vs. *right*; Wilcoxon; $p = 0.13$). These results imply that mDS neurons encode the correct direction on STOP trials more weakly than GO trials (as previously demonstrated in Fig. 2.1) but there is no appreciable difference during the response epoch between

directionality on STOP trials based on which trial type preceded it. However, the preparation for a STOP trial induced by a preceding STOP trial (sS trials) prohibited the encoding of the direction cued by the GO cue (i.e. direction miscoding) and allowed for the resolution of directional conflict in a speedier manner.

If the above effects seen in mDS increasing-type neurons were a result of the conflict induced by the previous trial and not simply the *identity* of the previous trial, the identity of the trial preceding a GO trial should not impact neuronal firing. To measure this, I analyzed the difference between GO trials preceded by GO trials (Fig. 2.3D; dark blue lines; 'gG') and GO trials preceded by STOP trials (Fig. 2.3D; light blue lines; 'sG'). The population histogram in figure 2.3D illustrates very little firing difference between gG and sG trials. Additionally, the index comparing the average firing rate of gG and sG trials was not significantly shifted (Fig. 2.3E; Wilcoxon; $p = 0.77$) and although the direction indices for both types of trials are significantly positively shifted, they did not differ from one another (Fig. 2.3F *left* vs. *right*; Wilcoxon; $p = 0.28$).

Summary: Increasing-type mDS neurons have a substantial bias toward the direction of the response made by the animal (not the one that cued it) such that the direction signal, early during STOP trials, is flipped until the animal correctly inhibits the incorrect direction and responds correctly. These neurons vary their firing patterns based on the direction of the response as well as the speed of the response but added modulation by the type of trial (STOP vs. GO) is minimal. Despite this propensity toward encoding the nature of the response, increasing-type mDS neurons are also sensitive to the conflict preceding STOP trials where the incorrect direction is not encoded and the correct direction is resolved earlier in the trial. This sensitivity to conflict however is likely due

to the neurons encoding the faster and more accurate movements made when conflict is minimal. Indeed, it has been suggested before that mDS is invariant to trial sequence, rather, it tracks the response being made even if that was response was in error (*80*).

Decreasing-type cells

Population activity: A large proportion (38%) of the recorded mDS cells can be characterized as "decreasing-type" cells. That is, activity during the response epoch is significantly lower than the baseline firing rate. These neurons (Fig. 2.4A,B) are presented and analyzed in the exact same manner as their increasing-type counterparts. A cursory comparison of firing between decreasing- and increasing-type neurons reveals similar direction-based activity. In these decreasing-type cells, the contrast between preferred and nonpreferred direction on GO trials (Fig. 2.4A; blue ticks) is significantly distinct near GO cue illumination and robustly different just before port exit. On STOP trials (Fig. 2.4A; red ticks), even though there is no significant miscoding of direction, the correct direction is still not significantly discerned until after the SCRT. Due to the increased activity on STOP trials compared to GO trials in both directions during the response (quantified below), one could argue that determining the correct direction during behavior is not an integral function of these neurons. However, during STOP errors (Fig. 2.4A,B; dashed lines), activity tends to be higher for the direction the animal responded to rather than the direction instructed by the STOP cue. In fact, activity during STOP error trials remains comparable to activity on correct GO trials throughout the response (Fig. 2.4B) when the ultimate response direction was the same (e.g. thick blue vs. thick dashed red).

Figure 2.4: **Direction and trial type encoding of decreasing-type mDS neurons. A-B)** Average firing rate (spikes/s) over time aligned on port exit (A) and well entry (B) for all mDS neurons that fired less strongly during the 'response epoch' (port exit to well entry) relative to baseline (1s epoch beginning 2s prior to trial initiation). The time necessary to inhibit a response (stop change reaction time; SCRT) is defined as the difference between STOP trial movement time and GO trial movement time. SCRT is marked as the vertical dotted line labeled 'SCRT' at 121ms. 'GO cue' and its associated vertical dashed line indicates the average onset of the GO cue as measured by the latency from port exit (-340ms). Blue lines refer to GO trials, red lines refer to STOP trials, and dashed lines refer to errant trials (incorrect direction). Due to the heterogeneous direction specificity of individual cells, each cell was characterized as having a preferred direction and a nonpreferred direction. This preference was determined by asking which direction (contra- or ipsilateral to the recorded hemisphere) elicited the highest firing rate during the response epoch for each cell. Therefore, as defined by the analysis, preferred direction (thick lines) is always higher than the nonpreferred direction (thin lines) during the response epoch. Tick marks represent significant p-values in temporal space after preferred direction was compared to nonpreferred direction in the population for GO trials (blue ticks) and STOP trials (red ticks) in 100ms epochs that slid by 10ms after each iteration (t-test; $p < 0.01$). Although each tick mark signifies statistical difference for a 100ms epoch, tick width is 10ms for the purpose of presentational detail. Arrowheads denote the average movement time (well entry) during GO trials (blue arrowhead = 488ms) and STOP trials (red arrowhead = 608ms). GO cue, SCRT, and movement times (arrowheads) are variable values based on the behavior of the animals in the analyzed sessions. These values (except SCRT) are estimates with variance and cannot be treated as constants relative to port exit. **C)** Stop indices for preferred (*left*) and nonpreferred (*right*) directions. Stop indices are calculated by taking the activity during the response epoch from STOP trials, subtracting activity during the response epoch on GO trials, and dividing it by the sum of the two ((STOP-GO/(STOP+GO)) in each direction for every cell. Significant shifts from zero (as calculated by Wilcoxon) denote that neuronal activity is significantly different between STOP and GO trials in a given direction. **D)** Directional index distributions defined as activity during the response epoch in the preferred direction minus activity during the response epoch in the nonpreferred direction divided by the sum ((preferred-nonpreferred)/(preferred+nonpreferred)) in every cell. These calculations are specific to GO trials (*left*), STOP trials (*middle*), and STOP errors (*right*). Significant shifts from zero (as calculated by Wilcoxon) signify that activity is greater in one direction than the other at the neuronal level. Asterisks in C and D indicate that two distributions are significantly different via Wilcoxon.

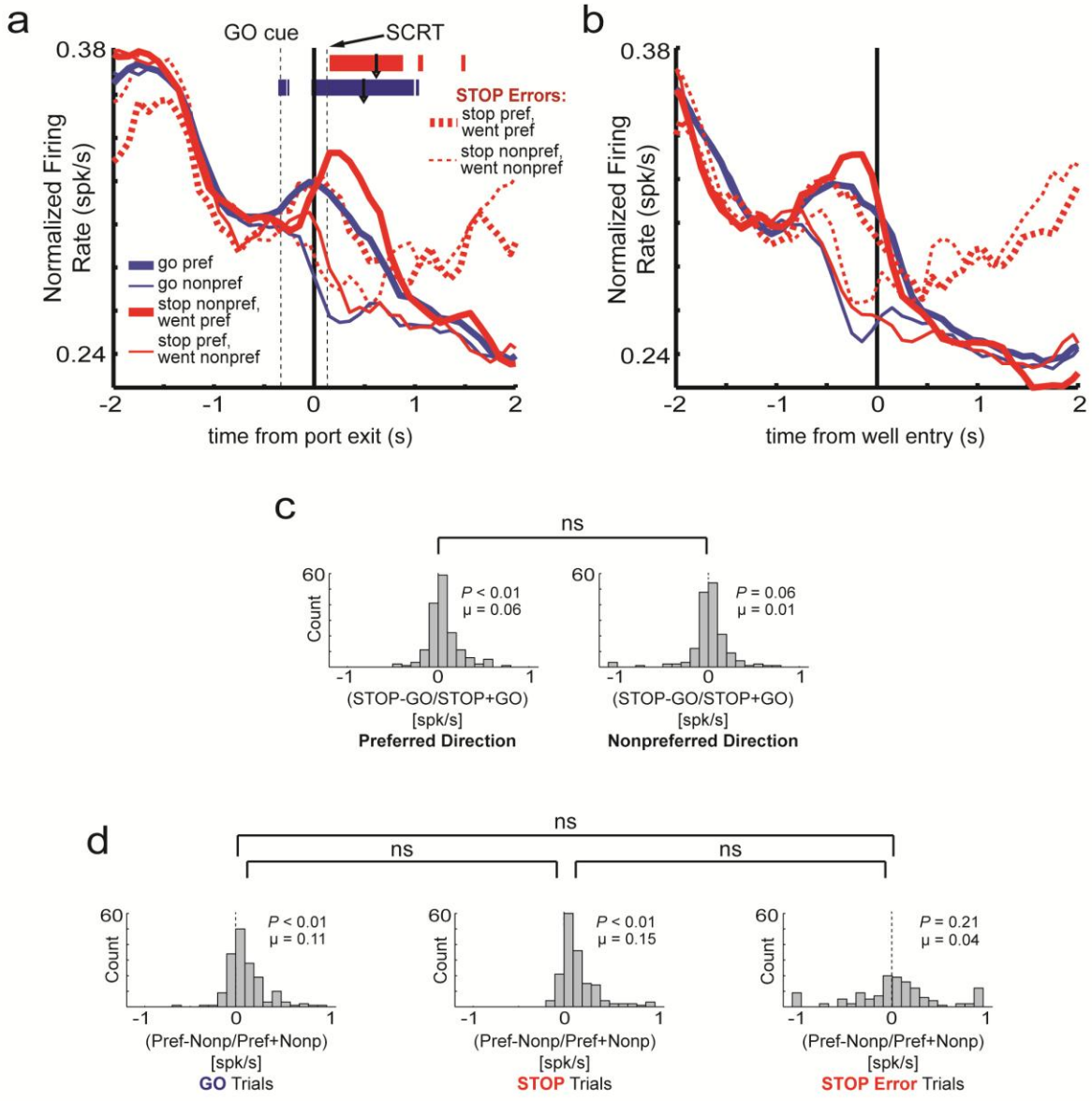
a
GO cue
SCRT
0.38
0.24
Normalized Firing Rate (spk/s)
STOP Errors:
stop pref, went pref
stop nonpref, went nonpref
go pref
go nonpref
stop nonpref, went pref
stop pref, went nonpref
-2
-1
0
1
2
time from port exit (s)
b
0.38
0.24
Normalized Firing Rate (spk/s)
-2
-1
0
1
2
time from well entry (s)
c
ns
60
Count
P < 0.01
μ = 0.06
-1
0
1
(STOP-GO/STOP+GO)
[spk/s]
Preferred Direction
60
P = 0.06
μ = 0.01
-1
0
1
(STOP-GO/STOP+GO)
[spk/s]
Nonpreferred Direction
d
ns
ns
ns
60
Count
P < 0.01
μ = 0.11
-1
0
1
(Pref-Nonp/Pref+Nonp)
[spk/s]
GO Trials
60
P < 0.01
μ = 0.15
-1
0
1
(Pref-Nonp/Pref+Nonp)
[spk/s]
STOP Trials
60
P = 0.21
μ = 0.04
-1
0
1
(Pref-Nonp/Pref+Nonp)
[spk/s]
STOP Error Trials

Stop Index: To quantify the above proclamations, activity at the neuronal level tended to be higher on STOP trials than GO trials in the preferred direction (Fig. 2.4C *left*; Wilcoxon; $p < 0.01$) and although this was only a trend in the nonpreferred direction (Fig. 2.4D *right*; Wilcoxon; $p = 0.06$), the two distributions are not different (Fig. 2.4C *left* vs. *right*; Wilcoxon; $p = 0.13$). Therefore, at the population level, there tends to be greater firing on STOP trials than GO trials regardless of direction.

Directional Index: When comparing direction-based activity in decreasing-type neurons, I found that the distribution of directional indices was significantly shifted positively on both GO trials (Fig. 2.4D *left*; Wilcoxon; $p < 0.01$) and STOP trials (Fig. 2.4D *middle*; Wilcoxon; $p < 0.01$) and the two distributions do not differ (Fig. 2.4E *left* vs. *middle*; Wilcoxon; $p = 0.13$). Additionally, the directional index distribution for STOP error trials was not significantly shifted (Fig 2.4D *right*; Wilcoxon; $p = 0.21$) but also did not differ from the GO trial (Fig. 2.4D *left* vs. *right*; Wilcoxon; $p = 0.06$) or STOP trial distributions (Fig. 2.4D *middle* vs. *right*; Wilcoxon; $p = 0.06$).

Although it appears that differential activity patterns are elicited under STOP trials relative to GO trials, the lack of direction specificity in the SCRT time window implies that this population cannot be the sufficient driving force for response inhibition. However, decreasing-type mDS neurons are likely important for refining a motor response due to the nearly identical firing patterns across trial types within a direction once the response is completed (Fig. 2.4B). In this sense, if the STOP versus GO contrast cannot be explained by response inhibition, it can only be explained by the motor differences necessary to change a response on STOP trials. Therefore, the best explanation for the increase in activity on correct STOP trials relative to the other trial

types is that decreasing-type mDS cells are tuning the response trajectory via projections to the indirect pathway known to pause or alter the kinetics of a movement.

Multiple regression analysis: The average population activity described in the previous sub-section does not capture the nuances of signal cell variability so I therefore implemented the multiple regression procedure used previously in figure 2.2. Of the 164 decreasing-type neurons collected, 34% (n = 56) were significantly modulated by the direction of the response when variance accounted for by movement speed and trial type were regressed out (Fig. 2.5; direction). Of these 56, equal numbers showed positive and negative β-values (33 vs. 23; binomial sign test; $p = 0.11$). When this procedure was repeated for the movement time parameter, 28 neurons (17%) were significantly modulated, a greater proportion of which exhibited positive β-values meaning reduced firing for faster movement times (Fig. 2.5; movement time; 22 vs. 6; binomial sign test; $p < 0.01$). Although a low total percentage of neurons were significantly modulated by trial type (9%; n = 15), a significant proportion of those fifteen had positive associated β-values (Fig. 2.5; trial type; 12 vs. 3; binomial sign test; $p < 0.05$).

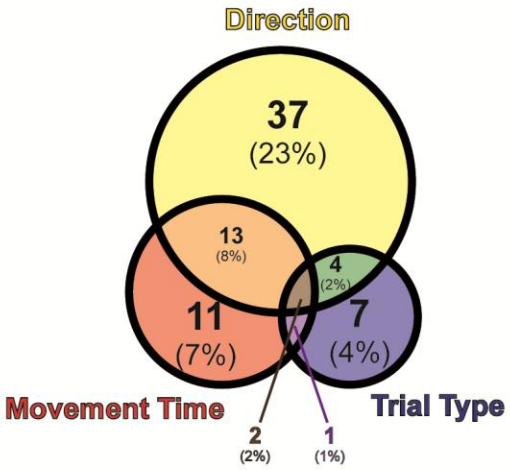

	Direction		Movement Time		Trial Type	
β-valence	+	-	+	-	+	-
	33	23	***22****	6	***12****	3

Figure 2.5: **Multiple regression results for decreasing-type mDS neurons.** Circle sizes represent the relative proportions of neurons showing significant partial r^2 values for the individual task parameters. Top circle encompasses the proportion of neurons that show significant partial r^2 values for the direction parameter. Conventions as above for the movement time (red circle) and trial type (blue circle) parameters. Non-overlapping portions represent the counts (and percentages) of neurons with significant partial r^2 values for one parameter. Overlapping portions denote the counts (and percentages) of single cells that exhibited significant partial r^2 values for two (orange, green, purple) or all three (brown) parameters. The table specifies the counts of neurons significant within a variable that have associated positive ("+") or negative ("-") β-values. As specified by the model, positive β-values indicate greater firing for the contralateral direction (direction), greater firing for slower movement times (movement time), and greater firing for STOP over GO trials (trial type). Asterisks indicate significantly more β-values for one valence within a parameter (binomial sign test; $p < 0.05$).

These results first demonstrate that a low percentage of mDS decreasing-type neurons are modulated by any of the three main task parameters relative to mDS increasing-type neurons (decreasing-type = 46%; increasing-type = 75%; χ^2; $p < 0.01$). However, the decreasing-type mDS neurons that were modulated by individual parameters tended to vary by the direction, as well as the speed, of the response. Importantly, although the number of trial type specific neurons were low, significantly more showed higher firing on STOP trials (positive β-values) which fits with the greater activation of STOP trials in both directions at the population level (Fig. 2.4C).

Modulation of conflict by identity of the previous trial: In pursuit of ascertaining the function of decreasing-type mDS neurons during conflict adaptation, I replotted these neurons where current STOP trials (Fig. 2.6A-C) and GO trials (Fig. 2.6D-F) are respectively split by the identity of the previous trial. Perusal of figure 2.6A shows that the correct direction on STOP trials is not statistically determined until after the SCRT, regardless of the previous trial type (Fig. 2.6A; orange ticks; red ticks). Quantitatively, neither the "stop index" is significantly shifted between gS and sS trials (Fig. 2.6B *right*; Wilcoxon; $p = 0.63$) nor is the direction signal between gS trials and sS trials significantly different (Fig. 2.6C *middle* vs. *right*; Wilcoxon; $p = 0.17$). Therefore, despite a "preparedness" for response inhibition on sS trials (as indicated by the faster movement speeds relative to gS trials; Fig. 2.6A; red vs. orange arrowheads) the neurons largely do not reflect this behavioral change.

Figure 2.6: **Impact on neuronal encoding based on conflict induced by the previous trial in decreasing-type mDS neurons. A)** Population histogram of mDS neurons that decreased significantly below baseline. Activity is aligned to port exit. Blue lines refer to all GO trials. Red lines represent STOP trials preceded by GO trials ('gS'). Orange lines indicate trials where a STOP trial is preceded by a STOP trial ('sS'). Calculation of direction preference remained unchanged from figure 2.4. Tick marks represent 100ms epochs where the preferred direction was significantly different from the nonpreferred direction (t-test; $p < 0.01$) for GO trials (blue), gS trials (red), and sS trials (orange). Although each tick mark signifies statistical difference for a 100ms epoch, tick width is 10ms for the purpose of presentational detail. Arrowheads indicate average movement times (port exit to well entry) for GO trials (blue; 491ms), gS trials (red; 620ms), and sS trials (608ms). Note the longer movement times for gS trials relative to sS trials consistent with reduced preparation for conflict. Vertical dashed lines mark the times of the stop change reaction time (SCRT; 121ms) and the average GO cue onset as measured as the latency from port exit (GO cue; -340ms) for the analyzed sessions. **B)** Indices compare the difference in firing between the three trial types presented in A. Leftmost distribution calculates the differences between gS and GO trials for each cell. The middle distribution marks the difference between sS and GO trials. Rightmost distribution computes the difference between gS and sS trials. **C)** Directional index distributions calculate the difference between the preferred and nonpreferred direction in each neuron during GO trials (*left*), gS trials (*middle*), and sS trials (*right*). **D)** Population histogram of increasing-type mDS neurons is aligned to port exit. All lines represent accurate GO trials that either followed a GO trial ('gG'; dark blue) or followed a STOP trial ('sG'; light blue). Thick lines refer to the preferred direction and thin lines refer to the nonpreferred direction. Tick marks denote the 100ms epochs where the preferred direction significantly differed from the nonpreferred direction (t-test; $p < 0.01$) during gG trials (dark blue) and sG trials (light blue). Arrowheads mark the average movement times for gG trials (dark blue; 492ms) and sG trials (light blue; 487ms). **E)** Distribution calculates the difference between firing on gG versus sG trials. **F)** Directional index distributions calculate the difference between the preferred and nonpreferred direction in each neuron during gG trials (*left*) and sG trials (*right*). Activity for all distributions was taken during the response epoch and significant shifts from zero are determined via Wilcoxon ($p < 0.05$). Asterisks indicate a direct comparison between two distributions is significant (Wilcoxon; $p < 0.05$ corrected for multiple comparisons).

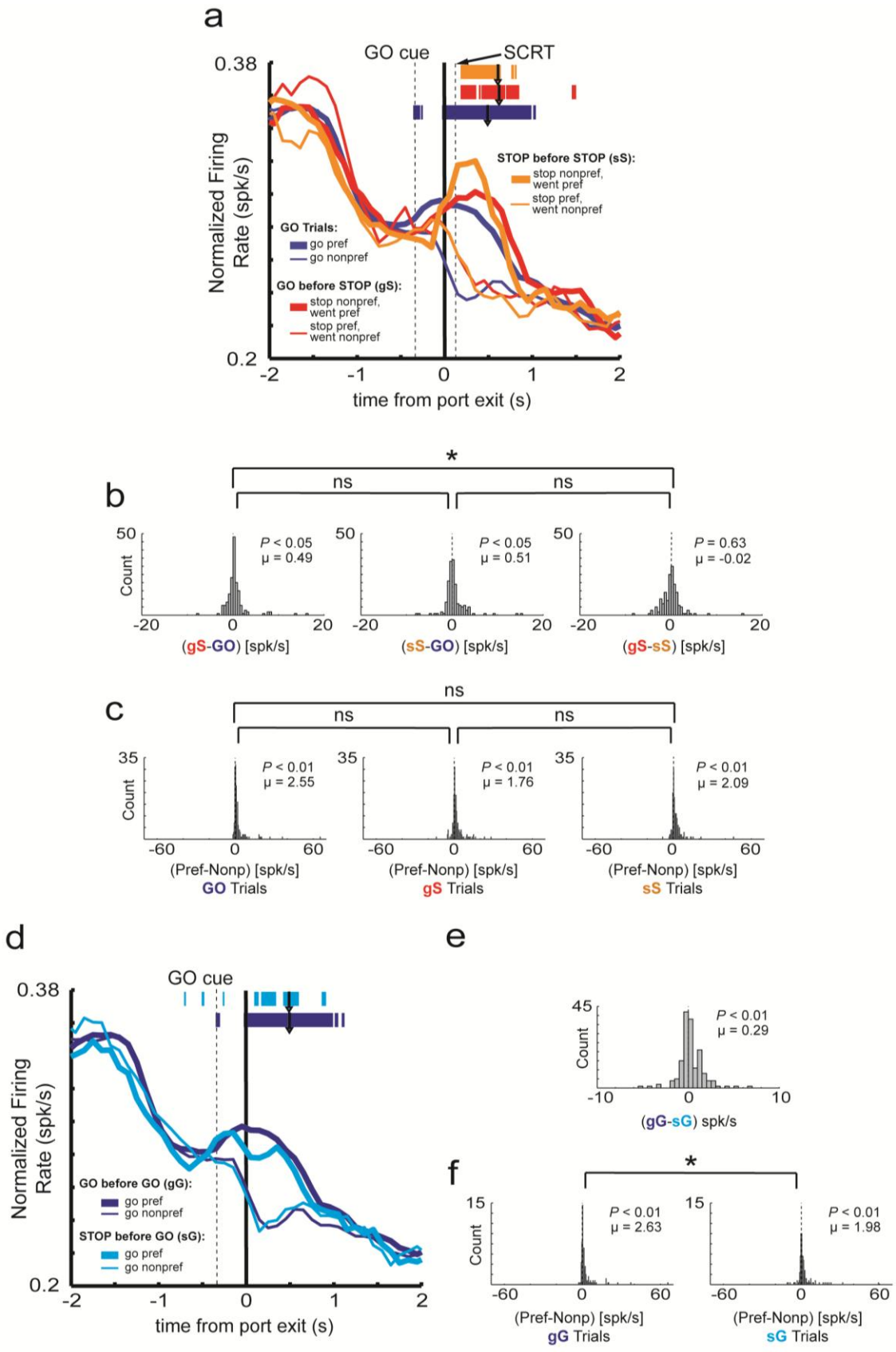
a
GO cue
SCRT
0.38
0.2
Normalized Firing Rate (spk/s)
STOP before STOP (sS):
stop nonpref, went pref
stop pref, went nonpref
GO Trials:
go pref
go nonpref
GO before STOP (gS):
stop nonpref, went pref
stop pref, went nonpref
-2
-1
0
1
2
time from port exit (s)
b
*
ns
ns
50
Count
P < 0.05
μ = 0.49
P < 0.05
μ = 0.51
P = 0.63
μ = -0.02
-20
0
20
(gS-GO) [spk/s]
(sS-GO) [spk/s]
(gS-sS) [spk/s]
c
ns
ns
ns
35
P < 0.01
μ = 2.55
P < 0.01
μ = 1.76
P < 0.01
μ = 2.09
-60
0
60
(Pref-Nonp) [spk/s]
GO Trials
gS Trials
sS Trials
d
GO cue
0.38
0.2
Normalized Firing Rate (spk/s)
GO before GO (gG):
go pref
go nonpref
STOP before GO (sG):
go pref
go nonpref
-2
-1
0
1
2
time from port exit (s)
e
45
Count
P < 0.01
μ = 0.29
-10
0
10
(gG-sG) spk/s
f
*
15
Count
P < 0.01
μ = 2.63
P < 0.01
μ = 1.98
-60
0
60
(Pref-Nonp) [spk/s]
gG Trials
sG Trials

When the current trial was a GO trial, however, previous trial conflict minimally impacted firing on the current trial. That is, activity during the response epoch tended to be higher on gG trials than sG trials at the neuronal level (Fig. 2.6E; Wilcoxon; $p < 0.01$) and the directional index distribution was significantly more positive in gG trials relative to sG trials (Fig. 2.6F; Wilcoxon; $p < 0.05$). Although it is difficult to reconcile this firing difference in the context that it is the only comparison where the previous trial impacts firing on the current trial in mDS, I propose that the mDS decreasing-type activity is simply firing at a higher rate and with greater directional strength when animals are slower (Fig. 2.6D; dark blue vs. light blue arrowheads). This explanation is consistent with the relatively large proportion of mDS decreasing-type neurons that exhibit a significant partial r^2 for the movement time parameter and have a positive valence (greater firing for slower movement speeds; Fig. 2.5; movement time).

Summary: Decreasing-type mDS cells show elevated firing on trials when the response is successfully inhibited/redirected (correct STOP trials) where activity is similar on trials where the initial response is commenced either correctly (GO trials) or in error (STOP errors). Despite this, directional signaling on STOP trials becomes significant after the SCRT suggesting that it is unlikely that this population can signal an inhibition/redirection signal in enough time to *promote* stopping. Therefore this population may play a role in informing downstream neurons of the direction of the terminal response as well as the necessity to change the course of action and/or to refine the motor response.

Though these increasing- and decreasing-type neurons were recorded from the same brain region, in the same rats, and often on the same electrode, there are important

differences between these populations. Firstly, increasing-type neurons are highly directional in the sense that they robustly encode the direction of the intended response prior to its ultimate execution, even when it is incorrect within a short temporal window (early direction miscoding on STOP trials). This is the case to a lesser extent in decreasing-type cells. Additionally, the direction of the response is resolved sooner under STOP trials with reduced conflict (sS trials) in increasing- but not decreasing-type neurons. Accordingly, increasing-type mDS neurons have a large proportion of direction specific neurons (65%) relative to decreasing-type neurons (34%).

Disparate waveform characteristics as a means to define increasing- and decreasing populations

As a means to disclose any cell-type (i.e. projection vs. local interneuron) differences between increasing- and decreasing-type cells, I have plotted the interspike interval (i.e. average duration between action potentials), baseline firing rate, and waveform peak width independently for each type (Fig. 2.7A,B). Although there is no perfect way to classify neurons based on waveform shape or firing characteristics, and attempts to do so often lead to debate and controversy, here I simply ask if neurons that exhibit these different activity patterns might show differential characteristics often used to define the two main types of striatal neurons: fast-spiking interneurons (FSIs) and medium spiny neurons (MSNs) (*77, 81-87*). Additionally, these characteristics are plotted based on the significance of their regression parameter(s). For clarity, FSIs should exhibit reduced inter-spike intervals and greater baseline firing rates relative to MSNs due to the greater functional and physiological capacity of FSIs to fire more frequently.

This concept extends to waveform peak width where FSI waveforms tend to be more condensed, that is, a reduced time from depolarization to repolarization.

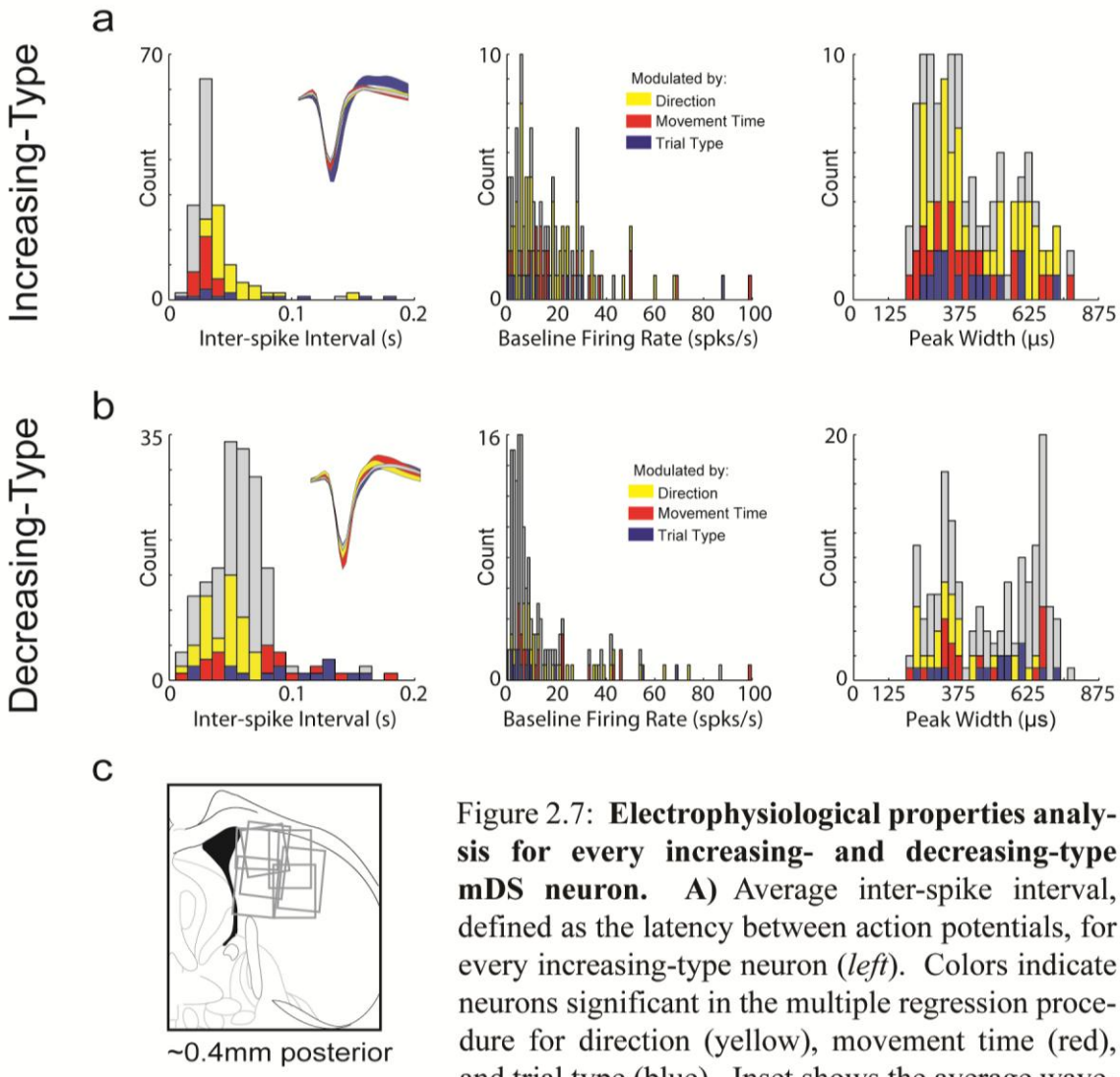

Figure 2.7: **Electrophysiological properties analysis for every increasing- and decreasing-type mDS neuron.** **A)** Average inter-spike interval, defined as the latency between action potentials, for every increasing-type neuron (*left*). Colors indicate neurons significant in the multiple regression procedure for direction (yellow), movement time (red), and trial type (blue). Inset shows the average waveform ±SEM for all increasing-type neurons (gray) and the neurons significant in the multiple regression procedure (colors). Average baseline firing rate (spikes/s) taken from the 1s epoch beginning 2s prior to trial initiation is plotted for each increasing-type cell (*middle*). Average peak width defined as the time between the two highest peaks in the waveform is plotted for every increasing-type cell (*right*). **B)** Conventions as in A for decreasing-type neurons. **C)** Coronal slices approximately 0.4mm posterior to bregma. Each box represents an electrode track, the dorso-ventral extent of which represents the estimated recorded area.

Notably, the division in waveform parameters between increasing- and decreasing-type neurons was not entirely clear cut; there was substantial overlap in all three measures. With that said, it appears from this analysis that, at minimum, a subset of neurons that exhibit different patterns fall into increasing- versus decreasing-type populations. Both the interspike interval (Fig. 2.7A,B *left*) and peak width (Fig 2.7A,B *right*) are significantly greater for decreasing-type neurons suggesting that increasing-type cells have a greater probability of being FSIs whereas decreasing-type cells have a greater likelihood of being MSNs that project downstream. The neurons that are significantly modulated by a specific parameter in the task tend to be evenly distributed across the three measurements. Despite any statistical differences among the recording measurements, the waveform shapes across all neurons are approximately identical (Fig. 2.7A,B *left*; insets).

Chapter Discussion

Functions of mDS

Few studies have examined neuronal activity in the context of response inhibition. Most of the work has been done in oculomotor countermanding tasks and/or have focused on frontal cortical regions (*57, 88-91*). Here, I designed a novel task that allows me to examine neural activity when rats had to inhibit a response that occurred on the large majority of trials and redirect behavior toward the opposite location. During performance of this task, rats were less accurate and slower to respond on STOP trials.

Slower movement speeds resulted from cancellation of an already initiated response (i.e. STOP cue was only signaled after response initiation).

Pharmacological and lesion studies have implicated mDS in the control of behavior during performance of stop signal tasks. Although rats with mDS lesions needed earlier warnings to be able to adequately inhibit movement as compared to controls, they were also slower on GO trials, suggesting that they not only had a deficit in response inhibition but also in general behavioral control (*5*). More recently, it has been suggested that dopamine in mDS may act to balance response inhibition independent of behavioral activation. Manipulation of striatal D1 and D2 receptors, commonly associated with neurons that give rise to the direct and indirect pathways, influenced the imposition and speed of inhibition during stop signal performance (*59*). These results, combined with the electrophysiological results reported here, suggest than signaling of movement in mDS is complicated and that the ultimate output depends on the integration of several signals that promote or inhibit behavior as discussed below.

Miscoding of direction and inhibition failure

Given that the mDS is the area functionally closest to the motor system, it is unsurprising that mDS exhibits a large directional bias (preferred relative to nonpreferred direction) toward one direction (70% contralateral preferring cells). As reviewed above, significant directional signaling on GO trials occurs early (i.e. before unpoke) and remains strong throughout the response in increasing-type mDS neurons (Fig. 2.1A; blue ticks). Since directionality on GO trials becomes significantly distinct before port

unpoke, this provides heightened encoding of the incorrect direction on STOP trials (becomes significant at 30ms before unpoke; Fig. 2.1A; pink ticks). Without sufficient correction (neuronally and behaviorally), the animal will continue to approach the incorrect direction on STOP trials as shown in the STOP error encoding. After a short delay, mDS neurons discontinue encoding the wrong direction and, consistent with the aforementioned role of mDS in signaling the direction of the response on STOP trials, neurons are directionally distinct prior to fluid well entry (Fig. 2.1A; red ticks). Critically, the temporal delay in mDS neurons encoding the ultimately correct direction is too long for this brain region to have a causal impact on inhibiting the behavior. Specifically, the correct direction is signaled after the SCRT. Therefore, mDS neurons appear to be tied to the response direction, but not the ability to inhibit the incorrect direction when necessary. This suggests that when there was a miscoding of direction by these neurons, rats were unable to correctly inhibit responding.

On one hand, these neurons might be driving behavior through what has been described as the "direct" pathway in which activity from mDS directly modulates activity in substantia nigra pars reticulata (SNr), which is the main output structure in basal ganglia (*42, 43, 55, 92-97*)(Fig. 1.1). Increased firing of mDS neurons would inhibit firing in these areas which would release downstream structures (e.g. superior colliculus and other motor outputs) from GABAergic inhibition to promote behavior (*98, 99*).

On the other hand, these neurons might impact local circuits before influencing more motor-related downstream regions. Many of these neurons shared characteristics common to interneurons, having shorter waveforms and lower inter-spike intervals (*77, 83*)(Fig. 2.7A). Further, their activity patterns were similar to what has been described

previously for interneurons in lateral parts of dorsal striatum, firing more strongly for contralateral action at the time of the choice (*83*). Interneurons are thought to shape firing of MSNs in mDS through feed-forward inhibition (*83, 87, 100*). Thus, activity of these neurons might also shape behavior by impacting local circuits that then project downstream. Regardless of how these neurons ultimately impact behavior, their miscoding of direction was clearly related to failures in response inhibition.

Inhibition of movement

Decreasing-type neurons in mDS *appear* to better serve an inhibitory function. Many of these neurons increased firing on correctly performed STOP trials when the rat had to inhibit and redirect its response. However, very few of these neurons fell under the "inhibitory signal" hypothesis (Fig. 1.3C; significant partial r^2 for trial type; Fig. 2.5; 9%) and the correct direction was not significantly encoded until after the SCRT on STOP trials. If these neurons are not causally contributing to the inhibition of a response, how can one explain the significant difference between STOP and GO trials in both directions (Fig. 2.4C *left*, *right*)? Given the proximity of mDS to the motor system and the known function of mDS in coordinating the correct muscles necessary for a movement (*78*), I propose that these neurons are refining the newly initiated motor response on correct STOP trials. Evidence for this inference lies in the observation that firing patterns are similar between successful GO trials (Fig. 2.4A; blue lines) and errant STOP trials (Fig. 2.4A; dashed red lines) and the comparable firing rates within a direction once the response was completed (Fig. 2.4B). Thus, unlike the increasing-type

neurons, decreasing-type mDS neurons appear to inform downstream regions of dramatic changes in spatial response properties necessary for correct STOP trial performance.

Consistent with this hypothesis, these neurons shared firing and waveform characteristics that have been used to categorize neurons as MSNs. MSNs are thought to project out of the striatum to impact behavior via direct and indirect pathways through basal ganglia (*42, 43, 55, 92-97, 101-104*). Based on the relationship that these neurons have with movement speed and errant responses, I suspect that they must be part of the indirect pathway which projects to globus pallidus external (GPe) then to subthalamic nucleus (STN) before impacting SNr and motor outputs (Fig. 1.1). Since GPe and STN are inhibitory and excitatory, respectively, excitation of mDS would increase activity in SNr, whereas inhibition (GABA) would reduce it. Thus, increased activity in striatum would indirectly increase activity in SNr, which would subsequently inhibit downstream motor structures critical for controlling body movements in rats such as superior colliculus (*98*).

Control of behavior

Patterns observed here, in mDS, resemble firing in primate oculomotor regions such as the frontal eye field (FEF) during performance of a countermanding task in which monkeys were signaled to make a saccade to the periphery by brief illumination of a visual stimulus (*56, 57, 91, 105, 106*). During performance of this task, on 20% of trials, a stop signal (re-illumination of the fixation point) instructed the monkey to not make the instructed saccade and to remain fixating at a central location.

They found, as I have here, neurons related to generating and inhibiting behavior. Activity of many neurons was correlated with faster eye movements contralateral to the recording site. Other neurons fired more strongly on stop trials when the monkey had to maintain fixation. From these studies it has been suggested that generation of movement results from the activity of motor-related neurons reaching some activation threshold at which point a movement is generated. The response that is made depends on what neurons cross threshold first. This process has been described as a race between two (or more) competing movement signals (*107*). In the oculomotor example, if the firing of neurons that generate eye movements crossed threshold before the competing signal to maintain fixation, the eye movement was erroneously generated. Models such as the race model could explain the relationship between cells that promote responses and those that globally inhibit behavior in my task. That is, if a cell reaches threshold before the cells that shut it down, then the response would be erroneously generated.

In conclusion, I show activity in mDS is related to both the promotion and refinement of spatial responses. Miscoding of directional information was correlated with poor performance. Against this backdrop I can better address what happens in several mental disorders where the ability to inhibit behavior is impaired. Deficits observed in certain disorders or after lesions might reflect abnormalities in one or both of the increasing- and decreasing-type populations. However, as previously mentioned, my results do not support a causal function for mDS neurons to inhibit an action. That is, an upstream region must provide a timely warning signal to mDS in order for mDS to alter its activity and reorient the animal toward the appropriate destination.

Chapter 6: An inhibitory hypothesis for lateral orbitofrontal neurons

I have shown that mDS neurons are responsible for the encoding of direction and/or motor refinement. Although the directional signal in increasing-type mDS neurons is initially miscoded, and ultimately weaker on STOP trials, accurate representations of direction do emerge. It has been shown that optogenetic activation of dorsal striatal medium spiny neurons can alter basal ganglia firing and cause generation or suppression of movements/actions (*108, 109*). While mDS and downstream basal ganglia regions are more closely tied to motor output, information from afferent cortical regions has been hypothesized to play a role in alerting mDS neurons of the necessity to cancel or redirect an ongoing movement within a short temporal window. One candidate region for this function is lOFC based on its role in executive function (*110-112*).

Research has suggested that OFC acts as a critical frontal structure that informs downstream regions of the need to suppress a prepotent behavior. Evidence for this arose as damage to OFC was shown to promote disinhibition operationalized as perseveration during extinction tasks (*113*), reduced reversal ability (*51, 52, 114-123*), impulsive choice in both delay discounting (*124*) and stop tasks (*125, 126*), and impaired gambling behavior (*127, 128*). Many of these studies suggest that OFC provides a type of inhibitory signal that overrides or dampens behavioral responding when such control is necessary for accurate performance. Indeed, imaging studies have shown heightened BOLD signal generating from OFC on trials that require subjects to inhibit behavior (*18, 126, 129-131*). Based on its anatomical connections to mDS (*30, 132*) and the previous literature linking OFC with response inhibition, OFC appears to be a logical brain region to explore response inhibition preformed in my stop signal task.

Over the past decade, the theory that inhibitory function is causally linked to OFC has lost some ground due to data revealing that OFC lesioned animals can exhibit certain forms of inhibitory restraint as well as healthy control animals (*53, 133-135*). For example, rats with OFC lesions can discontinue responding to stimuli that unpredictably lead to punishment during discrimination learning (*123*) or suddenly predict no reward during set-shifting (*117, 136, 137*).

With the abundance of attention OFC has received during the past few decades, it comes as a surprise that there have been few recordings from OFC during performance of a task that independently probes response inhibition. Most tasks vary both the need to inhibit behavior and aspects related to expected outcomes. To address these issues I recorded from single lOFC neurons in my rodent variant of the stop signal task (*1*).

I analyzed single cell recording data from 548 neurons in lOFC of five rats over 113 sessions (recording locations in figure 3.7C). Neural analyses will be identical to the previous mDS recording experiment. Briefly, I found that lOFC increasing-type cells tend to signal the direction of the ultimate response and this signal was able to distinguish the correct direction on STOP trials prior to the SCRT placing lOFC in a position to guide spatial response behavior. Additionally, the strength of this direction signal was significantly enhanced on STOP trials where preparedness was high (sS trials) providing a conflict adaptation signal useful for response inhibition. Although there were many decreasing-type neurons, these cells appear to be driven mainly by the speed of responding (movement time) as opposed to flexible inhibitory signaling.

As in the mDS section described above, to qualify activity over the increasing-type neurons in lOFC, I constructed population histograms that represent the average

firing over time during the execution of a trial. I found 209 neurons (38%) that significantly increased activity during the response epoch relative to baseline.

Increasing-type Cells

Population Activity: As described in previous literature, increasing-type neurons in rat lOFC are spatially selective (*62, 63, 65*), firing more strongly for movements made in one direction over another. On correct GO trials (blue), activity differentiated between the preferred (thick) and nonpreferred (thin) directions before withdrawal from the nose port. This can be observed via the tick marks in figure 3.1A that represent statistically significant (t-test; $p < 0.01$) directional activity (preferred vs. nonpreferred directions) in 100ms windows that slide every 10ms. This direction specificity on GO trials (blue ticks) shows that the correct direction was encoded between GO cue and port exit. On correct STOP trials, the correct direction was encoded after the rat exited the nose-port as can be observed by the red tick marks. On STOP trials, activity became directionally significant after the onset of the STOP cue and *before* the SCRT suggesting that these neurons can have a causal impact on response inhibition during STOP trials.

Figure 3.1: **Direction and trial type encoding of increasing-type lOFC neurons. A-B)** Average firing rate (spikes/s) over time aligned on port exit (A) and well entry (B) for all lOFC neurons that fired more strongly during the 'response epoch' (port exit to well entry) relative to baseline (1s epoch beginning 2s prior to trial initiation). The time necessary to inhibit a response (stop change reaction time; SCRT) is defined as the difference between STOP trial movement time and GO trial movement time. SCRT is marked as the vertical dotted line labeled 'SCRT' at 205ms. 'GO cue' and its associated vertical dashed line indicates the average onset of the GO cue as measured by the latency from port exit (-339ms). Blue lines refer to GO trials, red lines refer to STOP trials, and dashed lines refer to errant trials (incorrect direction). Due to the heterogeneous direction specificity of individual cells, each cell was characterized as having a preferred direction and a nonpreferred direction. This preference was determined by asking which direction (contra- or ipsilateral to the recorded hemisphere) elicited the highest firing rate during the response epoch for each cell. Therefore, as defined by the analysis, preferred direction (thick lines) is always higher than the nonpreferred direction (thin lines) during the response epoch. Tick marks represent significant p-values in temporal space after preferred direction was compared to nonpreferred direction in the population for GO trials (blue ticks) and STOP trials (red ticks) in 100ms epochs that slid by 10ms after each iteration (t-test; $p < 0.01$). Although each tick mark signifies statistical difference for a 100ms epoch, tick width is 10ms for the purpose of presentational detail. Arrowheads denote the average movement time (well entry) during GO trials (blue arrowhead = 558ms) and STOP trials (red arrowhead = 763ms). GO cue, SCRT, and movement times (arrowheads) are variable values based on the behavior of the animals in the analyzed sessions. These values (except SCRT) are estimates with variance and cannot be treated as constants relative to port exit. **C)** Stop indices for preferred (*left*) and nonpreferred (*right*) directions. Stop indices are calculated by taking the activity during the response epoch from STOP trials, subtracting activity during the response epoch on GO trials, and dividing it by the sum of the two ((STOP-GO/(STOP+GO)) in each direction for every cell. Significant shifts from zero (as calculated by Wilcoxon) denote that neuronal activity is significantly different between STOP and GO trials in a given direction. **D)** Directional index distributions defined as activity during the response epoch in the preferred direction minus activity during the response epoch in the nonpreferred direction divided by the sum ((preferred-nonpreferred)/(preferred+nonpreferred)) in every cell. These calculations are specific to GO trials (*left*), STOP trials (*middle*), and STOP errors (*right*). Significant shifts from zero (as calculated by Wilcoxon) signify that activity is greater in one direction than the other at the neuronal level. Asterisks in C and D indicate that two distributions are significantly different via Wilcoxon.

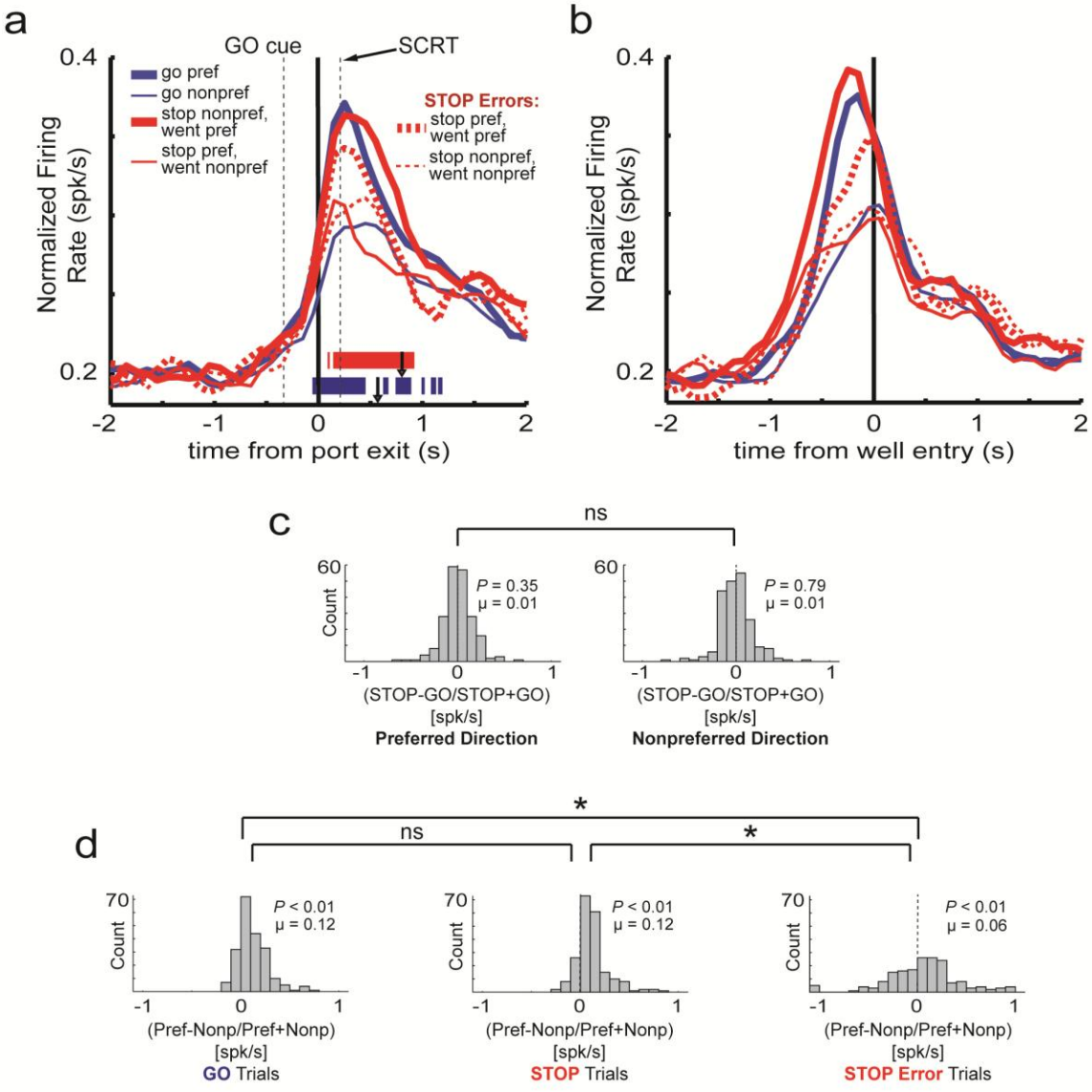
a
GO cue
SCRT
0.4
0.2
Normalized Firing Rate (spk/s)
go pref
go nonpref
stop nonpref, went pref
stop pref, went nonpref
STOP Errors:
stop pref, went pref
stop nonpref, went nonpref
-2
-1
0
1
2
time from port exit (s)
b
0.4
0.2
Normalized Firing Rate (spk/s)
-2
-1
0
1
2
time from well entry (s)
c
ns
60
Count
P = 0.35
μ = 0.01
-1
0
1
(STOP-GO/STOP+GO)
[spk/s]
Preferred Direction
60
P = 0.79
μ = 0.01
-1
0
1
(STOP-GO/STOP+GO)
[spk/s]
Nonpreferred Direction
d
*
ns
*
70
Count
P < 0.01
μ = 0.12
-1
0
1
(Pref-Nonp/Pref+Nonp)
[spk/s]
GO Trials
70
P < 0.01
μ = 0.12
-1
0
1
(Pref-Nonp/Pref+Nonp)
[spk/s]
STOP Trials
70
P < 0.01
μ = 0.06
-1
0
1
(Pref-Nonp/Pref+Nonp)
[spk/s]
STOP Error Trials

Stop index: Despite temporal differences in significant direction encoding between STOP and GO trials, activity throughout the response was not different between STOP and GO trials in either the preferred or nonpreferred direction (Fig. 3.1C *left*, *right*; Wilcoxon; ps > 0.35) and the two distributions were not different from one another (Fig. 3.1C *left* vs. *right*; Wilcoxon; p = 0.80).

Directional index: Although I observed behavioral evidence of response conflict on STOP trials and directional signals took longer to develop, the strength of the directional signal during the entire response epoch was not significantly weaker on STOP relative to GO trials. This is illustrated in figure 3.1C *left* and *middle* which plot the distributions of directional indices for both correct GO and STOP trials during the response epoch. The same analysis performed on data from mDS increasing-type neurons illustrated weaker directional signals on STOP trials (Fig 2.1D). In lOFC, the directional index distribution for both GO and STOP trial types was shifted significantly above zero (Fig. 3.1D *left*, *middle*; Wilcoxon; ps < 0.01) but there was no difference between the two distributions (Fig. 3.1D *left* vs. *middle*; Wilcoxon; p = 0.84), suggesting that even though the directional signal took longer to develop under STOP trials, it was resolved before the completion of the response as is evident in the neural activity aligned to well entry in figure 3.1B. On STOP error trials, the distribution of directional indices was significantly lower compared to both correct STOP trials (Fig. 3.1D *middle* vs. *right*; Wilcoxon; p < 0.05) and correct GO trials (Fig. 3.1D *left* vs. *right*; Wilcoxon; p < 0.05). Therefore, on STOP error trials (Fig. 3.1A,B; dashed lines), the directional signal during the response epoch is reduced implying that adequate encoding of direction in lOFC is necessary for correct performance.

Despite the bias in lOFC firing toward one response direction over another, the incorrect direction is never miscoded on STOP trials (Fig. 3.1A) as it was in mDS (Fig. 2.1A; pink ticks). Due to this absence, firing in lOFC increasing-type neurons was able to discern between the incorrect and newly correct response direction on STOP trials within the behavioral time window necessary for the brain to recruit inhibitory machinery (SCRT). This is intriguing because it suggests that in addition to "inhibitory signaling" (Fig. 1.3C), "directional signal" categorized neurons (Fig. 1.3A) can be also be important for response inhibition because it is necessary to resolve the response conflict, an idea never previously proposed.

Multiple regression analysis: Increasing-type lOFC neurons appear to be highly directional regardless of trial type but single cell variability is not captured when averaging neurons over population histograms. Therefore to determine if neuronal firing correlates with movement speed, direction, and/or type of trial at the single-cell level, I performed the multiple regression procedure identical to the one used in the mDS analysis. The size of the top circle in figure 3.2 indicates the proportion of increasing-type lOFC cells that were significantly modulated by the direction of the response when variance for movement time and trial type parameters was accounted for (partial r^2). Thirty seven percent of increasing-type neurons (n = 78) were significantly modulated by direction (Fig. 3.2; direction) and of these 78 neurons, 48 β-values of the direction parameter were negative (greater firing for the ipsilateral direction) whereas 30 were positive (binomial sign test; p = 0.05). Forty-nine cells (23%) were significantly modulated by movement time (Fig. 3.2; movement time). Of these 49, equal numbers showed positive and negative β-values for the movement time parameter (20 vs. 29;

binomial sign test; $p = 0.25$). In 26 neurons, both the direction and movement speed parameters showed significant partial r^2 values (Fig. 3.2; orange + brown). Thus, consistent with the population analysis described in the previous sub-section, lOFC increasing-type neurons encoded both response direction and movement speed.

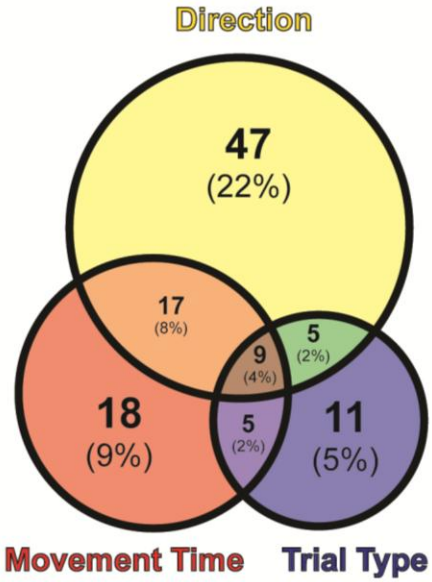

	Direction		Movement Time		Trial Type	
β-valence	+	-	+	-	+	-
	30	48	20	29	19	11

Figure 3.2: **Multiple regression results for increasing-type lOFC neurons.** Circle sizes represent the relative proportions of neurons showing significant partial r^2 values for the individual task parameters. Top circle encompasses the proportion of neurons that show significant partial r^2 values for the direction parameter. Conventions as above for the movement time (red circle) and trial type (blue circle) parameters. Non-overlapping portions represent the counts (and percentages) of neurons with significant partial r^2 values for one parameter. Overlapping portions denote the counts (and percentages) of single cells that exhibited significant partial r^2 values for two (orange, green, purple) or all three (brown) parameters. The table specifies the counts of neurons significant within a variable that have associated positive ("+") or negative ("-") β-values. As specified by the model, positive β-values indicate greater firing for the contralateral direction (direction), greater firing for slower movement times (movement time), and greater firing for STOP over GO trials (trial type). Asterisks indicate significantly more β-values for one valence within a parameter (binomial sign test; $p < 0.05$).

Clearly signals in lOFC are related to motor output and response direction. However, from these results it appears that lOFC does not encode a pure "inhibitory signal" which one might predict to be independent of response direction (*138*). At the single cell level, 30 neurons (14%) showed significant partial r^2 values in the regression procedure for the trial type variable (Fig. 3.2; trial type), but only 11 of those neurons, 5% of the population of increasing-type neurons, showed a significant partial r^2 independent of significant modulation by direction and movement speed factors; a number not significantly different from chance ($\chi^2 = 0.03.$; $p = 0.86$). The main caveat to these results is that the conclusions are based on activity throughout the entirety of the movement (response epoch). mDS neurons, direct projection recipients of lOFC, are closer to the motor system and can arbitrate between the two response directions, but it did not have the capability to correct response directions prior to the SCRT. lOFC neurons provide this temporally precise signal.

Modulation of conflict by identity of the previous trial: Conflict adaptation, the phenomenon defined as the readiness to resolve conflict under recent conflicting conditions, has been found in a number of brain regions including anterior cingulate cortex (*67*), dorsolateral prefrontal cortex (*139*), and orbitofrontal cortex (*69*), all of which are cortical regions. Because of this, minimal modulation based on the previous trial was expected in the sub-cortical mDS. However, lOFC may provide a neural substrate for conflict adaptation.

Figure 3.3: **Impact on neuronal encoding based on conflict induced by the previous trial in increasing-type lOFC neurons. A)** Population histogram of lOFC neurons that increased significantly above baseline. Activity is aligned to port exit. Blue lines refer to all GO trials. Red lines represent STOP trials preceded by GO trials ('gS'). Orange lines indicate trials where a STOP trial is preceded by a STOP trial ('sS'). Calculation of direction preference remained unchanged from figure 3.1. Tick marks represent 100ms epochs where the preferred direction was significantly different from the nonpreferred direction (t-test; $p < 0.01$) for GO trials (blue), gS trials (red), and sS trials (orange). Although each tick mark signifies statistical difference for a 100ms epoch, tick width is 10ms for the purpose of presentational detail. Arrowheads indicate average movement times (port exit to well entry) for GO trials (blue; 570ms), gS trials (red; 804ms), and sS trials (770ms). Note the longer movement times for gS trials relative to sS trials consistent with reduced preparation for conflict. Vertical dashed lines mark the times of the stop change reaction time (SCRT; 205ms) and the average GO cue onset as measured as the latency from port exit (GO cue; -339ms) for the analyzed sessions. **B)** Indices compare the difference in firing between the three trial types presented in A. Leftmost distribution calculates the differences between gS and GO trials for each cell. The middle distribution marks the difference between sS and GO trials. Rightmost distribution computes the difference between gS and sS trials. **C)** Directional index distributions calculate the difference between the preferred and nonpreferred direction in each neuron during GO trials (*left*), gS trials (*middle*), and sS trials (*right*). **D)** Population histogram of increasing-type mDS neurons is aligned to port exit. All lines represent accurate GO trials that either followed a GO trial ('gG'; dark blue) or followed a STOP trial ('sG'; light blue). Thick lines refer to the preferred direction and thin lines refer to the nonpreferred direction. Tick marks denote the 100ms epochs where the preferred direction significantly differed from the nonpreferred direction (t-test; $p < 0.01$) during gG trials (dark blue) and sG trials (light blue). Arrowheads mark the average movement times for gG trials (dark blue; 568ms) and sG trials (light blue; 580ms). **E)** Distribution calculates the difference between firing on gG versus sG trials. **F)** Directional index distributions calculate the difference between the preferred and nonpreferred direction in each neuron during gG trials (*left*) and sG trials (*right*). Activity for all distributions was taken during the response epoch and significant shifts from zero are determined via Wilcoxon ($p < 0.05$). Asterisks indicate a direct comparison between two distributions is significant (Wilcoxon; $p < 0.05$ corrected for multiple comparisons).

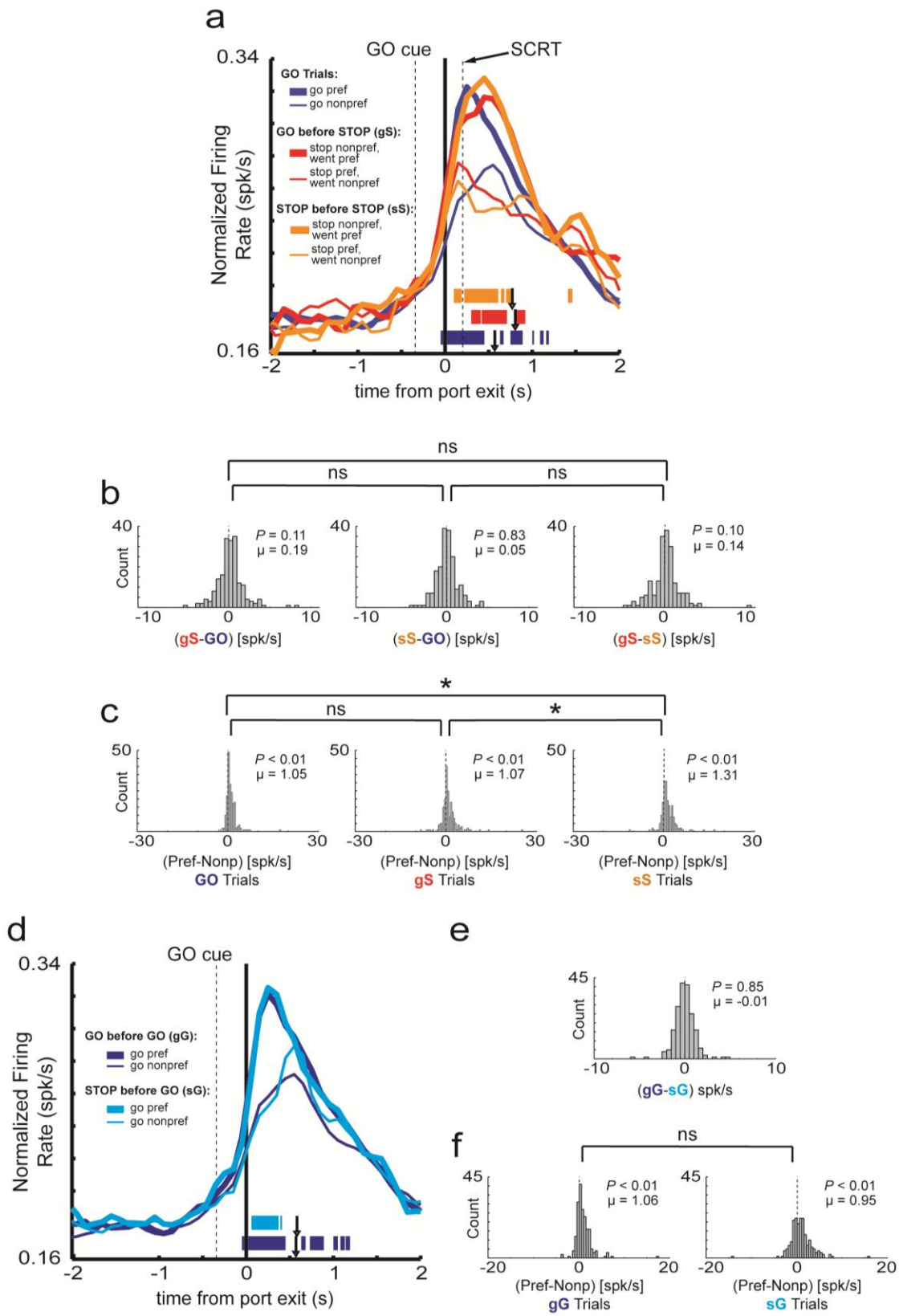
a
GO cue
SCRT
0.34
0.16
GO Trials:
go pref
go nonpref
GO before STOP (gS):
stop nonpref, went pref
stop pref, went nonpref
STOP before STOP (sS):
stop nonpref, went pref
stop pref, went nonpref
Normalized Firing Rate (spk/s)
time from port exit (s)
b
ns
ns
ns
Count
P = 0.11
μ = 0.19
(gS-GO) [spk/s]
P = 0.83
μ = 0.05
(sS-GO) [spk/s]
P = 0.10
μ = 0.14
(gS-sS) [spk/s]
c
*
ns
*
P < 0.01
μ = 1.05
(Pref-Nonp) [spk/s]
GO Trials
P < 0.01
μ = 1.07
(Pref-Nonp) [spk/s]
gS Trials
P < 0.01
μ = 1.31
(Pref-Nonp) [spk/s]
sS Trials
d
GO cue
GO before GO (gG):
go pref
go nonpref
STOP before GO (sG):
go pref
go nonpref
Normalized Firing Rate (spk/s)
time from port exit (s)
e
P = 0.85
μ = -0.01
(gG-sG) spk/s
f
ns
P < 0.01
μ = 1.06
(Pref-Nonp) [spk/s]
gG Trials
P < 0.01
μ = 0.95
(Pref-Nonp) [spk/s]
sG Trials

So far I have shown that directional signals on STOP trials are fairly resilient to the competition between two conflicting responses through the entirety of the response, demonstrating the lOFC is accurately signaling the correct direction during response inhibition. Here, I ask if directional tuning in lOFC might actually be enhanced during conflict adaption, when executive control is more engaged due to trial sequence. To address this issue, I plotted average firing of increasing-type cells broken down by STOP trials that were preceded by either a GO ("gS"; Fig. 3.3A; red lines) or a STOP ("sS"; Fig. 3.3A; orange lines) trial. Intriguingly, direction signals became significantly distinct prior to the SCRT only on sS trials (Fig. 3.3A; orange ticks). When GO trials, gS trials, and sS trials were compared directly, none of the average distributions were significantly shifted or different from one another (Fig. 3.3B; Wilcoxon; ps > 0.10). Quite strikingly however, direction signals on sS trials were larger than on gS trials. This observation is statistically validated in figure 3.3C which shows that the distribution of direction indices was greater on sS trials relative to gS trials (Fig. 3.3C *middle* vs. *right*; Wilcoxon; $p < 0.01$) *and* relative to directional signals on all correct GO trials (Fig. 3.3C *left* vs. *right*; Wilcoxon; $p < 0.05$).

Importantly, this effect was dependent on the current trial being a STOP trial, suggesting that directional signals were enhanced only when it was needed to inhibit and redirect behavior. This is illustrated in figure 3.3D-F which examines the impact of the previous trial on GO trials. Neither direct gG versus sG comparisons nor directional signals on correct GO trials were significantly modulated by the identity of the previous trial (Fig 3.3E; Wilcoxon; $p = 0.85$; Fig 3.3F *left* vs. *right*; Wilcoxon; $p = 0.36$).

Summary: I found that activity in lOFC increasing-type neurons does not appear to carry a pure "inhibitory signal." Population firing in lOFC was not significantly stronger under STOP trials, nor were there a preponderance of single neurons that fired significantly more strongly on STOP over GO trials. Instead I found that lOFC neurons exhibited directional tuning as previously reported (*62, 63, 65*), and that directional selectivity was enhanced by the need to suppress and redirect behavior during sequences of increased conflict resolution. This interpretation is broadly consistent with recent work in monkeys suggesting that OFC is involved in reconciling cognitive signals during conflict adaptation (*69*).

All of this suggests that OFC is more involved in executive functions that control and enhance response selectivity when unwanted movements are suppressed and redirected. I suspect that this signal is critical for resolving conflict observed in neural signals downstream of lOFC, such as mDS (*1*). Dysfunction of these correlates can explain why interference of OFC function impairs response inhibition. Although the most obvious interpretation is that OFC provides some sort of inhibition signal, my results suggest that lOFC plays an important role in conflict induced executive control (*69*). Such a function might be critical for performance on several tasks that require inhibition and are impaired after OFC lesions, including reversal learning (*140*), delay discounting (*124*), extinction (*141*), delayed alternation (*142*) and devaluation (*143*).

Decreasing-type cells

Population Activity: Of the 548 neurons recorded in lOFC, 131 (24%) fired significantly less during the response epoch compared to baseline.

Figure 3.4: **Direction and trial type encoding of decreasing-type lOFC neurons. A-B)** Average firing rate (spikes/s) over time aligned on port exit (A) and well entry (B) for all lOFC neurons that fired less strongly during the 'response epoch' (port exit to well entry) relative to baseline (1s epoch beginning 2s prior to trial initiation). The time necessary to inhibit a response (stop change reaction time; SCRT) is defined as the difference between STOP trial movement time and GO trial movement time. SCRT is marked as the vertical dotted line labeled 'SCRT' at 204ms. 'GO cue' and its associated vertical dashed line indicates the average onset of the GO cue as measured by the latency from port exit (-341ms). Blue lines refer to GO trials, red lines refer to STOP trials, and dashed lines refer to errant trials (incorrect direction). Due to the heterogeneous direction specificity of individual cells, each cell was characterized as having a preferred direction and a nonpreferred direction. This preference was determined by asking which direction (contra- or ipsilateral to the recorded hemisphere) elicited the highest firing rate during the response epoch for each cell. Therefore, as defined by the analysis, preferred direction (thick lines) is always higher than the nonpreferred direction (thin lines) during the response epoch. Tick marks represent significant p-values in temporal space after preferred direction was compared to nonpreferred direction in the population for GO trials (blue ticks) and STOP trials (red ticks) in 100ms epochs that slid by 10ms after each iteration (t-test; $p < 0.01$). Although each tick mark signifies statistical difference for a 100ms epoch, tick width is 10ms for the purpose of presentational detail. Arrowheads denote the average movement time (well entry) during GO trials (blue arrowhead = 569ms) and STOP trials (red arrowhead = 773ms). GO cue, SCRT, and movement times (arrowheads) are variable values based on the behavior of the animals in the analyzed sessions. These values (except SCRT) are estimates with variance and cannot be treated as constants relative to port exit. **C)** Stop indices for preferred (*left*) and nonpreferred (*right*) directions. Stop indices are calculated by taking the activity during the response epoch from STOP trials, subtracting activity during the response epoch on GO trials, and dividing it by the sum of the two ((STOP-GO/(STOP+GO)) in each direction for every cell. Significant shifts from zero (as calculated by Wilcoxon) denote that neuronal activity is significantly different between STOP and GO trials in a given direction. **D)** Directional index distributions defined as activity during the response epoch in the preferred direction minus activity during the response epoch in the nonpreferred direction divided by the sum ((preferred-nonpreferred)/(preferred+nonpreferred)) in every cell. These calculations are specific to GO trials (*left*), STOP trials (*middle*), and STOP errors (*right*). Significant shifts from zero (as calculated by Wilcoxon) signify that activity is greater in one direction than the other at the neuronal level. Asterisks in C and D indicate that two distributions are significantly different via Wilcoxon.

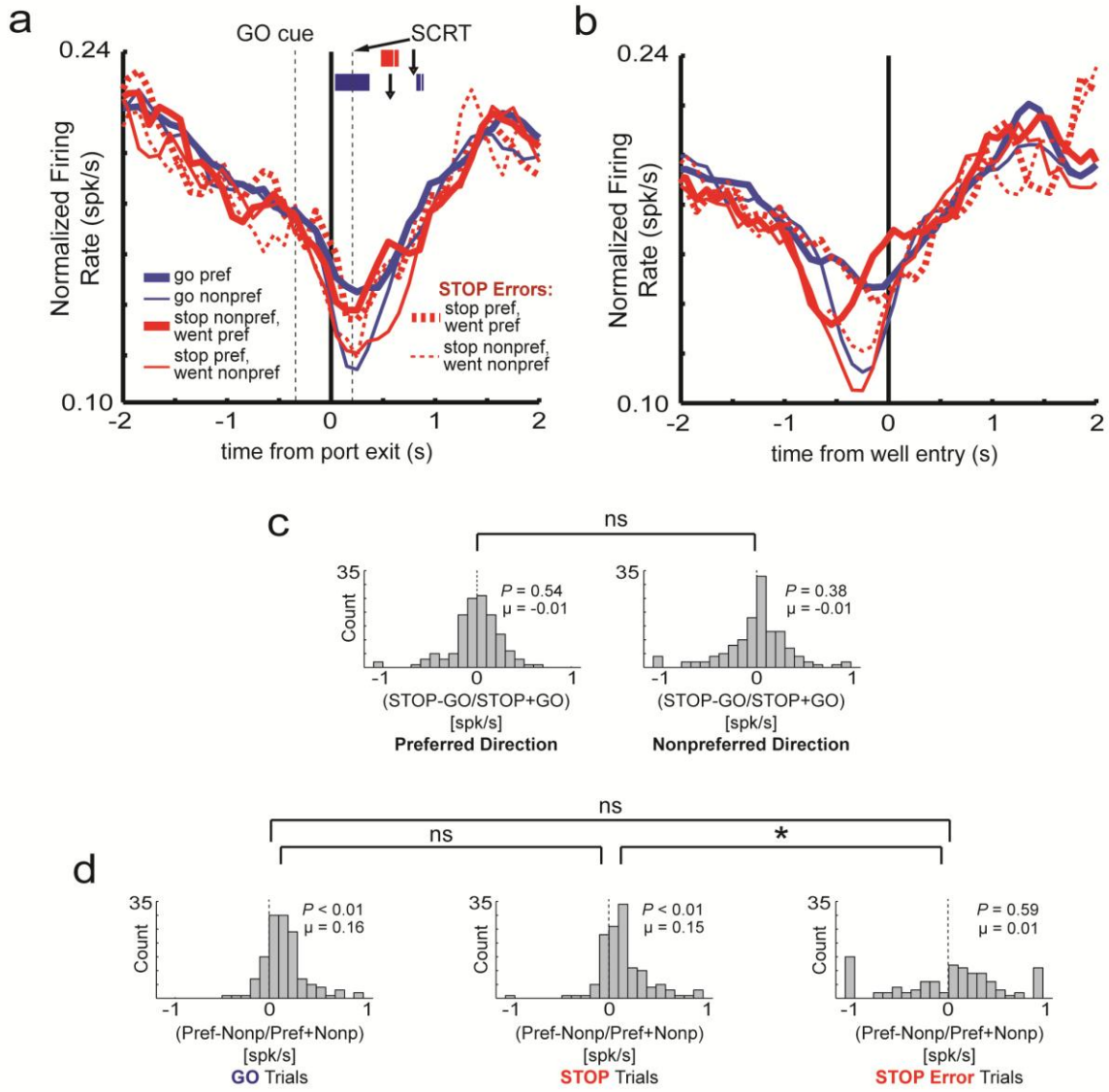
a
GO cue
SCRT
0.24
0.10
Normalized Firing Rate (spk/s)
go pref
go nonpref
stop nonpref, went pref
stop pref, went nonpref
STOP Errors:
stop pref, went pref
stop nonpref, went nonpref
-2
-1
0
1
2
time from port exit (s)
b
0.24
0.10
Normalized Firing Rate (spk/s)
-2
-1
0
1
2
time from well entry (s)
c
ns
35
Count
P = 0.54
μ = -0.01
-1
0
1
(STOP-GO/STOP+GO)
[spk/s]
Preferred Direction
35
P = 0.38
μ = -0.01
-1
0
1
(STOP-GO/STOP+GO)
[spk/s]
Nonpreferred Direction
d
ns
ns
*
35
Count
P < 0.01
μ = 0.16
-1
0
1
(Pref-Nonp/Pref+Nonp)
[spk/s]
GO Trials
35
P < 0.01
μ = 0.15
-1
0
1
(Pref-Nonp/Pref+Nonp)
[spk/s]
STOP Trials
35
P = 0.59
μ = 0.01
-1
0
1
(Pref-Nonp/Pref+Nonp)
[spk/s]
STOP Error Trials

Population firing for decreasing-type neurons exhibited subtle modulation by response direction (i.e. preferred vs. nonpreferred) with little modulation by trial type (Fig. 3.4A,B; solid lines). The **stop index** was not significantly shifted in either the direction. The minimal directional effect is apparent when observing the tick marks in figure 3.4A which represent the significant difference (t-test; $p < 0.01$) between the preferred and nonpreferred directions during sliding 100ms epochs for correct GO trials (blue ticks) and correct STOP trials (red ticks). Consistent with this observation, although **directional index** distributions for both preferred and nonpreferred directions are significantly shifted above zero for correct GO and STOP trial types (Fig. 3.4D *left*, *middle*; Wilcoxon; $ps < 0.01$), they are not significantly different from one another (Fig. 3.4D *left* vs. *middle*; Wilcoxon; $p = 0.84$). Thus, decreasing-type lOFC neurons appear to be sensitive to the direction of the action throughout the response regardless of trial type. To further support this assertion, I analyzed errant STOP trials and found that activity during these trials was not modulated by response direction as indicated by a non-significant shift in the directional index distribution (Fig. 3.4D *right*; Wilcoxon; $p = 0.59$). Importantly, the direction distribution for STOP errors was significantly reduced relative to correct STOP trials (Fig. 3.4D *middle* vs. *right*; Wilcoxon; $p < 0.05$). The lack of directionality on STOP errors suggests that when animals fail to inhibit and redirect their response, the activity involved in directional responding does not reliably distinguish between the two actions.

Multiple regression analysis: In the multiple regression analysis, 31 neurons (24%) were significantly modulated by movement time (Fig. 3.5; movement time). Significantly more of these neurons ($n = 25$) showed positive β-values (i.e. greater firing

for slower movement) than negative β-values (n = 6; binomial sign test; $p < 0.01$). Twenty eight neurons (15%) were modulated by the direction parameter (Fig. 3.5; direction) and equal numbers exhibited positive and negative β-values (10 vs. 18; binomial sign test; $p = 0.09$). Lastly, trial type yielded only five neurons (4%) that exhibited significant partial r^2s (Fig. 3.5; trial type). Thus, like lOFC increasing-type neurons, activity of decreasing-type cells was closely tied the direction and speed of behavior, rather than a direction unbiased signal to inhibit and redirect an action.

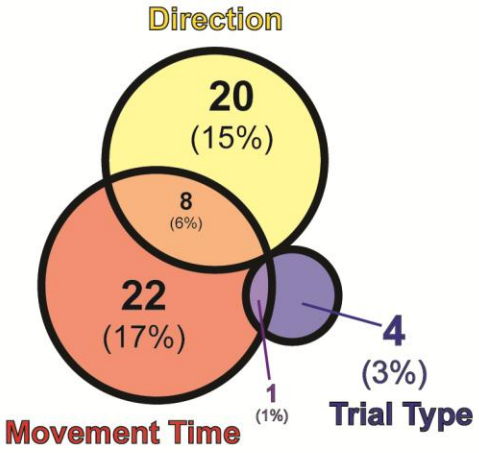

	Direction		Movement Time		Trial Type	
β-valence	+	-	+	-	+	-
	10	18	***25****	6	3	2

Figure 3.5: **Multiple regression results for decreasing-type lOFC neurons.** Circle sizes represent the relative proportions of neurons showing significant partial r^2 values for the individual task parameters. Top circle encompasses the proportion of neurons that show significant partial r^2 values for the direction parameter. Conventions as above for the movement time (red circle) and trial type (blue circle) parameters. Non-overlapping portions represent the counts (and percentages) of neurons with significant partial r^2 values for one parameter. Overlapping portions denote the counts (and percentages) of single cells that exhibited significant partial r^2 values for two (orange, green, purple) or all three (brown) parameters. The table specifies the counts of neurons significant within a variable that have associated positive ("+") or negative ("-") β-values. As specified by the model, positive β-values indicate greater firing for the contralateral direction (direction), greater firing for slower movement times (movement time), and greater firing for STOP over GO trials (trial type). Asterisks indicate significantly more β-values for one valence within a parameter (binomial sign test; $p < 0.05$).

Modulation of conflict by identity of the previous trial: I sought to determine whether direction signals in decreasing-type neurons, like increasing-type neurons, could provide a neural substrate for conflict adaptation. To accomplish this, I replotted decreasing-type lOFC cells under the same conventions as figure 3.3. Direct comparisons between GO trials, sS trials, and gS trials yielded no significant modulation by the type of trial (Fig. 3.6B; Wilcoxon; ps > 0.08). Intriguingly, significant directional signaling on gS trials was sparse (Fig. 3.6A; red ticks) and *nonexistent* on sS trials (Fig. 3.6A; no orange ticks). However, when direction indices were calculated, each type of trial featured significant positive shifts (Fig. 3.6C; Wilcoxon; $p < 0.05$) and, whereas increasing-type lOFC cells showed increased direction strength on sS trials, decreasing-type neurons show *decreased* direction strength (Fig. 3.6C *left* vs. *right*; Wilcoxon; $p < 0.05$; Fig. 3.6C *middle* vs. *right*; Wilcoxon; $p < 0.01$). Therefore, although counterintuitive, the direction of the response was reduced under circumstances where the animal was better prepared to inhibit a response. The identity of the previous trial did not impact activity on current GO trials, however. Figures 3.6D-F shows the lack of significant shift when gG and sG trials were compared directly (Fig. 3.6E; Wilcoxon; $p = 0.18$) and figure 3.6F demonstrates the lack of directional difference between the two trial types (Wilcoxon; $p = 0.41$).

Figure 3.6: **Impact on neuronal encoding based on conflict induced by the previous trial in decreasing-type lOFC neurons. A)** Population histogram of lOFC neurons that decreased significantly below baseline. Activity is aligned to port exit. Blue lines refer to all GO trials. Red lines represent STOP trials preceded by GO trials ('gS'). Orange lines indicate trials where a STOP trial is preceded by a STOP trial ('sS'). Calculation of direction preference remained unchanged from figure 3.4. Tick marks represent 100ms epochs where the preferred direction was significantly different from the nonpreferred direction (t-test; $p < 0.01$) for GO trials (blue), gS trials (red), and sS trials (orange). Although each tick mark signifies statistical difference for a 100ms epoch, tick width is 10ms for the purpose of presentational detail. Arrowheads indicate average movement times (port exit to well entry) for GO trials (blue; 608ms), gS trials (red; 791ms), and sS trials (756ms). Note the longer movement times for gS trials relative to sS trials consistent with reduced preparation for conflict. Vertical dashed lines mark the times of the stop change reaction time (SCRT; 204ms) and the average GO cue onset as measured as the latency from port exit (GO cue; -341ms) for the analyzed sessions. **B)** Indices compare the difference in firing between the three trial types presented in A. Leftmost distribution calculates the differences between gS and GO trials for each cell. The middle distribution marks the difference between sS and GO trials. Rightmost distribution computes the difference between gS and sS trials. **C)** Directional index distributions calculate the difference between the preferred and nonpreferred direction in each neuron during GO trials (*left*), gS trials (*middle*), and sS trials (*right*). **D)** Population histogram of increasing-type mDS neurons is aligned to port exit. All lines represent accurate GO trials that either followed a GO trial ('gG'; dark blue) or followed a STOP trial ('sG'; light blue). Thick lines refer to the preferred direction and thin lines refer to the nonpreferred direction. Tick marks denote the 100ms epochs where the preferred direction significantly differed from the nonpreferred direction (t-test; $p < 0.01$) during gG trials (dark blue) and sG trials (light blue). Arrowheads mark the average movement times for gG trials (dark blue; 564ms) and sG trials (light blue; 579ms). **E)** Distribution calculates the difference between firing on gG versus sG trials. **F)** Directional index distributions calculate the difference between the preferred and nonpreferred direction in each neuron during gG trials (*left*) and sG trials (*right*). Activity for all distributions was taken during the response epoch and significant shifts from zero are determined via Wilcoxon ($p < 0.05$). Asterisks indicate a direct comparison between two distributions is significant (Wilcoxon; $p < 0.05$ corrected for multiple comparisons).

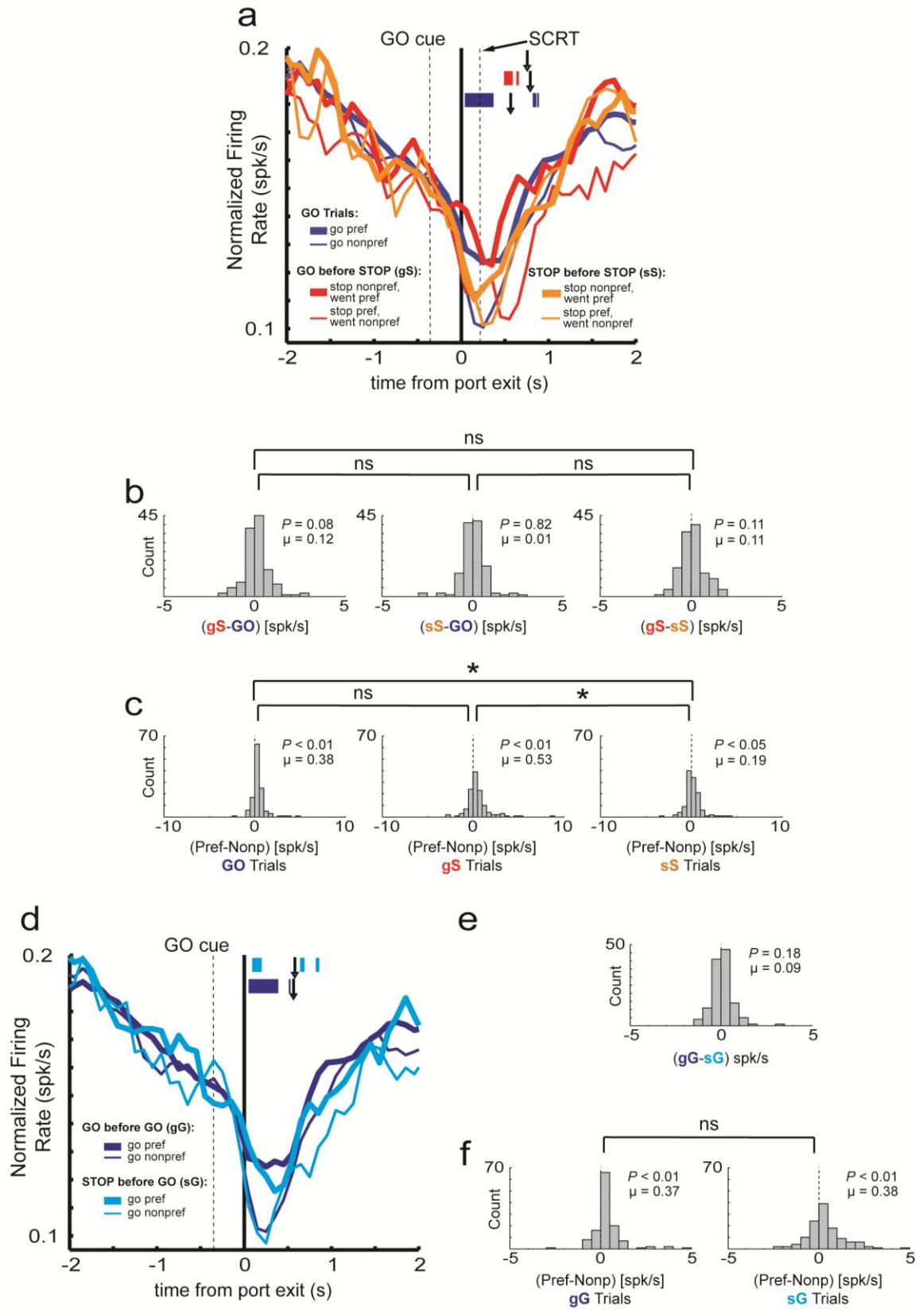
a
GO cue
SCRT
0.2
0.1
Normalized Firing Rate (spk/s)
GO Trials:
go pref
go nonpref
GO before STOP (gS):
stop nonpref, went pref
stop pref, went nonpref
STOP before STOP (sS):
stop nonpref, went pref
stop pref, went nonpref
-2
-1
0
1
2
time from port exit (s)
b
ns
ns
ns
45
Count
P = 0.08
μ = 0.12
P = 0.82
μ = 0.01
P = 0.11
μ = 0.11
(gS-GO) [spk/s]
(sS-GO) [spk/s]
(gS-sS) [spk/s]
c
*
ns
*
70
P < 0.01
μ = 0.38
P < 0.01
μ = 0.53
P < 0.05
μ = 0.19
(Pref-Nonp) [spk/s]
GO Trials
gS Trials
sS Trials
d
GO cue
GO before GO (gG):
go pref
go nonpref
STOP before GO (sG):
go pref
go nonpref
time from port exit (s)
e
50
P = 0.18
μ = 0.09
(gG-sG) spk/s
f
ns
P < 0.01
μ = 0.37
P < 0.01
μ = 0.38
gG Trials
sG Trials

Summary: Decreasing-type neurons tend to be most sensitive to the speed of responding as well as the direction of the response similar to its increasing-type counterparts. However, weak direction signaling across all trial types and the dearth of trial type specific neurons all but excludes this group of cells from playing a functional role in response inhibition. Instead, decreasing-type lOFC neurons appear to play a complimentary role to increasing-type cells by providing a redundant refining signal.

Disparate waveform characteristics as a means to define increasing- and decreasing populations in lOFC

Many OFC recording studies do not independently analyze decreasing- and increasing-type neurons. Some papers lump the two types together, some ignore decreasing-type cells, and some do not select cells based on differentiation from baseline at all. I believe that other approaches can lead to skewed perspectives on the function of a brain region. Theoretically a decreasing-type lOFC neuron has the capability to provide the identical code to recipient structures as increasing-type neurons given an intermediary inhibitory (GABAergic) neuron, an idea posited in (*144*). However, given the necessity for speed in my task, an additional chemical synapse may limit the usefulness of the decreasing-type population in downstream structures including mDS. Therefore, I measured the spiking properties separately for increasing- and decreasing-type lOFC populations in figures 3.7A-B. Remarkably, despite different firing valence from baseline, the average inter-spike interval, baseline activity, and peak width between increasing- and decreasing-types varied very little. Within populations, the significance of a cell in the regression procedure appeared to have minimal impact on its

electrophysiological properties. It is worth reporting that increasing- and decreasing-type lOFC neurons were found to be spatially heterogeneous within the recording tracts, a finding consistent with previous recordings in lOFC (*62*, *145*).

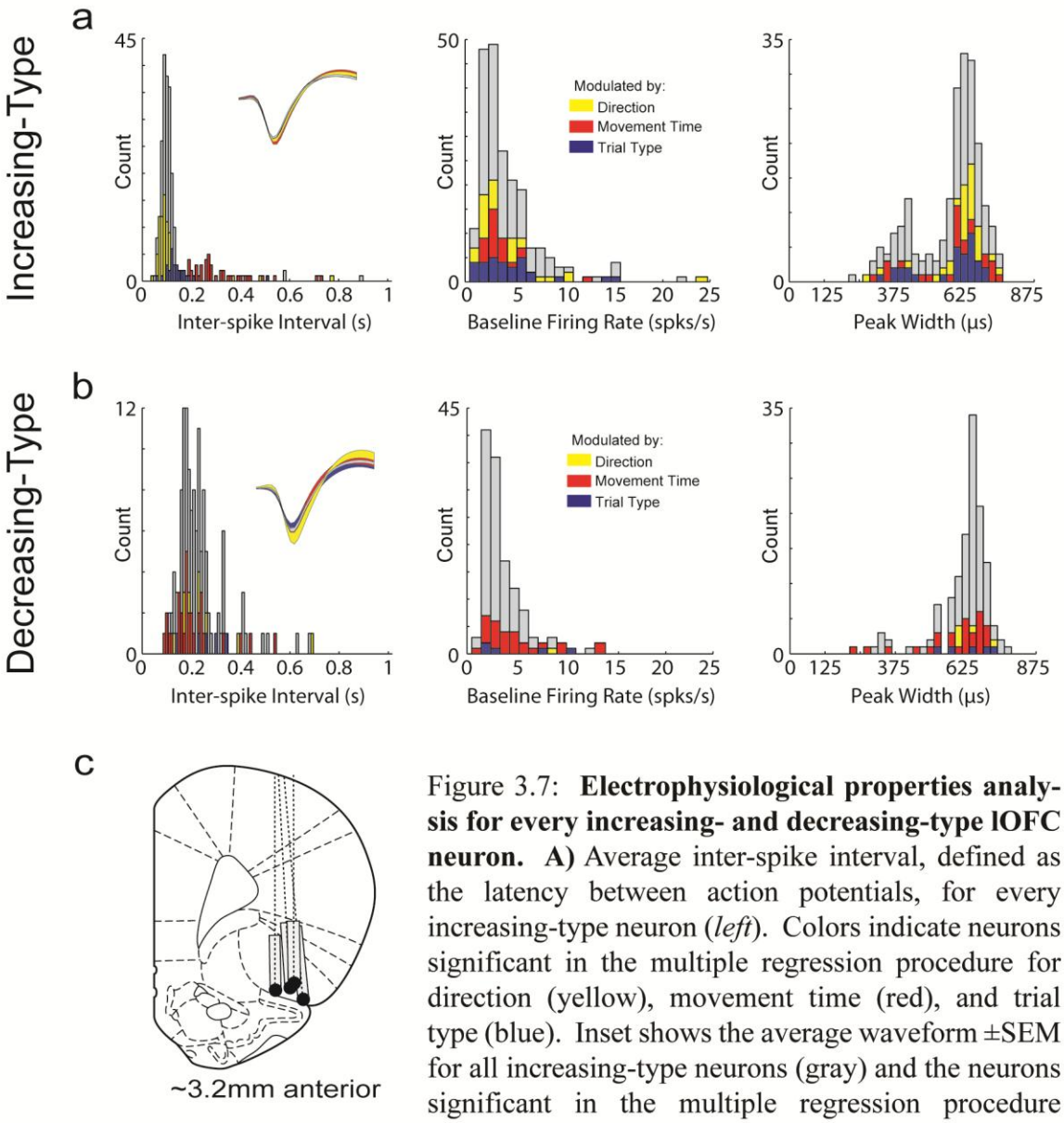

Figure 3.7: **Electrophysiological properties analysis for every increasing- and decreasing-type lOFC neuron. A)** Average inter-spike interval, defined as the latency between action potentials, for every increasing-type neuron (*left*). Colors indicate neurons significant in the multiple regression procedure for direction (yellow), movement time (red), and trial type (blue). Inset shows the average waveform ±SEM for all increasing-type neurons (gray) and the neurons significant in the multiple regression procedure (colors). Average baseline firing rate (spikes/s) taken from the 1s epoch beginning 2s prior to trial initiation is plotted for each increasing-type cell (*middle*). Average peak width defined as the time between the two highest peaks in the waveform is plotted for every increasing-type cell (*right*). **B)** Conventions as in A for decreasing-type neurons. **C)** Location of recording sites. Gray boxes mark extent of the recording locations. Black dots mark the bottom of the recording tract. Coronal slices approximately 3.2mm anterior to bregma.

Chapter Discussion

Research has suggested that orbitofrontal cortex (OFC) acts as a frontal area integral for inhibitory control. Dysfunction in OFC has been critically implicated in many disorders that impact inhibitory control including addiction, Tourette syndrome, obsessive compulsive disorder (OCD), and attention deficit hyperactivity disorder (*3-21, 146, 147*). In fact, recent work has demonstrated that optogenetic stimulation of lateral OFC and its terminals in striatum can restore normal levels of response inhibition in a mouse model of compulsive behavior (*148*) and pharmacological manipulation of this brain area in rats has been suggested to disrupt stopping with striking parallels to observations made in inferior frontal cortex in humans (*149*). Additionally, reductions of OFC activity have been observed when OCD-like symptoms were provoked experimentally (*150*).

Although this previous work suggests that OFC provides a type of inhibitory signal that can aid in response suppression, others have strongly refuted this theory arguing that rats with impaired OFC function can still perform a number of tasks that require response inhibition. Furthermore, a barrage of single unit studies over the past few years have suggested that neural activity in OFC better reflects expectations about future outcomes critical for reward-guided decision-making tasks that do not necessarily involve response inhibition (*151-155*). Decreased function after OFC lesions in tasks such as reversal and reinforcer devaluation can be parsimoniously explained by reward expectancy encoding rather than a decrement in the capacity to inhibit behavior.

Considering the debate on OFC's role in response inhibition, it comes as a surprise that no one has recorded from OFC in a task that requires response inhibition

independent from manipulations of expected outcomes. I chose to examine neural correlates during performance of a stop signal task for several reasons. First, stop signal performance is disrupted in a number of psychiatric disorders that are thought to impact function of the OFC circuit (*5, 6, 8, 18, 146, 147*). Second, imaging studies clearly suggest higher firing on stop relative to go trials in OFC in several tasks including ones that require suppression of specific response types (e.g. left/right)(*18, 126, 130*). The third reason I chose a stop signal task is that pharmacological studies suggest that OFC is critical for normal stop signal performance. Lesions disrupt performance on stop signal tasks and administration of atomoxetine (ADHD drug) into OFC improves stop signal performance (*61*). Although these studies do not "require" rats to redirect movement on STOP trials, rats do redirect their ongoing movement away from the habitual response directly to the food cup to receive reward. From these studies it is clear that during performance of stop signal tasks, OFC is critical for inhibition of movement on stop trials and that when subjects successfully suppress behavior, activity in OFC appears to be elevated.

The finding that BOLD signal is increased in OFC during response suppression can be interpreted in several different ways. On one hand, increased BOLD signal on stop relative to go trials might arise from neurons that signal the need for response inhibition. That is, single neurons in OFC elevate firing whenever subjects are required to suppress an ongoing movement. On the other hand, increased BOLD signal may arise from neurons active in conjunction with planning different actions. Similar to the argument originally posited by Nakamura and colleagues, on stop trials, there is simultaneous activation of neurons signaling the movement that needs to be stopped and the one

necessary for accurate performance (*156*). Thus, the net activity of this population of neurons might increase during response inhibition because neurons that signal for opposing actions will be active simultaneously.

My results are more consistent with the second explanation. Overall I found that activity in lOFC does not appear to carry a pure "inhibitory signal." Population firing in lOFC was not significantly stronger under STOP trials, nor were there a preponderance of single neurons that fired significantly more strongly on STOP over GO trials. Instead I found that lOFC neurons exhibited directional tuning as previously reported (*62, 63, 65*), and that directional selectivity was enhanced by the need to suppress and redirect behavior, especially during sequences of increased conflict resolution. This interpretation is broadly consistent with recent work in monkeys suggesting that OFC is involved in reconciling cognitive signals during conflict adaptation (*69*).

All of this suggests that OFC is more involved in executive functions that control and enhance response selectivity when unwanted movements are suppressed and redirected. I suspect that this signal is critical for resolving conflict observed in neural signals downstream of OFC, such as mDS (*1*). Dysfunction of these correlates can explain why interference of OFC function impairs response inhibition. Although the most obvious interpretation is that OFC provides some sort of inhibition signal, my results suggest that OFC plays an important role in conflict induced executive control (*69*). Such a function might be critical for performance on several tasks that require inhibition and are impaired after OFC lesions, including reversal learning (*140*), delay discounting (*124*), extinction (*141*), delayed alternation (*142*) and reinforcer devaluation (*143*).

Chapter 7: Medial prefrontal cortex and its role in conflict monitoring

Experimental work has reported that interference of medial prefrontal cortex (mPFC) impairs performance on response inhibition tasks as measured by stop trial accuracy and premature responding during reaction time tasks (*61, 157*). Taken together, this work points to mPFC as a critical player during response inhibition and suggests that reduced prefrontal activation/function in disorders such as ADHD drive behavioral impairments (*158*). However, the current literature possesses no single unit studies that probe the role of mPFC in response inhibition via the stop signal task. With the above data indicating that lOFC is a brain region responsible for timely signaling of the need to inhibit an action, I explored mPFC to determine its role in behavioral restraint.

The mPFC is a region in both humans and rats that functions as an executive control center important for decision-making, learning, and memory (*158*) that is disrupted in many psychiatric disorders, including ADHD (*159*). The circuit comprising the mPFC and mDS is important for premature/uncontrolled behavior as evidenced by a recent study where this network was disconnected in rats performing the 5-choice-serial-reaction-time task. After this perturbation, rats showed a persistent deficit characterized by a reduction in accuracy and speed in responding to a visual stimulus (*160*). More specifically, inactivating mPFC via the GABA agonist muscimol has demonstrated that mPFC is crucial for inhibiting an already initiated response during the stop signal task (*61*).

Despite suggestive evidence for the involvement of mPFC in successful inhibitory behavior, not all research has agreed with this notion (*125*). This accumulation of mPFC data propounds the necessity of a single cell recording study in rats that are actively

attempting to suppress their actions. To fill this void, and further pursue the frontal locus of response inhibition, I recorded from 636 mPFC neurons from eleven rats during performance of the stop signal task (recording locations in figure 4.7). Briefly, I found that mPFC neurons are highly directional, the correct direction on STOP trials is not discerned prior to the SCRT, and the overall directional strength is not different between STOP and GO trials. These characteristics preclude mPFC neurons from contributing to prompt response inhibition in the context of my task. However, mPFC is sensitive to the degree of conflict in the immediate past, providing a "monitor" that tracks the degree of conflict recently experienced. This is quite useful for a system since behavior is better controlled under difficult situations when preparation is high.

Increasing-type Cells

Population Activity: Of the 636 mPFC cells I recorded, 19% (n = 121) increased their firing during the response epoch (port exit until well entry) compared to baseline. As with the previously analyzed brain areas, mPFC is highly directional, firing more strongly for responses in one direction (Fig. 4.1A,B; thick lines; preferred) over the other (thin lines; nonpreferred). Activity appears higher for STOP relative to GO trials for responses made in the preferred direction (Fig. 4.1A, B; thick red vs. thick blue).

Figure 4.1: **Direction and trial type encoding of increasing-type mPFC neurons. A-B)** Average firing rate (spikes/s) over time aligned on port exit (A) and well entry (B) for all mPFC neurons that fired more strongly during the 'response epoch' (port exit to well entry) relative to baseline (1s epoch beginning 2s prior to trial initiation). The time necessary to inhibit a response (stop change reaction time; SCRT) is defined as the difference between STOP trial movement time and GO trial movement time. SCRT is marked as the vertical dotted line labeled 'SCRT' at 121ms. 'GO cue' and its associated vertical dashed line indicates the average onset of the GO cue as measured by the latency from port exit (-423ms). Blue lines refer to GO trials, red lines refer to STOP trials, and dashed lines refer to errant trials (incorrect direction). Due to the heterogeneous direction specificity of individual cells, each cell was characterized as having a preferred direction and a nonpreferred direction. This preference was determined by asking which direction (contra- or ipsilateral to the recorded hemisphere) elicited the highest firing rate during the response epoch for each cell. Therefore, as defined by the analysis, preferred direction (thick lines) is always higher than the nonpreferred direction (thin lines) during the response epoch. Tick marks represent significant p-values in temporal space after preferred direction was compared to nonpreferred direction in the population for GO trials (blue ticks) and STOP trials (red ticks) in 100ms epochs that slid by 10ms after each iteration (t-test; $p < 0.01$). Although each tick mark signifies statistical difference for a 100ms epoch, tick width is 10ms for the purpose of presentational detail. Arrowheads denote the average movement time (well entry) during GO trials (blue arrowhead = 610ms) and STOP trials (red arrowhead = 729ms). GO cue, SCRT, and movement times (arrowheads) are variable values based on the behavior of the animals in the analyzed sessions. These values (except SCRT) are estimates with variance and cannot be treated as constants relative to port exit. **C)** Stop indices for preferred (*left*) and nonpreferred (*right*) directions. Stop indices are calculated by taking the activity during the response epoch from STOP trials, subtracting activity during the response epoch on GO trials, and dividing it by the sum of the two ((STOP-GO/(STOP+GO)) in each direction for every cell. Significant shifts from zero (as calculated by Wilcoxon) denote that neuronal activity is significantly different between STOP and GO trials in a given direction. **D)** Directional index distributions defined as activity during the response epoch in the preferred direction minus activity during the response epoch in the nonpreferred direction divided by the sum ((preferred-nonpreferred)/(preferred+nonpreferred)) in every cell. These calculations are specific to GO trials (*left*), STOP trials (*middle*), and STOP errors (*right*). Significant shifts from zero (as calculated by Wilcoxon) signify that activity is greater in one direction than the other at the neuronal level. Asterisks in C and D indicate that two distributions are significantly different via Wilcoxon.

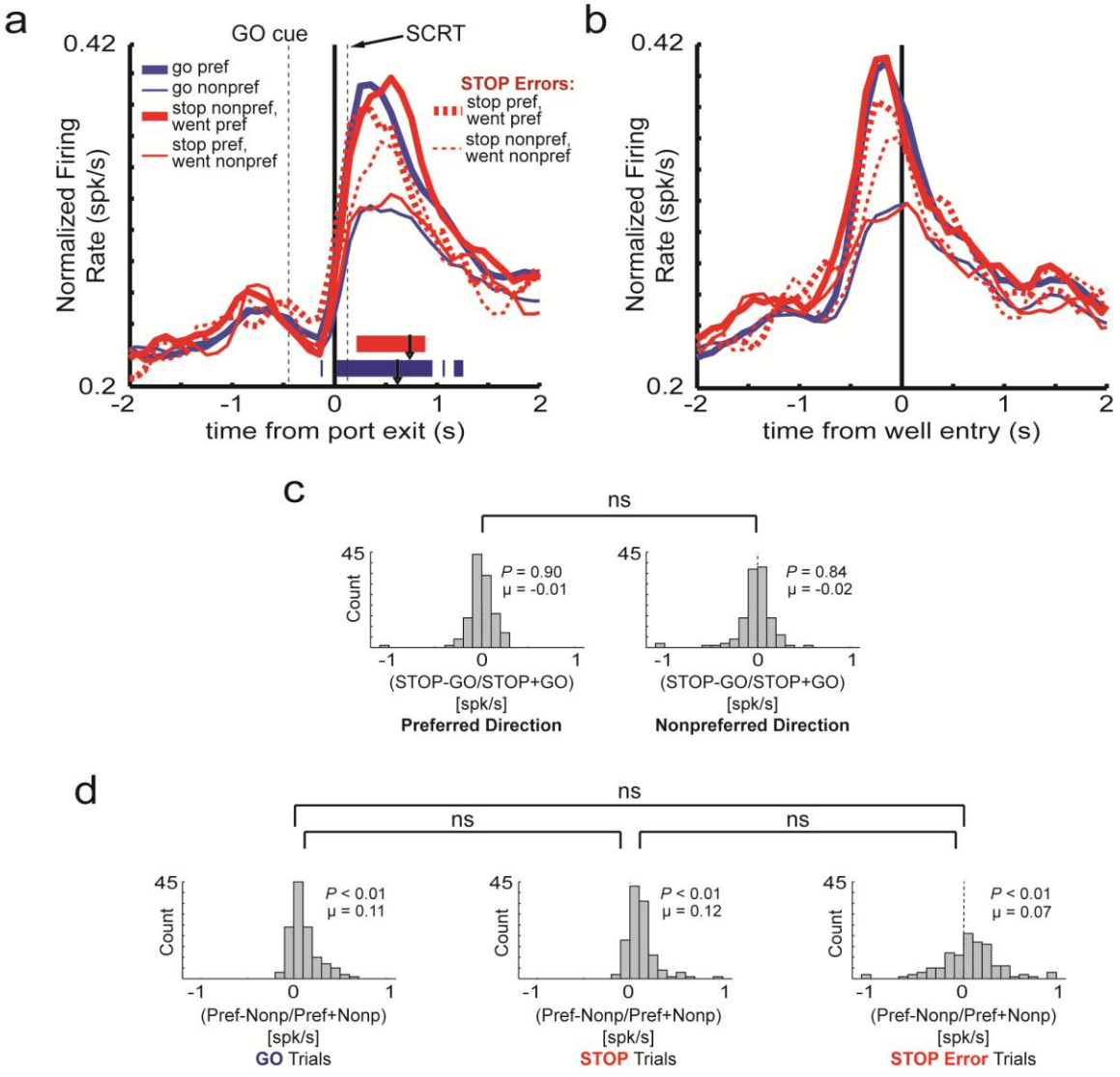
a
GO cue
SCRT
0.42
0.2
Normalized Firing Rate (spk/s)
go pref
go nonpref
stop nonpref, went pref
stop pref, went nonpref
STOP Errors:
stop pref, went pref
stop nonpref, went nonpref
-2
-1
0
1
2
time from port exit (s)
b
0.42
0.2
Normalized Firing Rate (spk/s)
-2
-1
0
1
2
time from well entry (s)
c
ns
45
Count
P = 0.90
μ = -0.01
-1
0
1
(STOP-GO/STOP+GO)
[spk/s]
Preferred Direction
45
P = 0.84
μ = -0.02
-1
0
1
(STOP-GO/STOP+GO)
[spk/s]
Nonpreferred Direction
d
ns
ns
ns
45
Count
P < 0.01
μ = 0.11
-1
0
1
(Pref-Nonp/Pref+Nonp)
[spk/s]
GO Trials
45
Count
P < 0.01
μ = 0.12
-1
0
1
(Pref-Nonp/Pref+Nonp)
[spk/s]
STOP Trials
45
Count
P < 0.01
μ = 0.07
-1
0
1
(Pref-Nonp/Pref+Nonp)
[spk/s]
STOP Error Trials

Stop index: To quantify differences between STOP and GO trials, I computed a stop index defined as the difference between STOP and GO trial activity (STOP-GO/STOP+GO) in both directions for each neuron. The distributions of these indices for preferred and nonpreferred directions are plotted in figure 4.1C. In these stop index plots, a shift in the positive direction indicates that neuronal firing was stronger for STOP relative to GO trials than the opposite effect (stronger firing for GO relative to STOP trials). In the preferred direction and nonpreferred direction, the stop index was not significantly shifted from zero (Fig. 4.1C *left*; Wilcoxon; $p = 0.90$; Fig. 4.1C *right*; Wilcoxon; $p = 0.84$) and were not significantly different from one another (Fig. 4.1C *left* vs. *right*; Wilcoxon; $p = 0.42$).

Directional index: As described previously, firing of neurons in mPFC is highly directional. To further assess the directional encoding for each trial type I computed a directional index during the response epoch independently for STOP and GO trials. In increasing-type mPFC cells, directional index distributions were shifted significantly above zero during both GO and STOP trials (Fig. 4.1D *left, middle*) but there was no significant difference between directionality of GO and STOP trials (Fig. 4.1D *left* vs. *middle*; Wilcoxon; $p = 0.50$).

Directional responding implies that mPFC is involved in executive functions pertaining to the spatial location of the response. If directional signals in mPFC are important for directing behavior, they should be attenuated on errors. Inconsistent with this hypothesis, the distribution of direction indices was not significantly different on STOP errors compared to correct STOP trials, suggesting that the lack of substantial directional selectivity did not lead to errant responding. Despite being the same strength

as correct STOP directional signals, the STOP error directional index distribution was still significantly positive suggesting that activity in mPFC better reflects the nature of the movement, not the sensory stimulus that triggered it.

Lastly, the timing of the directional signaling in mPFC neurons further illuminates the function of these cells. As a strategy to further assess this direction encoding as a function of time, I again used a sliding window analysis that, for STOP and GO trials independently, compares activity between the preferred and nonpreferred directions in 100ms epochs which slid 10ms after each iteration. Activity between the two directions on GO trials became significantly different (t-test; $p < 0.01$) around the time of port exit (Fig. 4.1A; blue ticks). Direction differences on STOP trials (Fig. 4.1A; red ticks) did not become significantly different until after the SCRT which precludes these neurons from being used to inhibit/redirect ongoing actions.

Multiple regression analysis: To complement the analyses above and the larger population effects, I have displayed the results of the multiple regression analysis done on each increasing-type cell in figure 4.2. The model used was designed to determine if neuronal firing correlates significantly and uniquely with movement speed, direction, and/or type of trial at the single cell level. The size of the top circle in figure 4.2 indicates the proportion of increasing-type mPFC cells that were significantly modulated by the direction of the response when variance for the other two parameters was factored out (partial r^2). Forty five neurons (37%) were significantly modulated by direction and of these 45 neurons, 21 β-values of the direction parameter were positive (greater firing for the contralateral direction) whereas 24 were negative, values not different from 50/50 split (binomial sign test; $p = 0.76$). Thirty seven neurons (31%) were significantly and

uniquely correlated with movement time and of these 37, the number of negative β-values (greater firing for faster movement speeds) differed significantly from the number of positive β-values (Fig. 4.2; movement time; 9 vs. 28; binomial sign test; $p < 0.01$). A substantial portion of the aforementioned neurons exhibited significant partial r^2 values for both the direction and movement time parameters (Fig. 4.2; orange + brown; n = 16) highlighting the role of mPFC in functions regarding spatial response and movement latency. A small proportion of increasing-type mPFC neurons featured significant partial r^2 values for the trial type (STOP vs. GO) parameter (Fig. 4.2; trial type; n = 13; 11%). Of these 13 neurons, equal numbers showed higher firing for STOP trials over GO trials and vice versa (binomial sign test; $p = 0.58$).

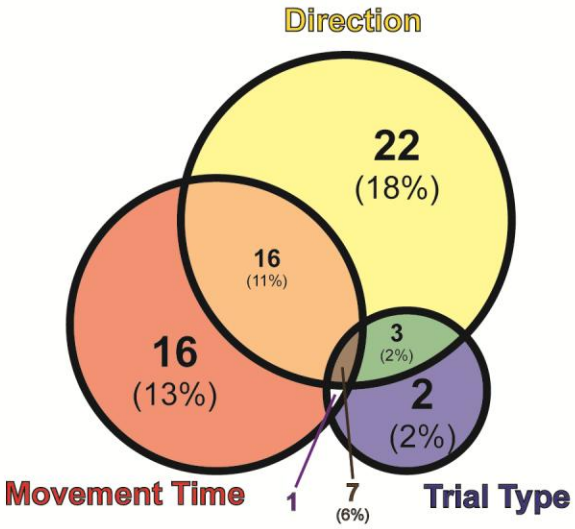

	Direction		Movement Time		Trial Type	
β-valence	+	-	+	-	+	-
	21	24	9	***28****	8	5

Figure 4.2: **Multiple regression results for increasing-type mPFC neurons.** Circle sizes represent the relative proportions of neurons showing significant partial r^2 values for the individual task parameters. Top circle encompasses the proportion of neurons that show significant partial r^2 values for the direction parameter. Conventions as above for the movement time (red circle) and trial type (blue circle) parameters. Non-overlapping portions represent the counts (and percentages) of neurons with significant partial r^2 values for one parameter. Overlapping portions denote the counts (and percentages) of single cells that exhibited significant partial r^2 values for two (orange, green, purple) or all three (brown) parameters. The table specifies the counts of neurons significant within a variable that have associated positive ("+") or negative ("-") β-values. As specified by the model, positive β-values indicate greater firing for the contralateral direction (direction), greater firing for slower movement times (movement time), and greater firing for STOP over GO trials (trial type). Asterisks indicate significantly more β-values for one valence within a parameter (binomial sign test; $p < 0.05$).

Modulation of conflict by identity of previous trial: Even though increasing-type mPFC neurons do not appear to serve a role in active inhibitory restraint, there is reason to believe that activity in mPFC may play a role in conflict adaptation. mPFC and neighboring structures (anterior cingulate and lOFC) have been shown to be sensitive to choices on trials in the recent past (*66-68, 161, 162*), therefore I asked whether mPFC was modulated by the added conflict induced by the identity of the previous trial. Therefore, increasing-type mPFC neurons may play a role in monitoring conflict to broadly increase preparedness for flexible response inhibition by aggregating current and past conflict history.

Figure 4.3: **Impact on neuronal encoding based on conflict induced by the previous trial in increasing-type mPFC neurons. A)** Population histogram of mPFC neurons that increased significantly above baseline. Activity is aligned to port exit. Blue lines refer to all GO trials. Red lines represent STOP trials preceded by GO trials ('gS'). Orange lines indicate trials where a STOP trial is preceded by a STOP trial ('sS'). Calculation of direction preference remained unchanged from figure 4.1. Tick marks represent 100ms epochs where the preferred direction was significantly different from the nonpreferred direction (t-test; $p < 0.01$) for GO trials (blue), gS trials (red), and sS trials (orange). Although each tick mark signifies statistical difference for a 100ms epoch, tick width is 10ms for the purpose of presentational detail. Arrowheads indicate average movement times (port exit to well entry) for GO trials (blue; 582ms), gS trials (red; 697ms), and sS trials (698ms). Vertical dashed lines mark the times of the stop change reaction time (SCRT; 119ms) and the average GO cue onset as measured as the latency from port exit (GO cue; -423ms) for the analyzed sessions. **B)** Indices compare the difference in firing between the three trial types presented in A. Leftmost distribution calculates the differences between gS and GO trials for each cell. The middle distribution marks the difference between sS and GO trials. Rightmost distribution computes the difference between gS and sS trials. **C)** Directional index distributions calculate the difference between the preferred and nonpreferred direction in each neuron during GO trials (*left*), gS trials (*middle*), and sS trials (*right*). **D)** Population histogram of increasing-type mDS neurons is aligned to port exit. All lines represent accurate GO trials that either followed a GO trial ('gG'; dark blue) or followed a STOP trial ('sG'; light blue). Thick lines refer to the preferred direction and thin lines refer to the nonpreferred direction. Tick marks denote the 100ms epochs where the preferred direction significantly differed from the nonpreferred direction (t-test; $p < 0.01$) during gG trials (dark blue) and sG trials (light blue). Arrowheads mark the average movement times for gG trials (dark blue; 608ms) and sG trials (light blue; 598ms). **E)** Distribution calculates the difference between firing on gG versus sG trials. **F)** Directional index distributions calculate the difference between the preferred and nonpreferred direction in each neuron during gG trials (*left*) and sG trials (*right*). Activity for all distributions was taken during the 1s epoch following port exit and significant shifts from zero are determined via Wilcoxon ($p < 0.05$). Asterisks indicate a direct comparison between two distributions is significant (Wilcoxon; $p < 0.05$ corrected for multiple comparisons).

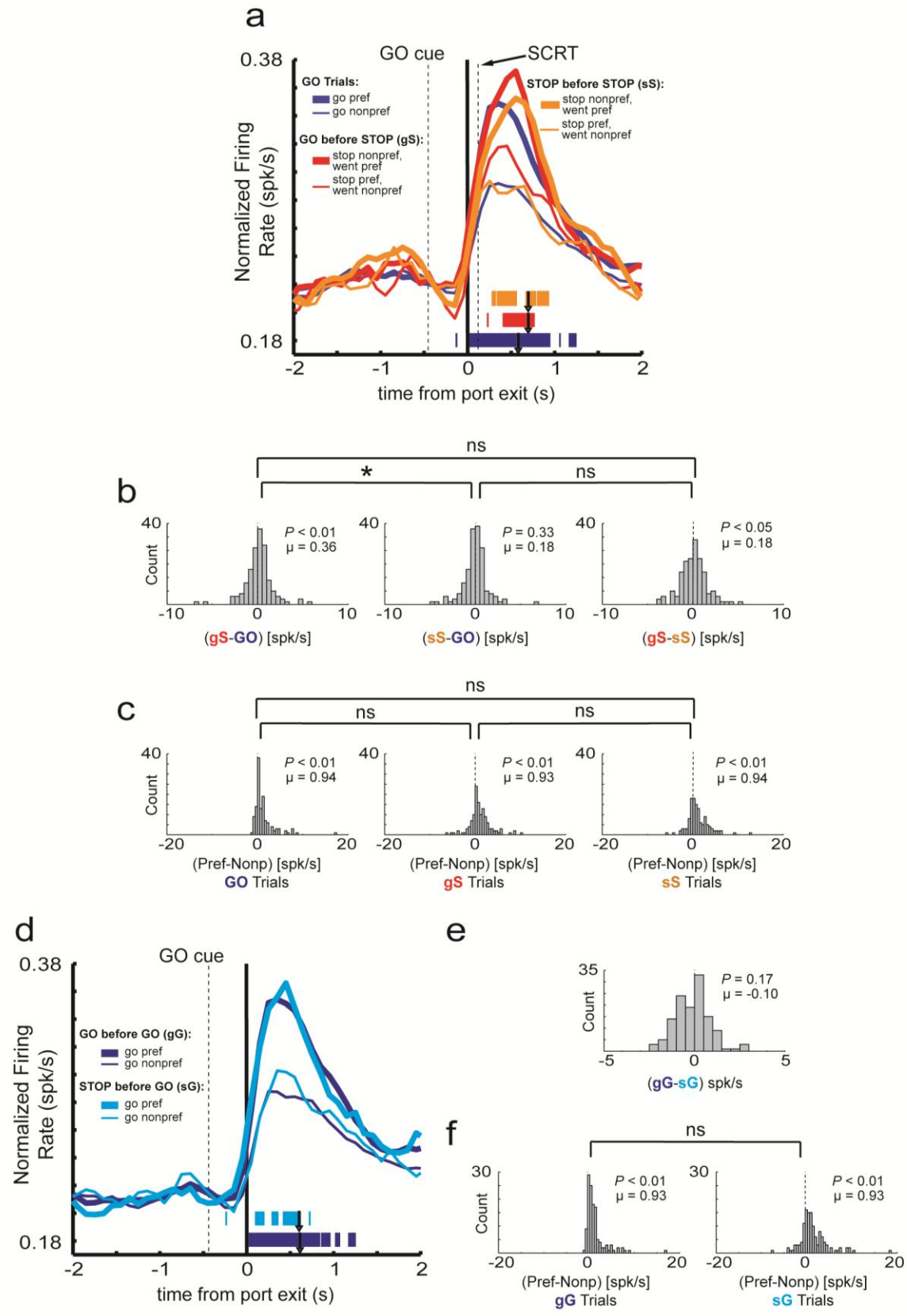
a
GO cue
SCRT
0.38
0.18
Normalized Firing Rate (spk/s)
GO Trials:
go pref
go nonpref
GO before STOP (gS):
stop nonpref, went pref
stop pref, went nonpref
STOP before STOP (sS):
stop nonpref, went pref
stop pref, went nonpref
-2
-1
0
1
2
time from port exit (s)
b
ns
*
ns
Count
P < 0.01
μ = 0.36
P = 0.33
μ = 0.18
P < 0.05
μ = 0.18
(gS-GO) [spk/s]
(sS-GO) [spk/s]
(gS-sS) [spk/s]
c
ns
ns
ns
P < 0.01
μ = 0.94
P < 0.01
μ = 0.93
P < 0.01
μ = 0.94
(Pref-Nonp) [spk/s]
GO Trials
gS Trials
sS Trials
d
GO cue
GO before GO (gG):
go pref
go nonpref
STOP before GO (sG):
go pref
go nonpref
e
P = 0.17
μ = -0.10
(gG-sG) spk/s
f
ns
P < 0.01
μ = 0.93
P < 0.01
μ = 0.93
gG Trials
sG Trials

Figures 4.3A plots average activity on STOP trials when the previous trial was either a GO (gS, red) or STOP trial (sS, orange). For reference, GO (low conflict) trials during these sessions are plotted in blue. Interestingly, mPFC increasing-type neurons did not fire differently on STOP trials discriminated by the previous trial type *during the response epoch*. However, it appears as though activity on gS trials differed from activity on sS and GO trials *later in the response*, therefore I extended the analysis epoch to 1s beginning at port exit to include post-response activity. After this extension, direct firing comparisons between trial types showed significant differences for the gS relative to GO comparison (Fig. 4.3B *left*; Wilcoxon; $p < 0.01$) and the gS relative to sS comparison (Fig. 4.3B *right*; Wilcoxon; $p < 0.05$). Interestingly, directional signals do not differ between trial types (Fig. 4.3C *left* vs. *middle*; Wilcoxon; $p = 0.69$; Fig. 4.4C *left* vs. *right*; Wilcoxon; $p = 0.74$; Fig. 4.4C *middle* vs. *right*; Wilcoxon; $p = 0.95$).

There was no significant effect for the previous trial impacting activity on current GO trials. That is, the direct comparison distribution between gG and sG trial types was not significantly shifted (Fig. 4.3E; Wilcoxon; $p = 0.17$) and the directional index distributions were not different from one another (Fig. 4.3F *left* vs. *right*; Wilcoxon; $p = 0.49$). This suggests that dissociable activity on gS relative to sS trials is due to the conflict induced by the current and previous trial, not a reflection of the simple identity of the preceding trial.

Ultimately, while mPFC activity is not responsible for the flexible control of behavior necessary for timely response inhibition, its firing patterns reflect a temporally broader (one to two previous trials) memory of the conflict experienced in the recent past and can presumably recruit attentional resources to better control subsequent inhibitory

behavior. It is important to note that this conflict monitoring signal need not arise *during* the response of a trial. In fact, this signal is better suited for post-decision activity where the degree of conflict endured on the present trial can be integrated with prior conflict to inform the system to prepare more carefully for upcoming demands.

Decreasing-type Cells

Population activity: Decreasing-type cells (39%; n = 249) are plotted in figure 4.4A,B. A glimpse at these population histograms reveals a noticeable increase in STOP trial activity in the preferred direction (Fig. 4.4A,B; thick red) relative to GO trials in the preferred direction (Fig. 4.4A,B; thick blue). The stop index in the preferred direction (Fig. 4.4C *left*; Wilcoxon; $p < 0.01$) substantiates this claim via a significantly positive shift. Interestingly, although the stop index was not significantly shifted from zero in the nonpreferred direction (Fig. 4.4C *right*; Wilcoxon; $p = 0.34$), the nonpreferred stop index distribution did differ from the preferred stop index distribution (Fig. 4.4C *left* vs. *right*; Wilcoxon; $p < 0.01$). This demonstrates that firing to response in the preferred direction varied by the type of trial. Interestingly, the directional signal was significantly *stronger* on correct STOP trials relative to GO trials (Fig. 4.4D *left* vs. *middle*; Wilcoxon; $p < 0.01$) which I have yet to observe in the previously analyzed brain regions. When comparing the directional index on correct STOP trials to incorrect STOP trials, the direction strength was significantly weaker when rats made errors (Fig. 4.4D *middle* vs. *right*; Wilcoxon; $p < 0.01$). Particularly in the preferred direction, activity on correct STOP trials tended to remain elevated related to correct GO trials even after the response had been completed (Fig. 4.4B; thick red vs. thick blue). Lastly, the direction signal of

decreasing-type mPFC cells in temporal space occurred after port exit and prior to the SCRT for both GO trials (Fig. 4.4A; blue ticks) and STOP trials (Fig. 4.4A; red ticks).

Figure 4.4: **Direction and trial type encoding of decreasing-type mPFC neurons. A-B)** Average firing rate (spikes/s) over time aligned on port exit (A) and well entry (B) for all mPFC neurons that fired less strongly during the 'response epoch' (port exit to well entry) relative to baseline (1s epoch beginning 2s prior to trial initiation). The time necessary to inhibit a response (stop change reaction time; SCRT) is defined as the difference between STOP trial movement time and GO trial movement time. SCRT is marked as the vertical dotted line labeled 'SCRT' at 141ms. 'GO cue' and its associated vertical dashed line indicates the average onset of the GO cue as measured by the latency from port exit (-420ms). Blue lines refer to GO trials, red lines refer to STOP trials, and dashed lines refer to errant trials (incorrect direction). Due to the heterogeneous direction specificity of individual cells, each cell was characterized as having a preferred direction and a nonpreferred direction. This preference was determined by asking which direction (contra- or ipsilateral to the recorded hemisphere) elicited the highest firing rate during the response epoch for each cell. Therefore, as defined by the analysis, preferred direction (thick lines) is always higher than the nonpreferred direction (thin lines) during the response epoch. Tick marks represent significant p-values in temporal space after preferred direction was compared to nonpreferred direction in the population for GO trials (blue ticks) and STOP trials (red ticks) in 100ms epochs that slid by 10ms after each iteration (t-test; $p < 0.01$). Although each tick mark signifies statistical difference for a 100ms epoch, tick width is 10ms for the purpose of presentational detail. Arrowheads denote the average movement time (well entry) during GO trials (blue arrowhead = 589ms) and STOP trials (red arrowhead = 730ms). GO cue, SCRT, and movement times (arrowheads) are variable values based on the behavior of the animals in the analyzed sessions. These values (except SCRT) are estimates with variance and cannot be treated as constants relative to port exit. **C)** Stop indices for preferred (*left*) and nonpreferred (*right*) directions. Stop indices are calculated by taking the activity during the 1s epoch beginning at port exit from STOP trials, subtracting activity during the 1s epoch beginning at port exit on GO trials, and dividing it by the sum of the two ((STOP-GO/(STOP+GO)) in each direction for every cell. Significant shifts from zero (as calculated by Wilcoxon) denote that neuronal activity is significantly different between STOP and GO trials in a given direction. **D)** Directional index distributions defined as activity during the 1s epoch beginning at port exit in the preferred direction minus activity during the 1s epoch beginning at port exit in the nonpreferred direction divided by the sum ((preferred-nonpreferred)/(preferred+nonpreferred)) in every cell. These calculations are specific to GO trials (*left*), STOP trials (*middle*), and STOP errors (*right*). Significant shifts from zero (as calculated by Wilcoxon) signify that activity is greater in one direction than the other at the neuronal level. Asterisks in C and D indicate that two distributions are significantly different via Wilcoxon.

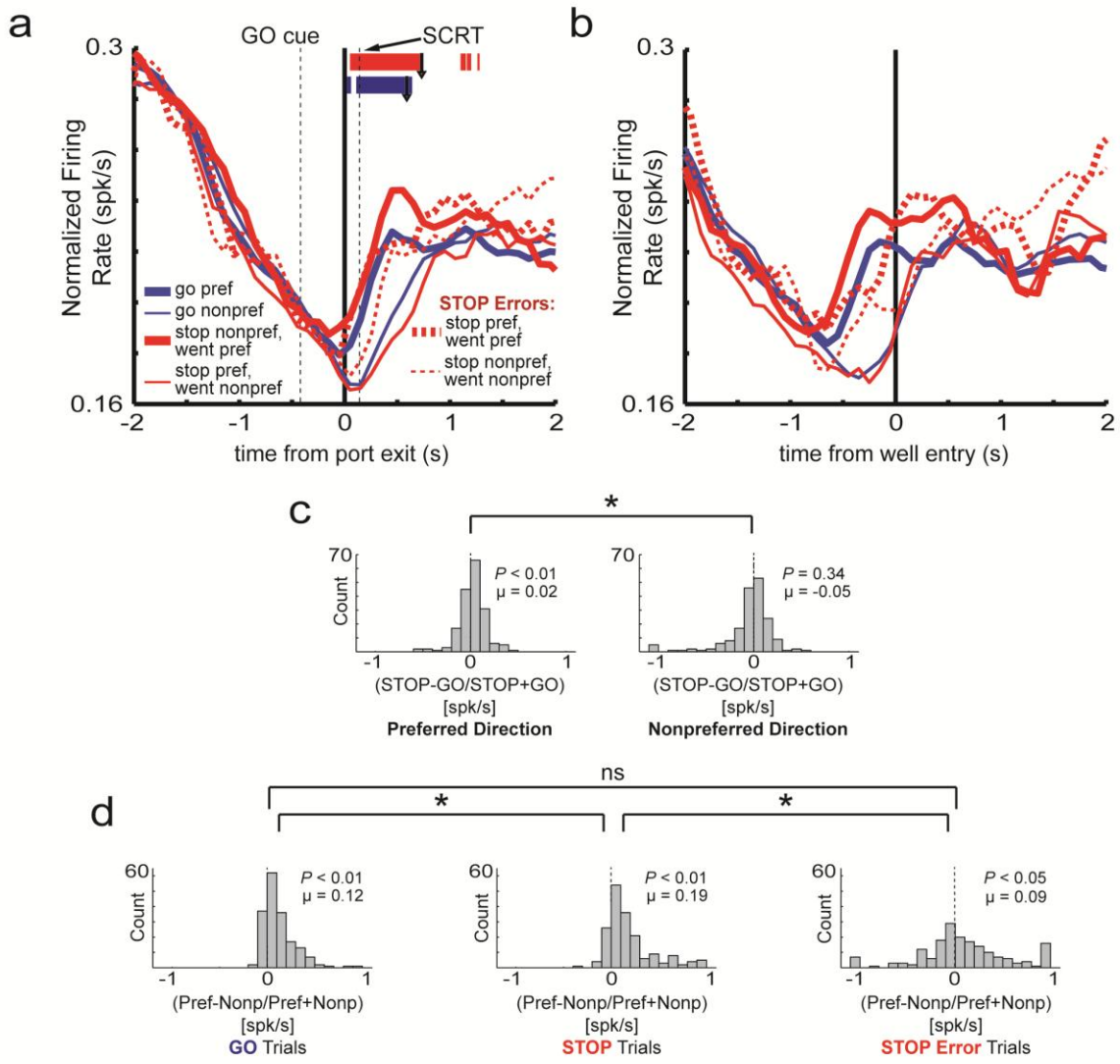
a
GO cue
SCRT
0.3
0.16
Normalized Firing Rate (spk/s)
go pref
go nonpref
stop nonpref, went pref
stop pref, went nonpref
STOP Errors:
stop pref, went pref
stop nonpref, went nonpref
-2
-1
0
1
2
time from port exit (s)
b
0.3
0.16
Normalized Firing Rate (spk/s)
time from well entry (s)
c
*
70
Count
P < 0.01
μ = 0.02
P = 0.34
μ = -0.05
(STOP-GO/STOP+GO)
[spk/s]
Preferred Direction
Nonpreferred Direction
d
ns
*
*
60
P < 0.01
μ = 0.12
P < 0.01
μ = 0.19
P < 0.05
μ = 0.09
(Pref-Nonp/Pref+Nonp)
[spk/s]
GO Trials
STOP Trials
STOP Error Trials

Relative to either lOFC or mDS, the directional signal on STOP trials in decreasing-type mPFC neurons is both greater and significantly distinct earlier relative to GO trials. This is an effect not seen in any of the previous populations of cells. It may then be the case that mPFC decreasing-type cells promote the correct direction on STOP trials since a comparable directional signal is observed between trials with similar speeds and movement mechanics: GO trials and errant STOP trials. However, a *stronger* directional signal on STOP trials does not fit with the "conflicted directional signal" hypothesis (Fig. 1.3B, 1.4B) where this signal should be *weaker* on STOP trials; instead it suggests that mPFC decreasing-type cells enhance directional encoding under conflict. Regardless, significant signaling of the correct direction early and strongly on STOP trials would provide an important mechanism useful for the flexible ability to alter behavior given new information.

Multiple regression analysis: When I isolated the impact that direction, movement time, and trial type had on individual mPFC decreasing-type cells, I first found that 54 cells (22%) significantly varied by the direction of the response outside of variance accounted for by movement speed or type of trial (Fig. 4.5; direction). Approximately equal proportions of these 54 cells had associated positive and negative β-values (28 vs. 26; binomial sign test; $p = 0.89$). The movement time variable generated significant partial r^2 values in 14% ($n = 34$) of cells (Fig. 4.5; movement time). Proportions of positive and negative β-values did not differ (22 vs. 12; binomial sign test; $p = 0.12$). Only a low number of cells ($n = 22$; 9%) were statistically modulated by the type of trial and the same number of these neurons had associated positive β-values (Fig. 4.5; trial type; 16 vs. 6; binomial sign test; $p = 0.05$). Therefore, a meaningful sub-set of

decreasing-type mPFC cells fall within the "inhibitory signal" hypothesis (Fig. 1.3C) although the majority of these neurons resemble "directional signal" encoding (Fig. 1.3A).

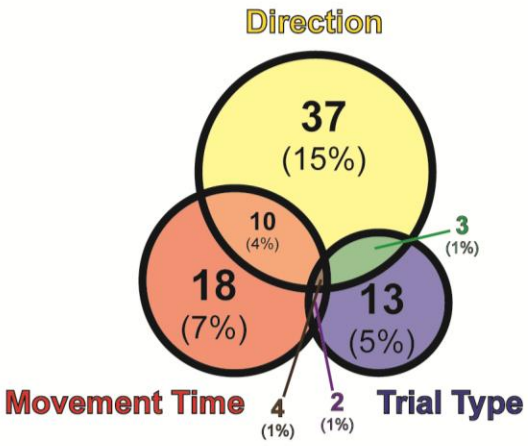

	Direction		Movement Time		Trial Type	
β-valence	+	-	+	-	+	-
	28	26	22	12	16	6

Figure 4.5: **Multiple regression results for decreasing-type mPFC neurons.** Circle sizes represent the relative proportions of neurons showing significant partial r^2 values for the individual task parameters. Top circle encompasses the proportion of neurons that show significant partial r^2 values for the direction parameter. Conventions as above for the movement time (red circle) and trial type (blue circle) parameters. Non-overlapping portions represent the counts (and percentages) of neurons with significant partial r^2 values for one parameter. Overlapping portions denote the counts (and percentages) of single cells that exhibited significant partial r^2 values for two (orange, green, purple) or all three (brown) parameters. The table specifies the counts of neurons significant within a variable that have associated positive ("+") or negative ("-") β-values. As specified by the model, positive β-values indicate greater firing for the contralateral direction (direction), greater firing for slower movement times (movement time), and greater firing for STOP over GO trials (trial type). Asterisks indicate significantly more β-values for one valence within a parameter (binomial sign test; $p < 0.05$).

Modulation of conflict by identity of previous trial: As in figure 4.3A, the population histogram for decreasing-type mPFC cells were replotted to distinguish STOP trials by the preceding trial type (Fig. 4.6A). When STOP trials discriminated by the previous trial type were compared to both GO trials and to each other (Fig. 4.6B), the only significant shift in the distributions came via the sS versus GO trial comparison (Fig. 4.6B *middle*; Wilcoxon; $p < 0.05$). When analyzing these two types of trials in figure 4.6A, one notices a peculiar pattern on sS trials (orange lines). Activity on these trials, in the preferred direction, diverges from the other trials in the preferred direction (thick red and blue lines), prior to port exit. This pattern is existent to a diminished degree in the nonpreferred direction. Despite this unique firing pattern, the directional signal is actually encoded later on sS trials (after the SCRT; Fig. 4.6A; orange ticks) relative to gS trials. Even though the directional strength throughout the entirety of the response was not different between these two "types" of STOP trials (Fig. 4.6C *middle* vs. *right*; Wilcoxon; $p = 0.75$), the earlier encoding of the correct direction on gS trials clashes with the reduced movement times (and presumably less conflict) on sS trials. No such comparable effect is found when comparing GO trials based on the identity of the previous trial (Fig. 4.6D). The direct comparison distribution between gG and sG trial types was not significantly shifted (Fig. 4.6E; Wilcoxon; $p = 0.75$) and the directional index distributions are not different from one another (Fig. 4.6F *left* vs. *right*; Wilcoxon; $p = 0.41$).

Figure 4.6: **Impact on neuronal encoding based on conflict induced by the previous trial in decreasing-type mPFC neurons. A)** Population histogram of mPFC neurons that decreased significantly below baseline. Activity is aligned to port exit. Blue lines refer to all GO trials. Red lines represent STOP trials preceded by GO trials ('gS'). Orange lines indicate trials where a STOP trial is preceded by a STOP trial ('sS'). Calculation of direction preference remained unchanged from figure 4.4. Tick marks represent 100ms epochs where the preferred direction was significantly different from the nonpreferred direction (t-test; $p < 0.01$) for GO trials (blue), gS trials (red), and sS trials (orange). Although each tick mark signifies statistical difference for a 100ms epoch, tick width is 10ms for the purpose of presentational detail. Arrowheads indicate average movement times (port exit to well entry) for GO trials (blue; 596ms), gS trials (red; 739ms), and sS trials (737ms). Vertical dashed lines mark the times of the stop change reaction time (SCRT; 141ms) and the average GO cue onset as measured as the latency from port exit (GO cue; -420ms) for the analyzed sessions. **B)** Indices compare the difference in firing between the three trial types presented in A. Leftmost distribution calculates the differences between gS and GO trials for each cell. The middle distribution marks the difference between sS and GO trials. Rightmost distribution computes the difference between gS and sS trials. **C)** Directional index distributions calculate the difference between the preferred and nonpreferred direction in each neuron during GO trials (*left*), gS trials (*middle*), and sS trials (*right*). **D)** Population histogram of increasing-type mDS neurons is aligned to port exit. All lines represent accurate GO trials that either followed a GO trial ('gG'; dark blue) or followed a STOP trial ('sG'; light blue). Thick lines refer to the preferred direction and thin lines refer to the nonpreferred direction. Tick marks denote the 100ms epochs where the preferred direction significantly differed from the nonpreferred direction (t-test; $p < 0.01$) during gG trials (dark blue) and sG trials (light blue). Arrowheads mark the average movement times for gG trials (dark blue; 597ms) and sG trials (light blue; 592ms). **E)** Distribution calculates the difference between firing on gG versus sG trials. **F)** Directional index distributions calculate the difference between the preferred and nonpreferred direction in each neuron during gG trials (*left*) and sG trials (*right*). Activity for all distributions was taken during the 1s epoch beginning at port exit and significant shifts from zero are determined via Wilcoxon ($p < 0.05$). Asterisks indicate a direct comparison between two distributions is significant (Wilcoxon; $p < 0.05$ corrected for multiple comparisons).

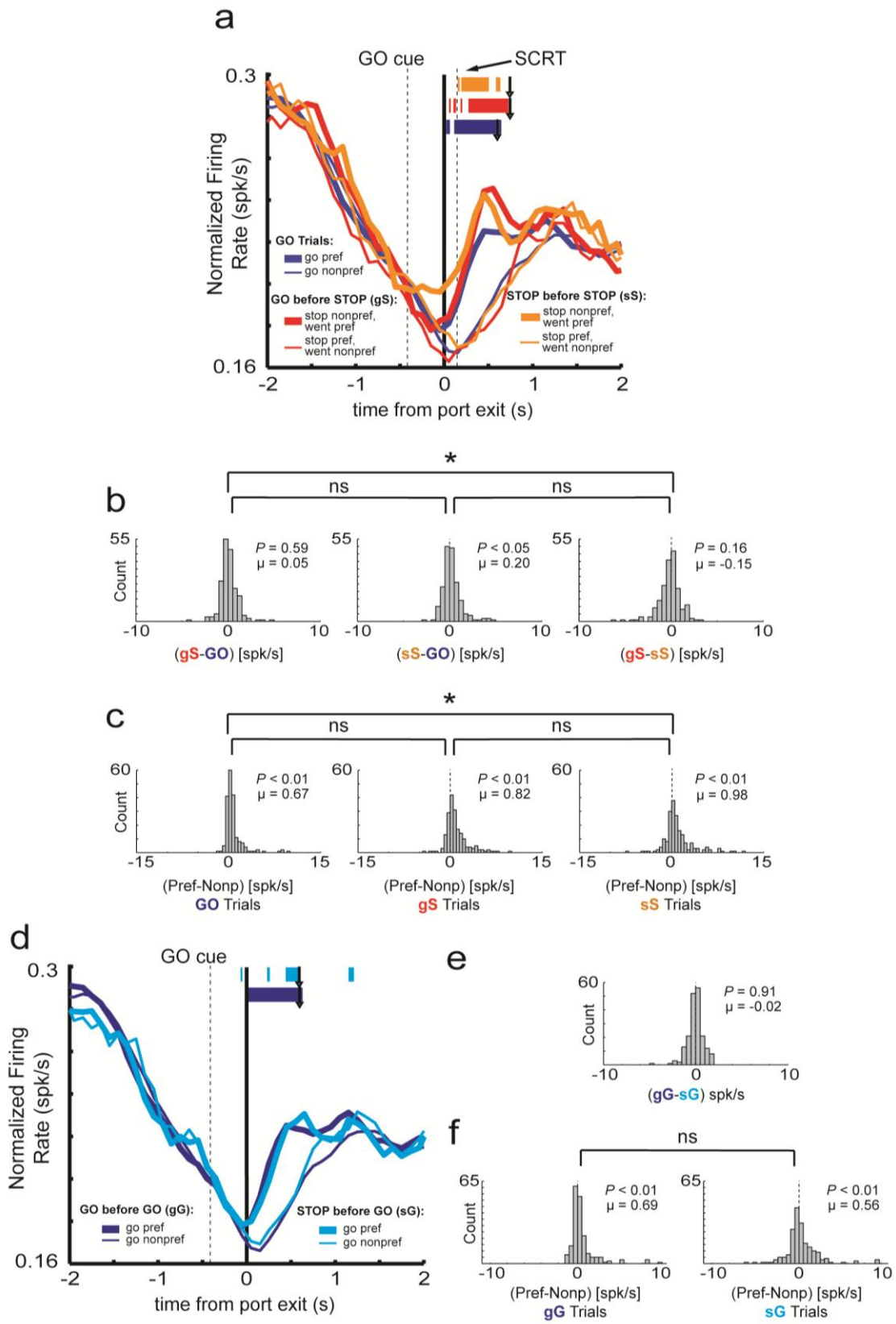
a
GO cue
SCRT
0.3
0.16
Normalized Firing Rate (spk/s)
GO Trials:
go pref
go nonpref
GO before STOP (gS):
stop nonpref, went pref
stop pref, went nonpref
STOP before STOP (sS):
stop nonpref, went pref
stop pref, went nonpref
-2
-1
0
1
2
time from port exit (s)
b
*
ns
ns
55
Count
P = 0.59
μ = 0.05
P < 0.05
μ = 0.20
P = 0.16
μ = -0.15
-10
0
10
(gS-GO) [spk/s]
(sS-GO) [spk/s]
(gS-sS) [spk/s]
c
*
ns
ns
60
Count
P < 0.01
μ = 0.67
P < 0.01
μ = 0.82
P < 0.01
μ = 0.98
-15
0
15
(Pref-Nonp) [spk/s]
GO Trials
(Pref-Nonp) [spk/s]
gS Trials
(Pref-Nonp) [spk/s]
sS Trials
d
GO cue
0.3
0.16
Normalized Firing Rate (spk/s)
GO before GO (gG):
go pref
go nonpref
STOP before GO (sG):
go pref
go nonpref
-2
-1
0
1
2
time from port exit (s)
e
60
Count
P = 0.91
μ = -0.02
-10
0
10
(gG-sG) spk/s
f
ns
65
Count
P < 0.01
μ = 0.69
P < 0.01
μ = 0.56
-10
0
10
(Pref-Nonp) [spk/s]
gG Trials
(Pref-Nonp) [spk/s]
sG Trials

Disparate waveform characteristics as a means to define increasing- and decreasing populations:

The difference in utility of mPFC increasing- and decreasing-type cells to the system may reside in the cell-types that characterize them. To distinguish whether these two mPFC populations occupy unique neuron types, I plotted inter-spike intervals, baseline firing frequencies, and waveform peak width (Fig. 4.7; A,B). There were no differences between increasing- decreasing-type neurons and effects appeared to be equally distributed across these electrophysiological properties.

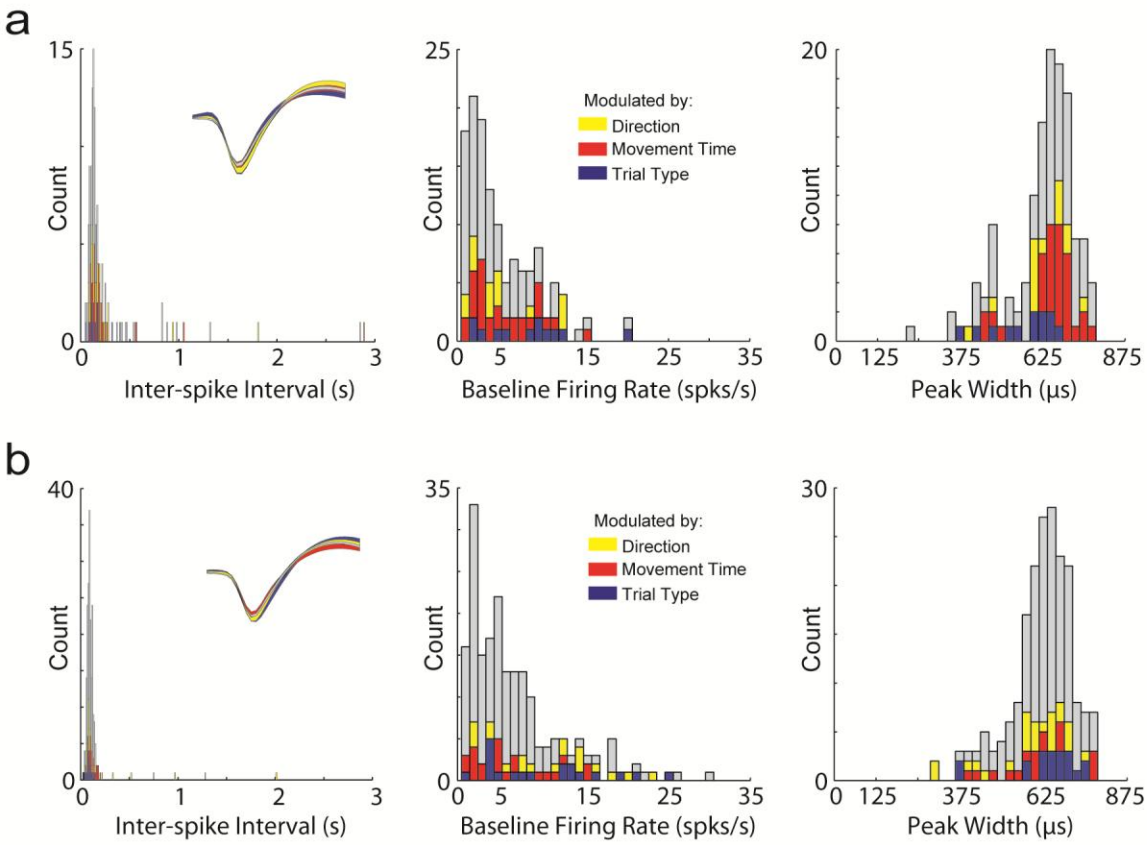

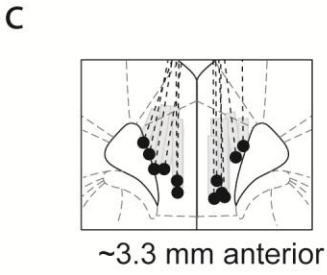

Figure 4.7: **Electrophysiological properties analysis for every increasing- and decreasing-type mPFC neuron. A)** Average inter-spike interval, defined as the latency between action potentials, for every increasing-type neuron (*left*). Colors indicate neurons significant in the multiple regression procedure for direction (yellow), movement time (red), and trial type (blue). Inset shows the average waveform ±SEM for all increasing-type neurons (gray) and the neurons significant in the multiple regression procedure (colors). Average baseline firing rate (spikes/s) taken from the 1s epoch beginning 2s prior to trial initiation is plotted for each increasing-type cell (*middle*). Average peak width defined as the time between the two highest peaks in the waveform is plotted for every increasing-type cell (*right*). **B)** Conventions as in A for decreasing-type neurons. **C)** Location of recording sites. Gray boxes mark extent of the recording locations. Black dots mark the bottom of the recording tract. Coronal slices approximately 3.3mm anterior to bregma.

Chapter Discussion

In the previous chapter regarding the function of lOFC neurons, I considered lOFC to be a cortical candidate for correcting STOP trial direction signaling via afferent connections to mDS. Increasing-type mPFC cells cannot be implicated in this function as activity does not show the time- or performance-sensitive flexibility in STOP trial directional signaling. For instance, in these neurons, direction differentiation during STOP trials does not occur until after the SCRT and therefore, in the context of swift response correction on STOP trials, mPFC does not serve this purpose early enough in the trial to impact immediate responding. The lack of temporal specificity for mPFC to control prompt behavior on trials that necessitate response inhibition does not mean that mPFC has no role in stop signal task behavior. It has been shown that mPFC neurons are sensitive to task components on the previous trial (*161*) and I have found that mPFC is the only region I studied where activity is significantly stratified based on the amount of previous conflict. The fact that this conflict signal appears *later* in the response suggests that instead of the mPFC guiding immediate behavior, it is tracking the prior conflict to ensure correct responding in the near future.

On the other hand, decreasing-type mPFC cells can have a causal impact on behavior during the current trial as direction differentiation on STOP trials occurs prior to the SCRT. Increased directional strength on STOP trials and a significant neuronal contrast between STOP and GO trials in the preferred direction offer further insight into the role of these neurons. Interestingly, firing in these cells differs only when an initial response is inhibited (correct STOP trials; Fig. 4.6; solid red lines) in the sense that activity is similar when the initial response is produced either correctly (GO trials; Fig.

4.6; blue lines) or in error (STOP errors; Fig. 4.6; dashed red lines). However, the resultant change in activity on correct STOP trials is a *stronger* directional signal relative to GO trials or STOP errors. This effect does not fit with either the "inhibitory signal" (Fig. 1.3C) or "conflicted directional signal" (Fig. 1.3B) hypotheses. Instead, these signals fit with what could be refer to as "enhanced directional signals" during difficult conflict trials (i.e. STOP trials). Therefore, decreasing-type mPFC cells are more likely functioning to refine a response rather than signal response inhibition. Further support for this notion comes from the analyses in figure 4.6 where early activity on sS trials (Fig. 4.6A; orange lines) begins to change its trajectory prior to exiting the port in preparation for an upcoming STOP cue that was induced by a prior STOP trial.

The two populations of mPFC neurons (increasing- and decreasing-type) provide evidence for dissociable functioning. Increasing-type cells encode for the increased need for conflict resolution based on the recent conflict history and decreasing-type cells provide response refinement function useful for guiding a change in responding behavior. These two divergent populations may provide a context for inconsistent findings on various response inhibition tasks after mPFC interference. For instance, perturbation of the rat prelimbic prefrontal cortex reveals stop signal reaction time deficits (*61*) and increased premature responses during performance of reaction time tasks (*157, 163*) while similar approaches yield conflicting results (*125, 160, 164*). The lack of a conflict monitor (increasing-type cells) could explain behavioral deficits on the stop signal task after mPFC inactivation while the absence of a speeded response refinement signal (decreasing-type cells) can explain increased premature responding.

Chapter 8: The prenatal nicotine exposure model of rodent impulsivity suggests that normal firing in medial prefrontal cortex is necessary for inhibitory control

Recording from three brain regions in healthy rats is a satisfactory approach for exploring the neural signals related to response inhibition. But what happens to the brain while animals with diseases characterized by reduced inhibitory capacity attempt to control/inhibit their responses? To answer this question, I recorded from the mPFC of rats who had been exposed to nicotine prenatally. Prenatal exposure to nicotine (PNE) has been shown to increase the incidence of psychiatric disorders in offspring, including but not limited to, attention deficit hyperactivity disorder (ADHD), conduct disorder, and addiction (*165-170*), all of which are characterized by diminished executive control (*166, 167, 171, 172*). In rodents, the behavioral disturbances described after PNE and the benefits observed after methylphenidate (Ritalin) treatment, have pinpointed prenatal nicotine exposure as a valuable animal model to investigate mechanisms that underlie poor impulse control as defined by the inability to inhibit prepotent movement (*173, 174*).

Although it is clear that PNE disrupts many brain systems involved in executive control, it is unknown how or what neural correlates related to the control of behavior are disturbed. It is known that dopaminergic and noradrenergic functions are affected by PNE (*175-177*), and that PNE alters morphology, volume, and dopamine turnover in mPFC (*173, 174, 178-180*), but it is still not understood how neural signals related to executive control mechanisms are affected. Although neighboring structures have been explored (*57, 88, 181*), prior to the work done in the previous chapter, it was unclear how firing in mPFC is normally modulated during tasks that probe response inhibition. This

is surprising considering the number of studies that have implicated mPFC in inhibitory control. For instance, perturbation of the rat prelimbic prefrontal cortex reveals stop signal reaction time deficits (*61*) and increased premature responses during performance of reaction time tasks (*157, 163*). However, similar approaches have yielded conflicting results (*125, 160, 164*). Elucidating the relationship between mPFC activity and response selection during the need for elevated executive and inhibitory control would help me to better understand dysfunctions observed in psychiatric disorders that impair inhibitory restraint.

To address this issue I recorded single mPFC cells from control and prenatal nicotine exposed (PNE) rats in my rodent variant of the stop signal task (methodology in Chapter 10: Detailed Methods). Due to the tractability of the rat, experimental prenatal nicotine exposure may provide a valuable tool to investigate mechanisms disrupted in animal models of impaired executive function and impulse control. It has been shown that mPFC is both affected by exposure to prenatal nicotine and is critical for normal performance on stop signal paradigms (*61, 173, 174*). Briefly, I show that PNE makes rats faster and more impulsive on the stop signal task. Additionally, PNE manifests in a hypoactive mPFC, diminished encoding of task parameters, and reduced capacity to maintain conflict information.

Prenatal nicotine exposure impairs inhibitory control

Full details of prenatal nicotine administration reside in Chapter 10: Detailed Methodology. Briefly, in a subset of nulliparous female rats, nicotine was added to their only source of drinking water at a dose akin to a human habitual smoker while control

mothers were provided with unadulterated drinking water. Nicotine exposed mothers in the present experiment consumed significantly less water than controls during pregnancy (98.89ml/kg/day; 131ml/kg/day; t-test; $p < 0.01$) and gained weight at a slower rate prior to pregnancy (0.21% gain per day; 0.68% gain per day; t-test; $p < 0.01$), characteristics that have been observed before by Schneider and colleagues (*182*). Pregnancy duration and fluid consumption comparisons are detailed in table 5.1. All pups were cross-fostered to control mothers in order to isolate the effects of nicotine exposure prenatally and minimize unique rearing practices by nicotine exposed mothers. Pups were not exposed to nicotine in any manner after birth.

Mothers			
	Nicotine (0.06mg/ml)	**Control (0mg/ml)**	***p***
Number of Pregnant Females	3	4	0.7055
Body Weight Prior to Exposure (g)	242.67	241.67	0.8615
Weight Increase Prior to Pregnancy (% per day)	0.21	0.68	0.0000 *
Maternal Weight on GD1 (g)	280.33	315.67	0.2475
Pregnancy Length	25.33	25.33	1.0000
Weight Gain during Pregnancy (total %)	42.33	38.11	0.1050
Fluid Consumption during Habituation (ml/kg/day)	87.63	112.39	0.0595
Fluid Consumption during Pregnancy (ml/kg/day)	98.89	131.00	0.0090 *

Offspring			
	Nicotine (0.06mg/ml)	**Control (0mg/ml)**	***p***
Litter Size	13.00	12.33	0.8946
Sex Ratio (% Females)	56.62	49.01	0.4720
Male Weights at Task Training (PND49)	270.65 (n = 17)	259.17 (n = 23)	0.5593

Table 5.1: Comparisons of physical characteristics between the PNE group (0.06mg/ml of nicotine in the drinking water) and the control group (unadulterated drinking water). All values are compared using a t-test ($p < 0.05$) except "Number of Pregnant Females" which was compared using a χ^2 test ($p < 0.05$).

Rats from both groups were trained prior to electrode surgery on my stop signal task. Rats in both control and PNE groups exhibited significantly slower movement speeds (latency from port exit to well entry; Fig. 5.1A) and reduced accuracy on STOP trials compared to GO trials (Fig. 5.1B). Slower latencies resulted in better STOP trial performance in both groups. Like in the analyses for the previous brain regions, during sessions in which rats were slower on STOP trials, performance was better (i.e. correlation between movement speed and percent correct) demonstrating a speed-accuracy tradeoff. Consistent with this finding, incorrect STOP trial movement times were significantly faster than movement times on correctly performed STOP trials (Fig. 5.1A; t-test; $p < 0.05$). These results demonstrate that PNE rats were planning and generating a movement prior to illumination of the STOP cue, in response to illumination of the first cue light, and that inhibition and redirection of the behavioral response was necessary to correctly perform STOP trials.

Figure 5.1: **Behavior and neuronal differences between control and PNE groups. A-B)**
Session averaged movement times (ms) (A) and percent of correct responses (B). Error bars indicate standard error of the mean. Asterisks indicate group comparisons (t-test; $p < 0.05$). **C)** Histogram represents the proportion of premature responses (withdraw from the nose-poke prior to GO light offset) for control and PNE rats per session. Inset represents the average proportion of premature responses for control and PNE rats. Asterisk indicates significant mean difference (t-test; $p < 0.05$). All behavior was taken from neural recording sessions. **D)** Percentage of cells that showed significantly greater (increasing-type) or less (decreasing-type) activity during the response epoch (unpoke to well entry) relative to baseline (1s epoch beginning 2s prior to nose-poke). There were a total of 636 control cells and 558 PNE cells. **E)** Percentage of cells per rat that were characterized as either increasing- or decreasing-type. Error bars indicate standard error of the mean. **F-G)** Average activity (spikes/s) across GO trials, STOP trials, and STOP errors ± SEM aligned on port exit for every increasing- (F) and decreasing-type (G) cell. As a temporally sensitive statistical comparison, the p-value for the t-test (black line) between control and PNE firing rates was taken from 100ms epochs that slid every 10ms and plotted in the graph below. The gray horizontal line refers to the p-value 0.05.

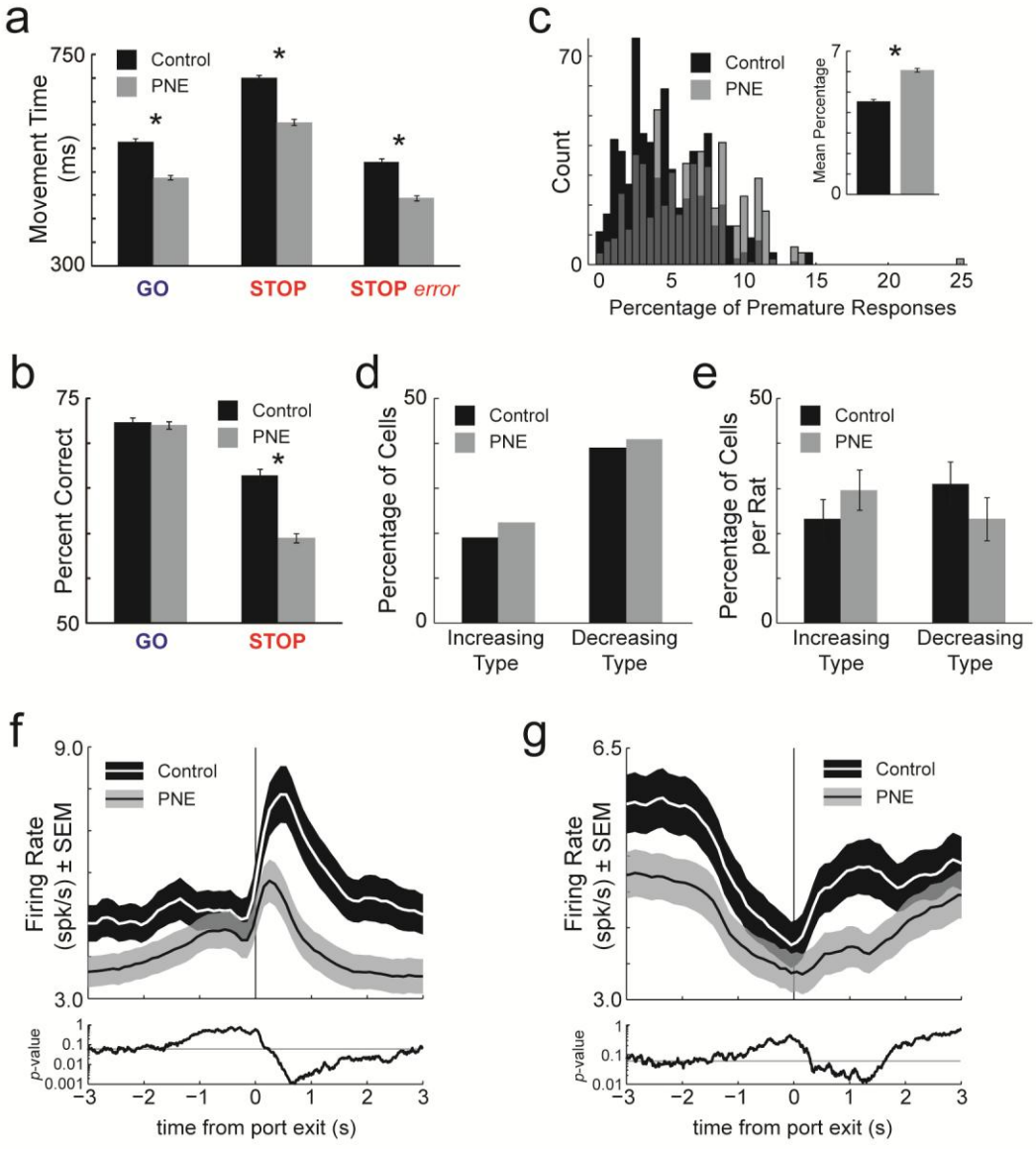
a
750
300
Movement Time (ms)
Control
PNE
*
*
*
GO
STOP
STOP error
c
70
0
Count
Control
PNE
7
0
Mean Percentage
*
0
5
10
15
20
25
Percentage of Premature Responses
b
75
50
Percent Correct
Control
PNE
*
GO
STOP
d
50
0
Percentage of Cells
Control
PNE
Increasing Type
Decreasing Type
e
50
0
Percentage of Cells per Rat
Control
PNE
Increasing Type
Decreasing Type
f
9.0
3.0
Firing Rate (spk/s) ± SEM
Control
PNE
1
0.1
0.01
0.001
p-value
−3
−2
−1
0
1
2
3
time from port exit (s)
g
6.5
3.0
Firing Rate (spk/s) ± SEM
Control
PNE
1
0.1
0.01
p-value
−3
−2
−1
0
1
2
3
time from port exit (s)

When comparing control and PNE rats I found that PNE rats were significantly faster on all trial types (Fig. 5.1A; black vs. gray; t-test; $p < 0.05$). Although the two groups did not differ significantly in accurate performance of GO trials, PNE rats made significantly more errors on STOP trials than control rats (Fig. 5.1B; black vs. gray; t-test; $p < 0.05$). Despite the difference in STOP trial movement speed and accuracy, the correlation between the two (speed/accuracy trade-off) was not altered between groups (control; $r = 0.33$; $p < 0.01$; PNE; $r = 0.38$; $p < 0.01$). This consistency between groups suggests that PNE rats were not fundamentally disabled or physically impeded from performing the task. Interestingly, PNE rats exhibited a greater proportion of premature responses (defined as leaving the nose port before offset of the first cue light) per session relative to control rats (Fig. 5.1C; t-test; $p < 0.01$). I conclude that PNE limits the capacity for successful inhibitory control, but not overall ability to meet the physical demands of the task.

Impact of prenatal nicotine exposure on population activity in mPFC

I recorded 636 and 558 mPFC neurons from control and nicotine exposed rats, respectively. The recording locations are illustrated in figure 4.7C and 5.7C. The neurons/sessions analyzed in the previous chapter serve as the control group here. I first determined how many neurons in each group exhibited activity that was significantly modulated during the response epoch (port exit to well entry) relative to baseline (1s epoch beginning 2s prior to trial initiation; t-test; $p < 0.05$).

In the control group, 19% ($n = 121$) and 39% ($n = 249$) of neurons significantly increased or decreased firing during the response epoch relative to baseline, respectively.

In the PNE group, 22% (n = 125) and 41% (n = 228) of neurons exhibited significant increases or decreases during the response epoch, respectively. The proportion of increasing- and decreasing-type cells did not differ between groups (Fig. 5.1D; increasing-type; χ^2; p = 0.17; decreasing-type; χ^2; p = 0.59). To provide evidence for homogeneity between rats within a group, I plotted the percentage of increasing- and decreasing-type neurons per rat. The control group did not differ from the PNE group (Fig. 5.1E; increasing-type; Wilcoxon; p = 0.43; decreasing-type; Wilcoxon; p = 0.49). Even though the proportions of task-related neurons did not differ between groups, average activity in numerous task epochs was reduced across the population of increasing- and decreasing-type neurons. This is illustrated by the mean firing rates (±SEM ribbons with sliding comparisons) in figures 5.1F and G, which plots the average firing (spikes/s) over time (aligned on port exit and averaged across trial types).

Even though activity was reduced in the PNE group, the proportions of task-modulated (i.e. increasing- or decreasing-type) did not change. This is important because it shows that the hypoactivation as a result of PNE was present both during the execution of the task and when the rats were in a relative state of quiescence (baseline). Additionally, both of these populations can be compared across groups with minimal concern that PNE firing reductions alone omitted cells from further analysis.

Multiple regression analysis of single-unit activity in mPFC

Since single cells tended to be modulated by the direction of the response and/or type of trial (STOP vs. GO; as in Fig. 1.4), I determined if the counts of neurons exhibiting task-related effects were different between the two groups. Specifically, I

performed the least-squares multiple regression approach described in Chapter 10: Detailed methods (identical to the model used in each of the previous chapters). The model used was designed to determine if neuronal firing during the response correlates significantly and uniquely with movement speed, direction, and/or type of trial at the single-cell level as done in the previous chapters.

Figure 5.2: **Multiple regression results for all increasing- and decreasing-type mPFC neuron in the control and PNE groups. A-D)** Results of the multiple regression procedure detailed in the *Methods* section for increasing- (A,C) and decreasing-type (B,D) cells in control (A,B) and PNE groups (C,D). The size specifications of the Venn diagrams map onto the proportion of neurons within a population that survived the regression procedure (i.e. exhibited partial r^2 values for at least one variable) relative to the other populations. Circle sizes represent the relative proportions of neurons showing significant partial r^2 values for the individual task parameters *within* a population. Top circle encompasses the proportion of neurons that show significant partial r^2 values for the direction parameter. Conventions as above for the movement time (red circle) and trial type (blue circle) parameters. Non-overlapping portions represent the counts (and percentages) of neurons with significant partial r^2 values for one parameter. Overlapping portions denote the number (and percentage) of single cells that exhibited significant partial r^2 values for two (orange, green, purple) or all three (brown) parameters. The table specifies the counts of neurons significant within a variable that have associated positive ("+") or negative ("-") β-values. As specified by the model, positive β-values indicate greater firing for the contralateral direction (direction), greater firing for slower movement times (movement time), and greater firing for STOP over GO trials (trial type). Asterisks indicate significantly more β-values for one valence within a parameter (binomial sign test; $p < 0.05$).

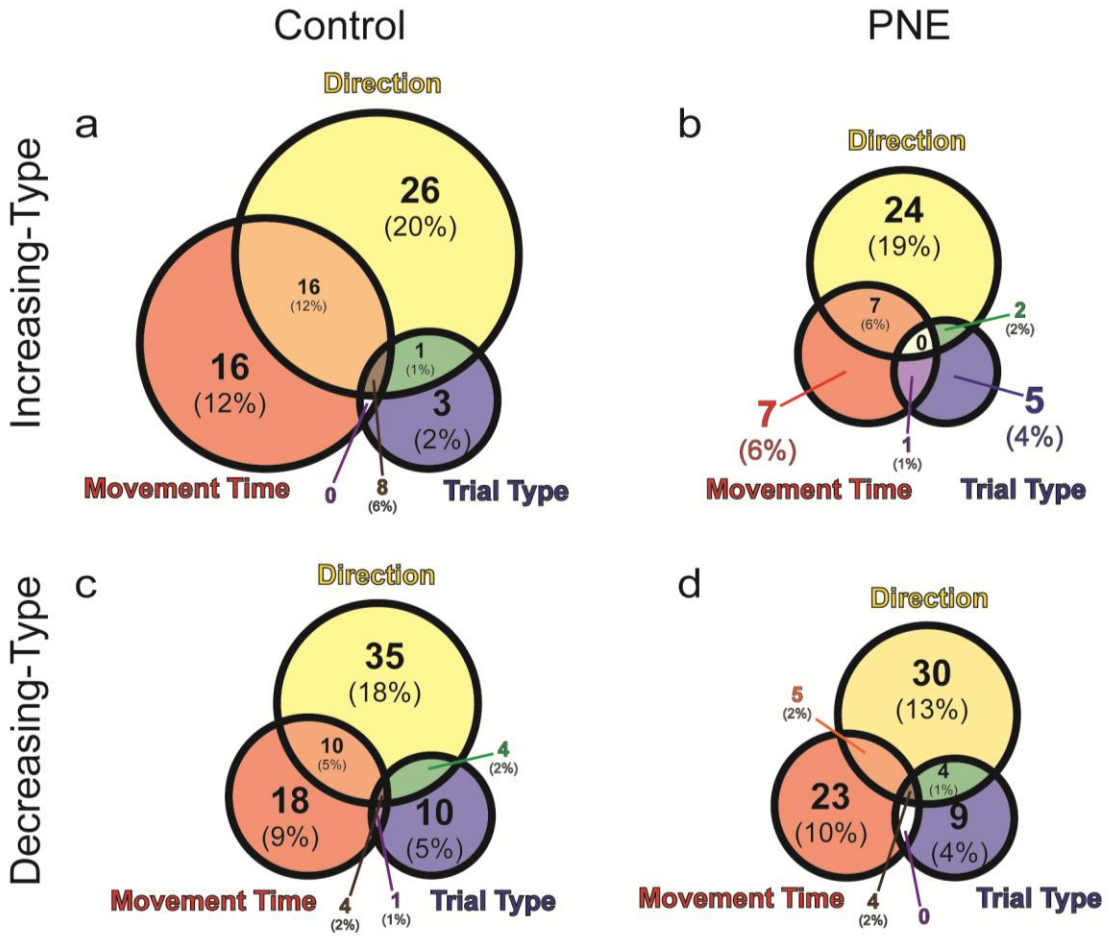

Increasing Type	Direction		Movement Time		Trial Type	
β-valence	+	-	+	-	+	-
Control	21	24	9	***28****	8	5
PNE	***24****	9	7	8	***8****	0

Decreasing Type	Direction		Movement Time		Trial Type	
β-valence	+	-	+	-	+	-
Control	28	26	22	12	16	6
PNE	***29****	14	21	11	9	8

The results of the regression procedure for the control group (originally shown in figures 4.2 and 4.5) are replicated in figure 5.2 A and C. The relative sizes of the Venn diagrams denote the proportions of task specific cells (significant partial r^2 for at least one parameter) in each population. In direct comparison to increasing-type control neurons, I examined increasing-type neurons in the PNE group (Fig. 5.2B). Of these cells, 26% (n = 33) were significantly modulated by direction. Twenty four of these 33 had associated positive β-values (greater firing in the contralateral direction) which is statistically greater than the number of neurons with associated negative β-values (Fig. 5.2B; direction; 24 vs. 9; binomial sign test; $p < 0.05$). Of the neurons that were significantly and uniquely correlated with movement speed (Fig. 5.2B; movement time; n = 15; 12%), an insignificant proportion featured positive β-values (Fig.5.2; movement time; 7 vs. 8; binominal sign test; $p = 1$). Lastly, increasing-type neurons of PNE rats had 8 neurons that were modulated by the trial type parameter; of which, statistically more featured positive β-values than negative β-values (Fig. 5.2B; trial type; 8 vs. 0; binomial sign test; $p < 0.01$).

Figure 5.2C and D detail the relatively similar results of the regression procedure for control (B) and PNE (D) decreasing-type mPFC cells. Eighteen percent (n = 43) of PNE decreasing-type cells exhibit significant partial r^2 values for the direction parameter where more β-values were positive than negative (Fig. 5.2D; direction; 29 vs. 14; binominal sign test; $p < 0.05$). Decreasing-type neurons in the PNE group showed 32 (14%) neurons significantly modulated by the movement time parameter but the proportion of the two β-values did not differ (Fig. 5.2D; movement time; 21 vs. 11; binominal sign test; $p = 0.11$). Lastly, the PNE group exhibited 17 (7%) significant

partial r^2 values for type of trial and the featured β-values did not differ from a 50/50 split (Fig. 5.2D; trial type; 9 vs. 8; binomial sign test; $p = 1$).

To more simply compare the proportions of neurons significantly correlated with individual task parameters, I collapsed increasing- and decreasing-type cells in both groups individually and plotted them in figure 5.3. The Venn diagrams featured in figure 5.2 detail the overlap in significance of the three task parameters in individual cells; because of this, I categorized neurons in figure 5.3 where a single neuron can contribute to more than one group. Specifically, the percentage of direction, movement time, and trial type neurons were compared between the control and PNE groups. Significantly more neurons were modulated by each of the individual parameters in the control group relative to the PNE group (χ^2; $ps < 0.05$). Therefore, along with behavioral changes and hypoactivation, PNE reduced the selectivity of individual mPFC neurons to important portions of the task.

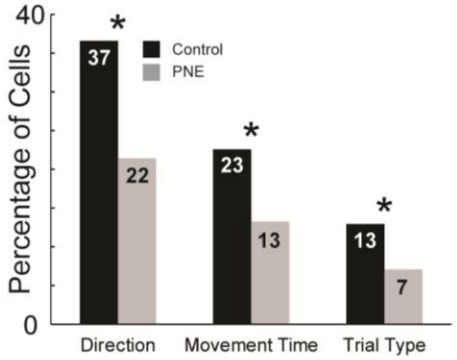

Figure 5.3: **Results of the multiple regression procedure compared between control and PNE groups.** Results of the regression analysis for every increasing- and decreasing-type cell. Each bar represents the percentage of cells where firing rate during the response epoch is correlated with a given parameter significantly and uniquely relative to the remaining parameters (partial r^2; $p < 0.05$). Many single neurons were selective for more than one parameter in this procedure. Details of this overlap in figure 5.2. Asterisks reveal significantly different proportions of cells (χ^2; $p < 0.05$).

Activity in mPFC is correlated with behavioral performance

The data described above demonstrates that both neural activity and performance were reduced in PNE rats. Here I ask if the two are correlated. Specifically, I determine via correlation whether average firing rates are correlated with behavioral measures of accuracy and movement speed between sessions.

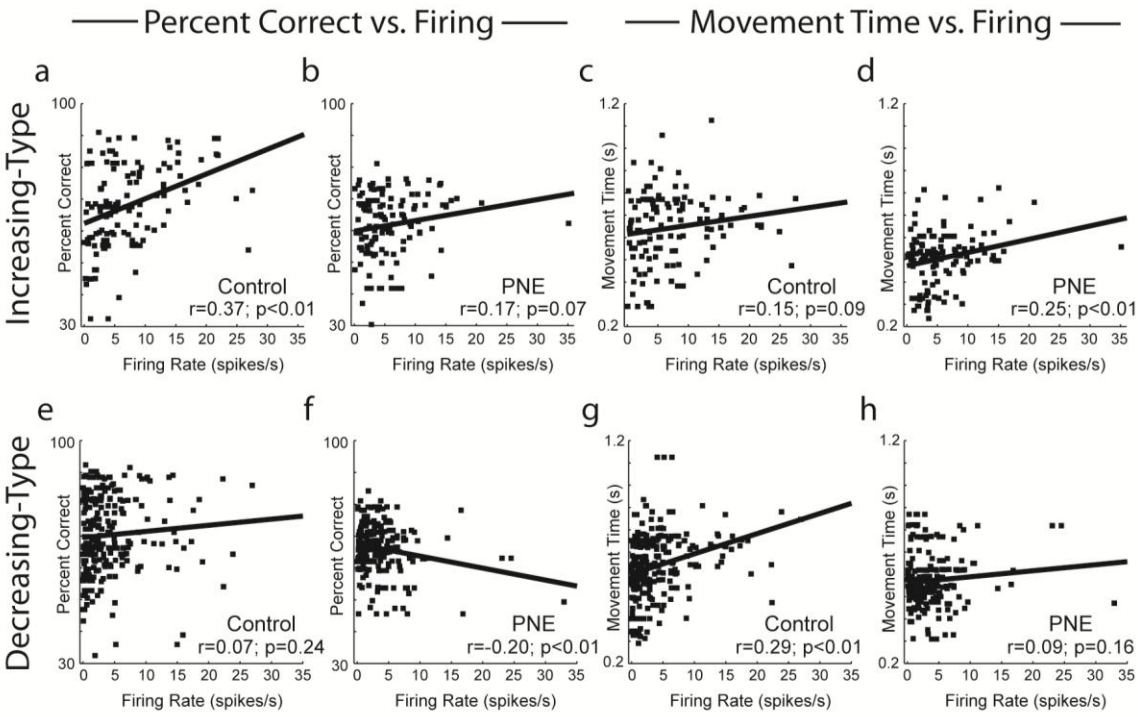

Figure 5.4: **Correlation between neuronal firing and behavior in the control and PNE groups. A-B,E-F)** Plots of firing rate on correct trials during the response epoch versus percent correct for all trial types averaged for each session are shown for increasing- (A,B) and decreasing-type (E,F) cells in the control (A,E) and PNE (B,F) groups. **C-D,G-H)** Plots of firing rate on correct trials versus movement time averaged on each session for increasing- (C,D) and decreasing-type (G,H) cells in control (C,G) and PNE (D,H) groups. Each dot represents a single neuron.

For increasing-type cells, firing during the response epoch was positively correlated with percent correct. That is, the greater the average firing rate during a session, the more accurate the animal was on that session. The regression was significant for the control (Fig. 5.4A; $r = 0.37$; $p < 0.01$) but not the PNE group (Fig. 5.4B; $r = 0.17$; $p = 0.07$). Further, these correlations were significantly different from one another (Fig. 5.4A vs. B; t-test; $p < 0.05$). The correlation between movement time and firing rate was significant for increasing-type cells only in the PNE group (Fig. 5.4D; $r = 0.25$; $p < 0.01$) but this correlation did not significantly differ from the control group (Fig. 5.4C vs. D; t-test; $p = 0.42$). However, for decreasing-type neurons, there *was* a positive correlation between movement time and firing rate, which was only significant in the control group (Fig. 5.4G; $r = 0.29$; $p < 0.01$) and was significantly different from the PNE group (Fig. 5.4G vs. H; t-test; $p < 0.01$). Finally, the correlation between firing rate and percent correct in decreasing-type cells was not significant in the control group (Fig. 5.4E; $r = 0.07$, $p = 0.24$), but was significantly *negatively* correlated in the PNE group (Fig. 5.4F; $r = -0.20$; $p < 0.01$). These correlations differed significantly (Fig. 5.4E vs. F; t-test; $p < 0.01$). Thus overall, when activity was high for increasing- and decreasing-type neurons, rats were better and slower, respectively. These correlations were largely not present in PNE rats. Furthermore, in sessions where decreasing-type neuronal activity was high, PNE rats tended to perform the task poorly. Importantly, the correlation results above are not simply a product of mPFC hypoactivation as these effects are maintained in a sub-selected population of firing-rate matched neurons between groups (data not shown).

Previous trial encoding and the ability to resolve conflict

Both groups of animals were less accurate on STOP trials following GO trials (gS) compared to STOP trials following STOP trials (sS; Fig. 5.5E, t-test, $p < 0.05$); however this effect was amplified in PNE rats (t-test, $p < 0.01$). This effect is presumably due to the heightened prepotency to respond to the first cue light induced by a previous GO trial which makes it more difficult for the rat to suppress the initial response on STOP trials. This demonstrates that the competition or 'conflict' between the two opposing responses (GO vs. STOP) is highest on gS trials, and it is during these trials that PNE rats perform the worst. It is well known that greater inhibitory control is necessary to overcome higher prepotency and frontal areas including mPFC (as supported by the previous chapter) are important for resolving conflict under these situations (*66-68*, *162*). Next I ask if this encoding of previous conflict is disrupted by PNE.

Figure 5.5: **Impact on neuronal encoding based on conflict induced by the previous trial in increasing-type control and PNE mPFC neurons. A-B)** Population histograms of all mPFC neurons that increased significantly above baseline in control (A) and PNE (B) groups. Activity is aligned to port exit. Blue lines refer to all GO trials. Red lines represent STOP trials preceded by GO trials ('gS'). Orange lines indicate trials where a STOP trial is preceded by a STOP trial ('sS'). Direction preference was determined in each cell by calculating the direction that elicited the greatest firing rate during the epoch from port exit to well entry ('response epoch'). Therefore, as defined by the analysis, the preferred direction (thick lines) is always higher than the nonpreferred direction (thin lines) during the response epoch. The direction of STOP trials is always referred to the ultimate response the animal made. The population histogram in A is a replication of figure 4.3A, but firing rate is not normalized in order to accentuate firing rate differences between control and PNE neurons. **C-D)** Indices compare the difference in firing between the three trial types presented in (A-B) for control (C) and PNE (D) groups. Leftmost distribution calculates the differences between gS and GO trials divided by the sum for each cell. The middle distribution marks the difference between sS and GO trials divided by the sum. Rightmost distribution computes the difference between gS and sS trials divided by the sum. Activity for all distributions was taken during the 1s epoch beginning at port exit in order to capture post decision activity and significant shifts from zero are determined via Wilcoxon ($p < 0.05$). Distributions between groups are compared via Wilcoxon ($p < 0.05$). **E-F)** Percent of correct responses (E) and movement latencies (F) per session for sS and gS trials. Movement times are calculated as the latency from port exit to well entry. Asterisks indicate significant mean differences (t-test; $p < 0.05$).

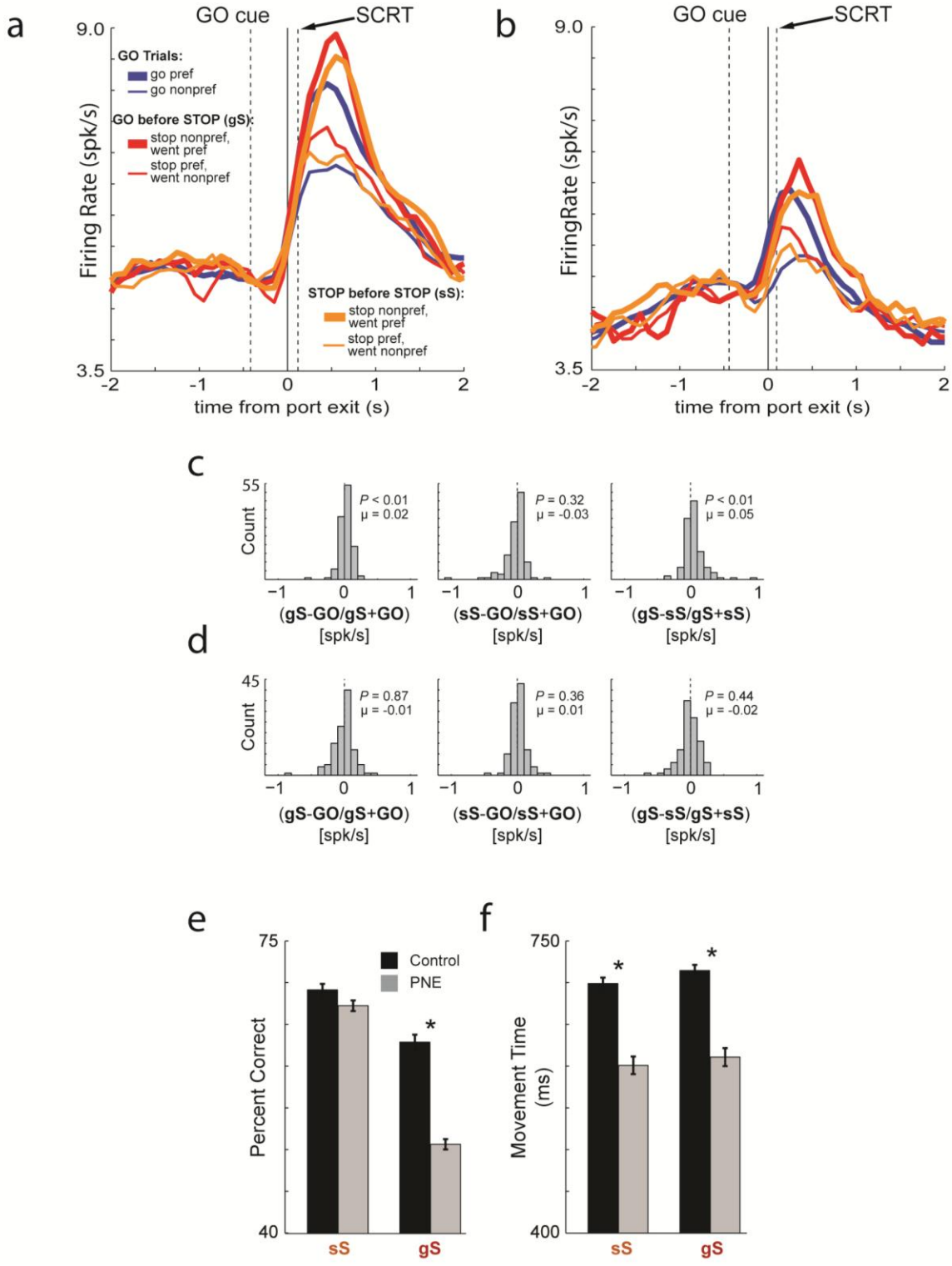
a
GO cue
SCRT
9.0
3.5
Firing Rate (spk/s)
GO Trials:
go pref
go nonpref
GO before STOP (gS):
stop nonpref, went pref
stop pref, went nonpref
STOP before STOP (sS):
stop nonpref, went pref
stop pref, went nonpref
-2
-1
0
1
2
time from port exit (s)
b
GO cue
SCRT
9.0
3.5
FiringRate (spk/s)
time from port exit (s)
c
55
Count
P < 0.01
μ = 0.02
P = 0.32
μ = -0.03
P < 0.01
μ = 0.05
(gS-GO/gS+GO)
[spk/s]
(sS-GO/sS+GO)
[spk/s]
(gS-sS/gS+sS)
[spk/s]
d
45
Count
P = 0.87
μ = -0.01
P = 0.36
μ = 0.01
P = 0.44
μ = -0.02
(gS-GO/gS+GO)
[spk/s]
(sS-GO/sS+GO)
[spk/s]
(gS-sS/gS+sS)
[spk/s]
e
75
40
Percent Correct
Control
PNE
*
sS
gS
f
750
400
Movement Time (ms)
*
*
sS
gS

Figures 5.5A and B plot average activity on STOP trials when the previous trial was either a GO trial (gS, red) or a STOP trial (sS, orange) for the control (Fig. 5.5A) and PNE (Fig. 5.5B) groups. For reference, GO (low conflict) trials during these sessions are plotted in blue. I have shown the effect of conflict monitoring in the control group previously in figure 4.3 but, in order to capture the reduction in firing rates in the PNE group, these population histograms are plotted using raw firing rates. This does not impact the statistical analyses and therefore, the results of figure 5.5C are identical those in figure 4.3B. Briefly, differences in firing between the three trials are quantified in figure 5.5C and D which compares the difference between higher and lower conflict trial types (i.e., gS-GO, sS-GO, and gS-sS) for each neuron during the 1s epoch beginning at port exit. In the control group, the distribution comparing gS to GO (i.e., gS-GO) was significantly shifted in the positive direction (Fig. 5.5C *left*; Wilcoxon; $p < 0.01$), whereas this distribution in the PNE group was not significantly shifted (Fig. 5.5D *left*; Wilcoxon; $p = 0.87$). When comparing activity on sS trials to GO trials, neither group exhibited a significantly shifted distribution (sS-GO; Fig. 5.5C,D *middle*; Wilcoxon; $ps > 0.32$). Importantly, direct comparison of gS and sS trials revealed a statistically shifted distribution in the control group (Fig. 5.5C; Wilcoxon; $p < 0.01$) which differed from the equivalent distribution in the PNE group (Fig. 5.5C *right* vs. D *right*; Wilcoxon; $p < 0.01$). Thus, when conflict was high, firing in mPFC tended to be significantly stronger in control but not PNE rats. Importantly, this group difference is not simply a product of the identity of the previous trial because these differences were not observed between gG and sG trials (Fig. 5.6A-D). That is, direct comparison of GO trials dissociated by the

previous trial type revealed no differences in either the control (Fig. 5.6A,C) or PNE (Fig. 5.6B,D) groups.

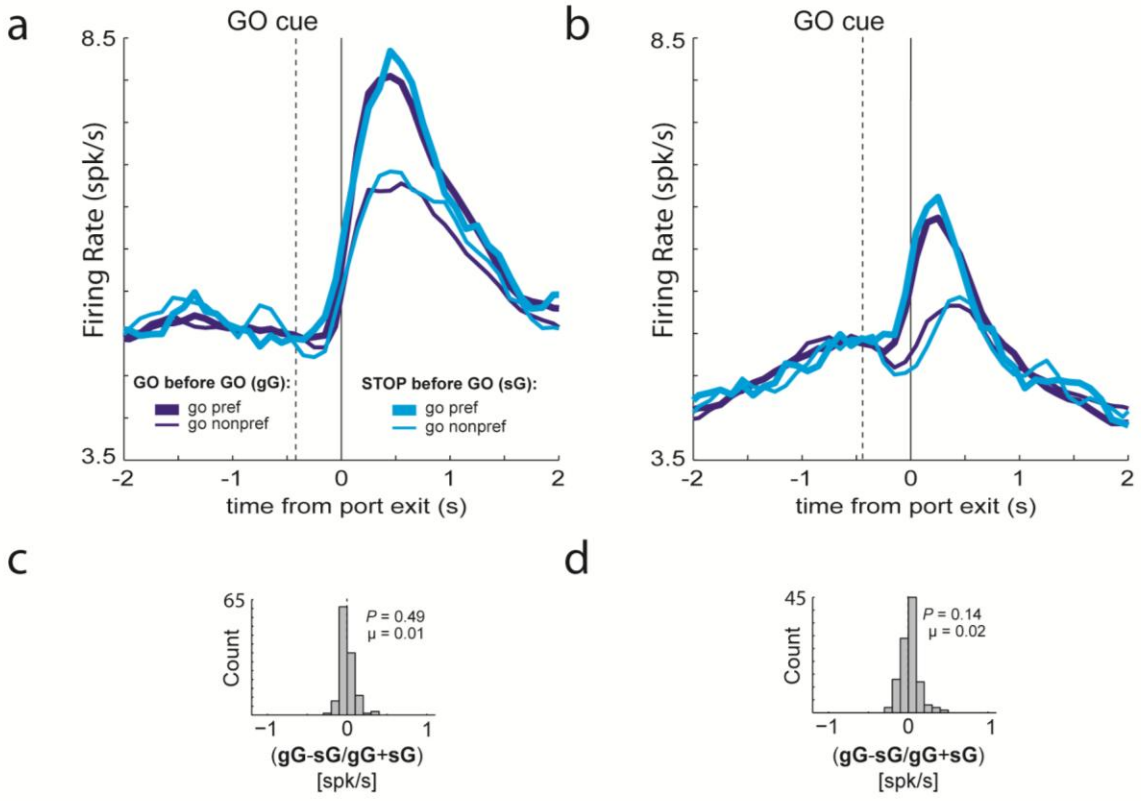

Figure 5.6: **Impact of the previous trial on current GO trial firing in control and PNE mPFC firing. A-B)** Population histograms of all mPFC neurons in the control (A) and PNE (B) groups that fired significantly above baseline between port exit to well entry (termed 'response epoch'). Activity is aligned to port exit. All lines represent accurate GO trials that either followed a GO trial ('gG'; dark blue) or followed a STOP trial ('sG'; light blue). Thick lines refer to the preferred direction defined as the direction that elicited the greatest firing rate during the response epoch. Thin lines refer to the nonpreferred direction. **C-D)** Distributions calculate the difference between firing during the 1s epoch following port exit on gG versus sG trials divided by the sum for control (C) and PNE (D) groups. Significance is determined via t-test ($p < 0.05$).

Together, these results demonstrate that the mPFC in control animals was able to differentiate STOP trials based on the conflict induced by the preceding trial type and this neural correlate of conflict monitoring was disrupted in animals prenatally exposed to nicotine. This could explain the marked behavioral deficits on gS trials relative to sS trials in the PNE group (Fig. 5.5E). Importantly, this conflict monitoring effect is not simply due to mPFC hypoactivation in PNE rats. In a group of sub-selected neurons matched for firing rate across groups, control neurons still capably differentiated between gS and sS trials (data not shown).

Disparate waveform characteristics as a means to define increasing- and decreasing populations in mPFC

As a means to electrophysiologically dissociate the morphology (type) of increasing- from decreasing-type cells, I plotted interspike intervals, baseline firing frequencies, and waveform peak width (Fig. 5.7; A,B). There were no differences between increasing- decreasing-type PNE neurons and effects appeared to be equally distributed across these properties.

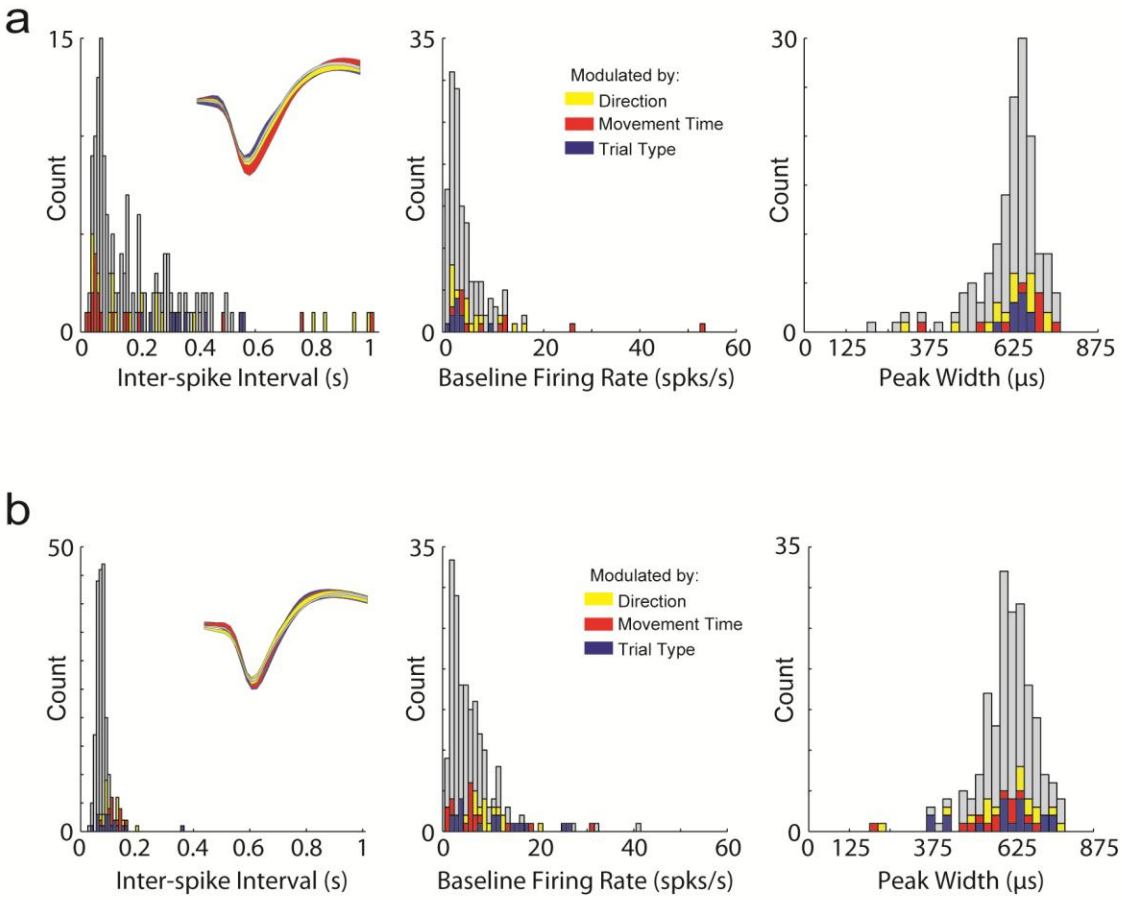

Figure 5.7: **Electrophysiological properties analysis for every increasing- and decreasing-type mPFC neuron in the PNE group. A)** Average inter-spike interval, defined as the latency between action potentials, for every increasing-type neuron (*left*). Colors indicate neurons significant in the multiple regression procedure for direction (yellow), movement time (red), and trial type (blue). Inset shows the average waveform ±SEM for all increasing-type neurons (gray) and the neurons significant in the multiple regression procedure (colors). Average baseline firing rate (spikes/s) taken from the 1s epoch beginning 2s prior to trial initiation is plotted for each increasing-type cell (*middle*). Average peak width defined as the time between the two highest peaks in the waveform is plotted for every increasing-type cell (*right*). **B)** Conventions as in A for decreasing-type neurons. **C)** Location of recording sites. Gray boxes mark extent of the recording locations. Black dots mark the bottom of the recording tract. Coronal slices approximately 3.3mm anterior to bregma.

Chapter Discussion

In summary, I show that PNE makes rats impulsive, disrupts neural signals related to response encoding and conflict monitoring, and reduces overall firing in mPFC. Further, I demonstrate that correlations between neuronal firing and performance (accuracy and movement speed) were altered after PNE.

An underactive prefrontal cortex (i.e. "hypofrontality") is commonly found in addiction, ADHD, and schizophrenia (*183-188*), all of which are psychiatric disorders characterized by diminished executive function. Experimental work has reported that interference of mPFC impairs performance on response inhibition tasks as measured by stop trial accuracy and premature responding during reaction time tasks (*61, 157*). Taken together, this work points to mPFC as a critical player during response inhibition and suggests that reduced prefrontal activation/function in disorders such as ADHD drive behavioral impairments (*158*).

Consistent with this hypothesis, patients diagnosed with ADHD have been successfully treated with noradrenaline and dopamine (e.g. methylphenidate; atomoxetine) reuptake inhibitors (*189-194*) that have been shown to impact prefrontal cortex in both humans and rats. For instance, in humans, atomoxetine administration increases inferior frontal activity in human participants (*195*) and methylphenidate reverses ADHD-associated hypofrontality (*196*). In rats, atomoxetine administration increases the immediate early gene c-Fos in mPFC (*197*). This all points to decreased prefrontal firing as a root of these and other psychiatric disorders that impair executive function. Consistent with this hypothesis I show that firing in mPFC is reduced in PNE rats. I further demonstrate reduced selectivity related to the direction of the response, the

speed of response, and the contrast between STOP and GO trials at the level of single units as well as an absence of correlations between firing and behavior output. My results provide a mechanism by which these drugs might ameliorate behavior deficits. Specifically, these drugs are likely to improve function by increasing frontal activity and driving selectivity for executive functions including response inhibition and conflict monitoring.

Maternal smoking is a risk factor for many psychiatric disorders (*166-169, 198-204*) and is still a common practice according to Substance Abuse & Mental Health Services which reported in 2012 that one in five women smoke during pregnancy. In addition to being an important issue in its own right, prenatal nicotine exposure has gained considerable traction as a suitable model for impulsive behavior as seen in ADHD. Exposing pregnant rodents to nicotine via drinking water produces offspring that bear striking resemblance to human ADHD both symptomatically and in treatment efficacy (*182, 205-207*). This exposure has also been shown to have a genetic component in that pups of prenatally exposed pups also show behavioral impairments (*208*). Previous studies have shown that prenatal nicotine exposure via drinking water at the same dose used in the current study (0.06mg/ml) produces increased anticipatory responses on the 5-choice serial reaction time task in rats (*174*). Similar results have been obtained in mice, where prenatal nicotine exposure via drinking water reduces cingulate cortex volume, reduces prefrontal dopamine turnover, and induces hyperactivity which was diminished by oral methylphenidate treatment (*173*). Thus, there is a substantial and meaningful overlap between human ADHD research and the rodent prenatal nicotine model.

It is highly unlikely that my results can be explained by impairments outside the realm of disrupted brain areas involved in executive control. As mentioned above, others have used the same method of nicotine administration, and shown impairment in the 5-choice serial reaction time task (*182*). Importantly, in that study, rats also performed a battery of sensorimotor tasks to assess different developmental milestones. PNE rats did exhibit lower birth weights and delayed sensorimotor development, but differences were not apparent prior to testing in the 5-choice task that occurred around three months of age. There were no significant differences in weight between PNE and control rats on the first day of my study (postnatal day 49). In addition, PNE rats were actually faster over all trial types and performed similarly on GO trials compared to control rats. Thus, as mentioned previously, it is unlikely that developmental problems beyond those related to executive and impulse control can account for the behavioral differences described here.

I conclude that PNE reduces activity in mPFC, an area known to be critical for executive control including response inhibition. Reduced activity in mPFC after PNE is correlated with poor impulse control and is likely to be directly related to elevated levels of drug seeking observed in ADHD and in rats that have chronically self-administered cocaine. Like prenatal nicotine, prolonged cocaine self-administration leads to mPFC hypoactivation and increased drug seeking, both of which are rescued through optogenetic stimulation of prelimbic prefrontal cortex (*209*). Together these results suggest that reduced firing in mPFC after exposure to prenatal nicotine might not only impair normal everyday executive control functions but increase one's predisposition to addiction (*210, 211*). Based on these findings and the existence of a positive correlation between firing and behavioral performance, this work implies that global increases in

mPFC firing may improve performance in animals during tasks that assess executive control and response inhibition.

Chapter 9: Comparison of areas and broad discussion

Through the results presented above, I have described how single cells in multiple brain areas might produce inhibitory control based on the context of the literature's current state. Since mine are the first studies to record single cells in the cortico-striatal circuit during performance of a task that exclusively probes response inhibition, there is no precedent for how mPFC, lOFC, and mDS cells interact to produce sufficient inhibitory action. Further, very few single unit studies record from different areas in the same task making direct comparisons difficult. As has been previously shown, the two cortical regions that I recorded from (lOFC and mPFC) are connected monosynaptically with mDS neurons (*32-34*) and communicate directly with one another (*35, 36*). I intend to detail the current prevailing theories on cortico-striatal function utilizing the established anatomical framework presented schematically in figure 1.1.

The cortico-striatal circuitry that mediates executive function/behavior in the human is largely conserved in the rodent. Although there are certainly cognitive behaviors that rats are not capable of, mediated by structures that rats do not possess, flexible response inhibition is a fundamental survival tactic for every mammal, particularly for smaller rodents under constant predation. Additionally, various clinical tasks including ones used to probe response inhibition have been successfully translated for use in the rat and previous research has shown a remarkable consistency between species in reaction time distributions (*212*). For these reasons, I propose that the invasive techniques used in the current rodent study can apply meaningfully to the state of human psychiatric research.

The cortex provides the majority of the input into the basal ganglia. Areas such as mPFC, OFC, and various sensory/motor cortices synapse directly onto medium spiny projection neurons of the dorsal striatum which tends to arbitrate between actions via mono- (mDS→SNr) or multi-synaptic (mDS→GPi→STN→SNr) connection to the output of the basal ganglia (SNr)(Fig. 1.1). Noticeably, the two afferent pathways onto SNr neurons release neurotransmitters of opposite valences; whereas STN is excitatory via glutamatergic connections, direct mDS to SNr connections are GABAergic. The importance of this is apparent after considering that SNr maintains tonic inhibition of motor outputs (superior colliculus, motor thalamus), the inhibition of which (disinhibition) allows for precise actions (*42*). Therefore, the balance between GABAergic and glutamatergic inputs onto SNr promotes or suppresses responding. The fact that this balance is largely mediated by the activity of dorsal striatum neurons makes mDS a logical brain region responsible for the initiation or inhibition of movement. By extension, the top-down modulation of mDS via frontal inputs becomes equally important as the majority of executive functions are linked to the cortex.

In the above chapters I describe the roles of mDS, lOFC, and mPFC individually and only hint at how their interactions can give rise to normal inhibitory functioning. In the subsequent section I intend to detail the advances afforded to the literature by my recent findings. Briefly, it appears as though mDS integrates all inputs into creating an appropriate motor response via its connections to the basal ganglia/motor system. Problematically, mDS alone cannot gather pertinent external information rapidly enough to pause, or redirect, an already programmed action. However, neurons in lOFC can inform the mDS of the appropriate response direction within the SCRT behavioral

window and allow the suppression of the initiated action. Interestingly, lOFC is also sensitive to previous conflict and can prepare the mDS of the necessary action based on recent response history. Although mPFC may not play a role in redirecting responses on the current trial, it appears as though it can broadly increase preparedness for flexible response inhibition by aggregating current and past conflict history.

In the next section, I better specify the interplay between the explored brain regions and compare their already reported results in figures 6.1-6.6 where individual properties are marked with letter symbols.

The comparative roles of mDS, lOFC, and mPFC in the stop signal task: Increasing-type

As a means to compare the functions of the explored brain regions, I begin by replicating the multiple regression results of the increasing-type neurons (Fig. 6.1) individually for mDS (A), lOFC (B), mPFC control neurons (C), and mPFC PNE neurons (D). The size specifications of the Venn diagrams map onto the relative proportion of increasing-type neurons that survived the regression procedure (i.e. exhibited partial r^2 values for at least one variable). Therefore, the first striking result is that more mDS neurons tend to encode task-related properties relative to the other populations. In fact, this is by a fairly large margin (percentage of neurons; mDS = 75%; lOFC = 54%; mPFC control = 53%; mPFC PNE = 37%). It is worth noting that the two healthy cortical regions (lOFC and mPFC) show comparable percentages of modulated neurons where PNE dramatically decreased the selectivity of these cells.

Figure 6.1: **Comparison of multiple regression results in increasing-type cells across brain regions. A)** A replication of figure 2.2 which displays the results of increasing-type mDS cells. **B)** A replication of figure 3.2 which displays the results of increasing-type lOFC cells. **C)** A replication of figure 4.2 which displays the results of increasing-type mPFC cells in the control group. **D)** A replication of figure 5.2B which displays the results of increasing-type mPFC cells in the PNE group. The relative size of each Venn diagram is proportional to the percentage of neurons in each population modulated by any of the three task parameters (e.g. mDS has the largest percentage). The table specifies the counts of neurons significant within a variable that have associated positive ("+") or negative ("-") β-values. As specified by the model, positive β-values indicate greater firing for the contralateral direction (direction), greater firing for slower movement times (movement time), and greater firing for STOP over GO trials (trial type). Asterisks indicate significantly more β-values for one valence within a parameter (binomial sign test; $p < 0.05$).

Medial Dorsal Striatum

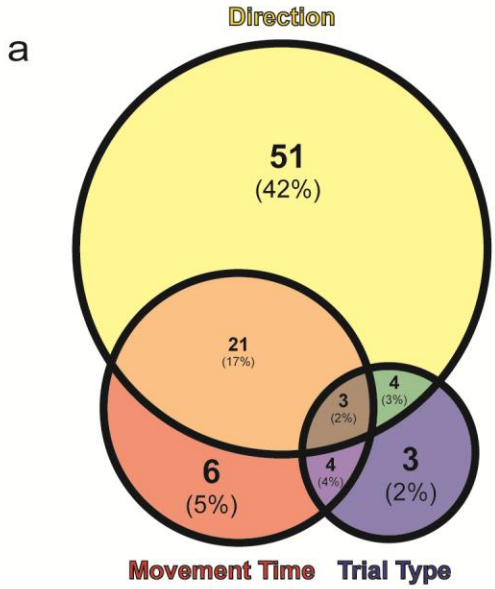

Lateral Orbitofrontal Cortex

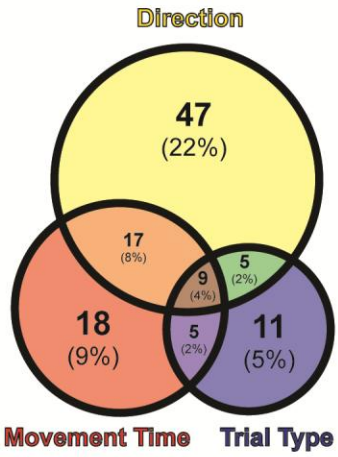

Medial Prefrontal Cortex (control)

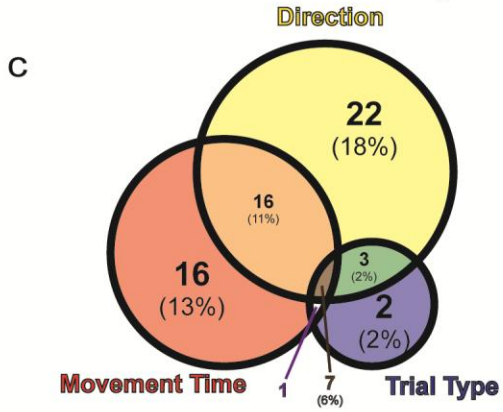

Medial Prefrontal Cortex (PNE)

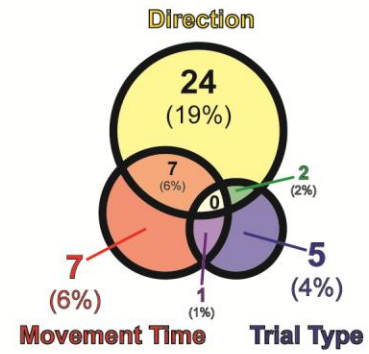

Increasing Type		Direction		Movement Time		Trial Type	
	β-valence	+	-	+	-	+	-
	mDS	***59****	20	6	***28****	9	5
	lOFC	30	48	20	29	19	11
	$mPFC^{CON}$	21	24	9	***28****	8	5
	$mPFC^{PNE}$	***24****	9	7	8	***8****	0

The size of the individual circles within the Venn diagrams offer a rather accurate comparison of the relative sensitivity to individual tasks parameters between brain regions. Given that the mDS is the area functionally closest to the motor system, it is unsurprising that mDS exhibits the greatest proportion of directionally specific neurons. In fact, 65% of increasing-type mDS cells are modulated by the direction of the response even after variance relegated to movement speed and the type of trial is accounted for. Additionally, of the healthy regions shown in A-C, mDS has the largest bias toward one direction; that is, significantly more neurons showed positive correlations (contralateral preferring; table; n = 59) than negative correlations (ipsilateral preferring; table; n = 20). These effects in mDS are in contrast to 37% of direction modulated cells in both lOFC and control mPFC while PNE diminished the direction encoding to 26%. These effects were somewhat anticipated as mDS has been shown to promote responding and articulate which muscles are necessary for any given movement (*41, 78*). However, it is somewhat surprising that greater than one third of healthy cortical neurons (lOFC, mPFC control) vary with regard to the direction of the response as lOFC and neighboring regions have been largely implicated in direction agnostic functions such as reward value, anticipatory control, and economic choice (*213-216*). As alluded to in the lOFC chapter, collapsing across directions in the increasing-type lOFC population would have eliminated the response inhibition and conflict adaptation effects. Therefore, the direction of responding in operant conditioning and decision-making paradigms should be examined more closely, particularly in regards to OFC function. Lastly, the relative lack of direction encoding in mPFC after PNE suggests that the ability of single neurons to dissociate between two spatial directions is linked to performance in the stop signal task.

Firing specificity to the speed of responding (movement time) in single neurons largely overlaps with the direction of responding in each analyzed brain region (i.e. a large orange portion in each Venn diagram). This suggests that the degree to which a neuron is modulated by the spatial attributes of an action is related to the modulation by the speed of an action on any given trial. Intriguingly, approximately equal proportions of neurons across healthy brain regions significantly vary with the movement speed (Fig. 6.1A-C; movement time; mDS = 28%; lOFC = 23%; mPFC control = 31%) whereas PNE diminishes the capacity for single neurons to encode the movement speed (Fig. 6.1D; movement time; 12%). Additionally, only mDS and control mPFC neurons show a preponderance of single neurons that exhibit greater firing with faster movement times (negative β-values; Fig. 6.1; table) implying that regardless of other task variables, greater firing in mDS and mPFC results in faster movement speeds. With regard to the effects of PNE on movement time encoding, the reduction in the ability of single neurons to control the speed of movement is clearly a contributing factor in inhibitory deficits in these animals.

Although a large fraction of neurons in each increasing-type population tended to be related to the spatial and speed attributes of a response, relatively few exhibited a direction/speed unbiased encoding of the type of trial (STOP vs. GO) that one might expect from regions implicated in response inhibition (*5*). Interestingly, the brain region displaying the largest percentage of trial type specific neurons was lOFC (Fig. 6.1B; trial type; 14%). This is in comparison to mDS (11%), mPFC control (11%), and mPFC PNE (6%). Admittedly, this difference between brain areas is not overwhelming, but the increasing-type population most closely associated with the ability to inhibit an ongoing

response in a temporally precise manner (Fig. 3.1) was lOFC. As with the other parameters in the preceding paragraphs, PNE reduced the percentage of neurons within mPFC that differentiated STOP from GO trials and therefore, STOP trial accuracy was reduced.

In the next section, using figure 6.2 as a guide, I intend to review the functions of healthy increasing-type mDS, lOFC, and mPFC populations in response inhibition and propose a collaborative mechanism for these regions to drive successful behavior in my task. Comparing across increasing-type populations is not meant to suggest that increasing-type cells form a separate network from decreasing-type cells. It is simply designed to be a comparative exercise between populations analyzed in the same manner.

Figure 6.2: **Comparison of population firing in increasing-type cells across brain regions. Top)** A replication of figure 2.1A which shows average firing of increasing-type mDS cells. **Middle)** A replication of figure 3.1A which shows average firing of increasing-type lOFC cells. **Bottom)** A replication of figure 4.1A which shows average firing of increasing-type mPFC cells.

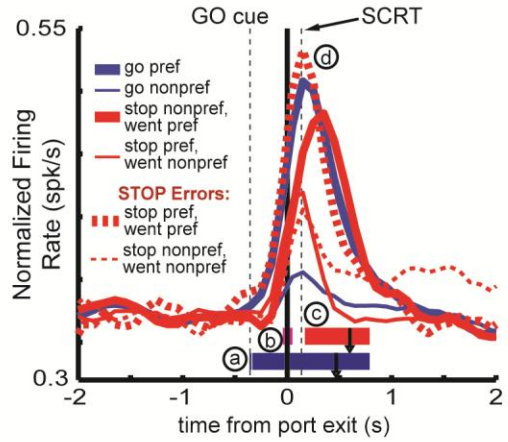

mDS: HABITUAL DIRECTIONAL RESPONDING

A region driving the response being made.

a) Early directional signalling during GO trials.

b) Incorrect direction encoded early on correct STOP trials followed by a period of direction correction.

c) The correct direction signalled after SCRT, prior to terminal well on correct STOP trials.

d) On STOP errors, incorrect direction signalled throughout the response.

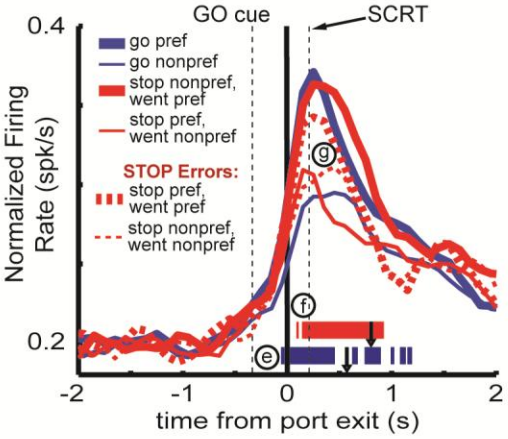

IOFC: DIRECTIONAL CONFLICT RESOLUTION

A region that swiftly rectifies incorrect directional responding

e) GO trial direction encoded at movement onset.

f) STOP trial direction encoded shortly after GO trial direction, prior to SCRT. No directional miscoding, quickly adapts to direction conflict.

g) On STOP errors, weak directional signal. Correct response not adapted to.

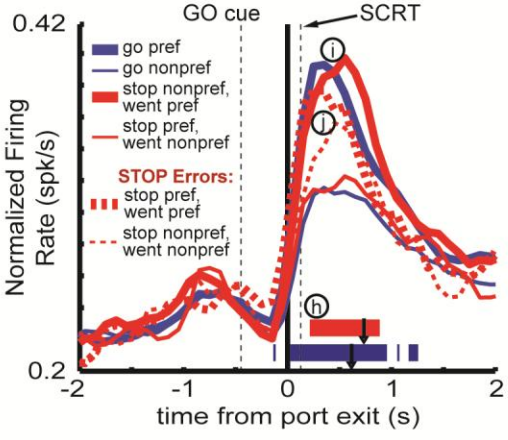

mPFC: CONFLICT MONITORING

A region that tracks the degree of conflict

h) On correct STOP trials, directional encoding well after SCRT.

i) Activity higher on correct STOP relative to correct GO trials after SCRT.

j) On STOP errors, minimal directional signalling.

Figure 6.2 places the population of increasing-type histograms together for direct comparison where mDS is the top figure, lOFC is in the middle, and mPFC control is at the bottom. The role of mDS increasing-type neurons in response inhibition appears to be one of habitual directional control. From the previous section, I described a large portion of direction specific neurons in mDS; it is therefore unsurprising that the direction signal is robust on GO trials and becomes distinct just after average GO cue onset in mDS (Fig. 6.2a) but later in both lOFC (Fig. 6.2e) and mPFC (Fig. 6.2 *bottom*). Intriguingly, this directional response in mDS was so robust that firing on correct STOP trials initially miscoded the ultimate direction (Fig. 6.2b) whereas this was not the case in lOFC and mPFC. This direction miscoding closer to the motor system (mDS) provides a signal that must be reconciled if the correct response is to be made in a timely manner. Importantly, this direction miscoding is not reconciled prior to the time-point necessary to recruit inhibitory machinery (SCRT) in mDS (Fig. 6.2c) or mPFC neurons (Fig. 6.2h), but it *is* reconciled in lOFC (Fig. 6.2f). Therefore, the lOFC increasing-type population can provide the temporally precise signal of the correct response direction to rescue the incorrect response signaled by mDS. The importance of this is accentuated in the context that on STOP errors, the incorrect direction is signaled throughout the response in mDS (Fig. 6.2d) and in lOFC and mPFC, the direction signal is weak and nondiscriminatory (Fig. 6.2g,i). Activity of the increasing-type mPFC population during the response is mainly driven by the direction taken by the animal. However, near the end of the response, mPFC exhibits greater firing on STOP trials relative to GO trials (Fig. 6.2i). This dissociation is late and likely not useful on the current trial but it appears to "monitor" which trial type was recently executed. As discussed in the previous chapters,

this can be interpreted in many ways so to further understand this signal, I plotted STOP trials in figure 6.3 based on the identity of the immediately preceding trial type (STOP or GO).

STOP trials inherently promote a directional conflict in the animals performing them due to the necessity to suppress an initiated response to a spatial location and redirect it to the opposite location. However, a recent history (previous trial) of STOP trials reduces the conflict produced by STOP trials, an effect referred to as conflict adaptation or "Gratton effect." Therefore, when STOP trials occur with a preceding history of GO trials, conflict is at its highest. In contrast, when a STOP trial had recently been performed, the conflict on the current STOP trial is easier to reconcile. Lastly, there is no inherent conflict on GO trials as animals are simply producing movements toward a well-conditioned stimulus. In increasing-type mDS neurons (Fig. 6.3 *top*), the miscoding of direction on high conflict STOP trials (gS) is exaggerated (Fig. 6.3a), but non-existent on lower conflict STOP trials (Fig. 6.3b). While stronger in mDS neurons, this direction miscoding on gS trials is not observed in lOFC (Fig. 6.3 *middle*) or mPFC (Fig. 6.3 *bottom*) even during high conflict. Importantly, in mDS neurons, the correct direction on STOP trials is *still* not reconciled prior to the SCRT regardless of prior conflict (Fig. 6.3c). Increasing-type lOFC cells lose the ability to discriminate between directions on STOP trials prior to the SCRT when conflict is high (Fig. 6.3e), but this ability is maintained when conflict is lower (Fig. 6.3d). In fact, lOFC neurons encode the correct direction even more strongly on lower conflict STOP trials than GO trials (Fig. 6.3f) which argues that preparedness for conflict induces accuracy on STOP trials. This is not the case for increasing-type mPFC neurons. Interestingly, the impact of prior conflict on

activity in mPFC cells is minimal when the animal is initiating its response (Fig. 6.3g) however, activity in both directions scales with the amount of conflict experienced on the current and previous trials once the decision on the current trial has been made (Fig. 6.3h). Therefore, mPFC has the ability to monitor the degree of conflict in the immediate past (current and previous trial) and inform the system to allocate requisite attentional resources for subsequent behavior.

Figure 6.3: **Comparison of population firing based on prior conflict in increasing-type cells across brain regions. Top)** A replication of figure 2.3A which shows average firing of increasing-type mDS cells. **Middle)** A replication of figure 3.3A which shows average firing of increasing-type lOFC cells. **Bottom)** A replication of figure 4.3A which shows average firing of increasing-type mPFC cells.

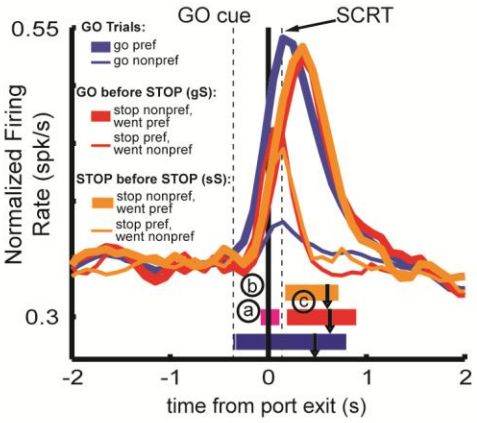

mDS: HABITUAL DIRECTIONAL RESPONDING

Neural encoding of the response.

a) When conflict is high (gS), miscoding of direction.

b) When conflict is low (sS), no miscoding.

c) Correct direction is signalled *after* the SCRT on STOP trials regardless of degree of conflict.

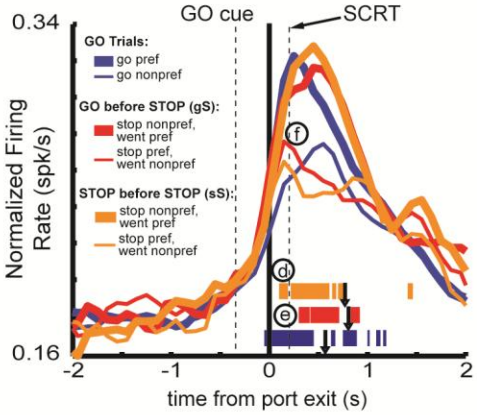

IOFC: CONFLICT ADAPTATION

Greater directional strength under conflict preparation

d) Adapts direction strength to heightened conflict in recent past. Signals correct response before SCRT.

e) Correct direction signaled after SCRT when preparation for conflict low.

f) Strong directional signal under conflict preparation.

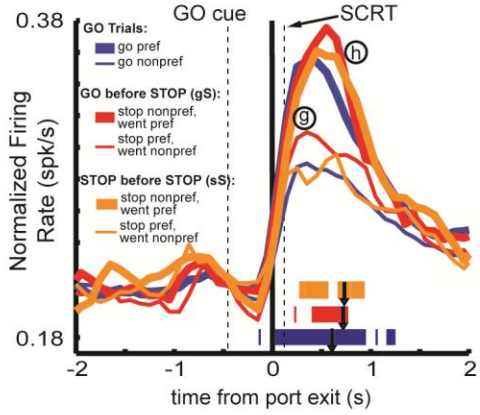

mPFC: CONFLICT MONITORING

Current and previous conflict history monitored

g) Directional strength invariant to conflict degree.

h) Activity scales to degree of conflict (gS>sS>GO) regardless of direction.

One can reasonably presume that greater firing during the highest conflict STOP trials in mPFC (Fig. 6.3 *bottom*; red lines) can provide the preparation for lOFC to signal the correct direction early and strongly on the next trial (Fig. 6.3 *middle*; orange lines) which then eliminates direction miscoding in mDS neurons (Fig. 6.3b) and provides greater accuracy on STOP trials. Given this framework, each node in this circuit is necessary for response inhibition in very different ways.

The comparative roles of mDS, lOFC, and mPFC in the stop signal task: Decreasing-type

Decreasing-type neurons are excluded from many single unit studies, but this is due to convenience rather than lack of importance. Decreasing-type neurons do, however, have a reputation for being highly variable and difficult to interpret so one should exercise caution while attempting to infer functions of a brain area from these populations. Regardless, given the large proportion of decreasing-type cells in each of the brain regions recorded from, I subjected decreasing-type cells to the identical analyses as above and review them in the current section.

Figure 6.4: **Comparison of multiple regression results in increasing-type cells across brain regions. A)** A replication of figure 2.5 which displays the results of decreasing-type mDS cells. **B)** A replication of figure 3.5 which displays the results of decreasing-type lOFC cells. **C)** A replication of figure 4.5 which displays the results of decreasing-type mPFC cells in the control group. **D)** A replication of figure 5.2D which displays the results of decreasing-type mPFC cells in the PNE group. The relative size of each Venn diagram is proportional to the percentage of neurons in each population modulated by any of the three task paramters. The table specifies the counts of neurons significant within a variable that have associated positive ("+") or negative ("-") β-values. As specified by the model, positive β-values indicate greater firing for the contralateral direction (direction), greater firing for slower movement times (movement time), and greater firing for STOP over GO trials (trial type). Asterisks indicate significantly more β-values for one valence within a parameter (binomial sign test; $p < 0.05$).

Medial Dorsal Striatum

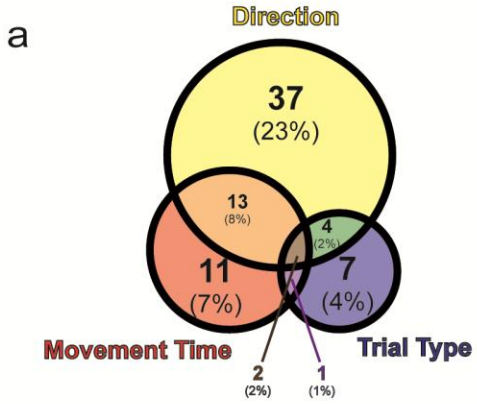

Lateral Orbitofrontal Cortex

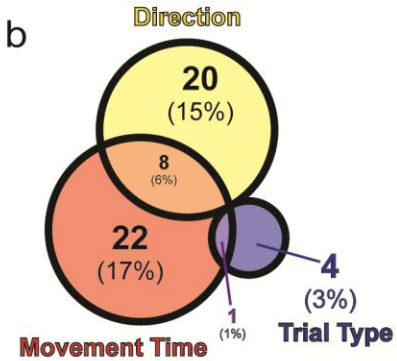

Medial Prefrontal Cortex (control)

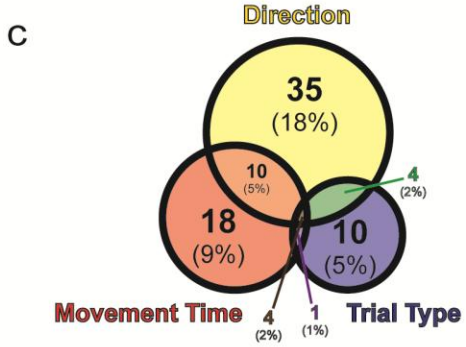

Medial Prefrontal Cortex (PNE)

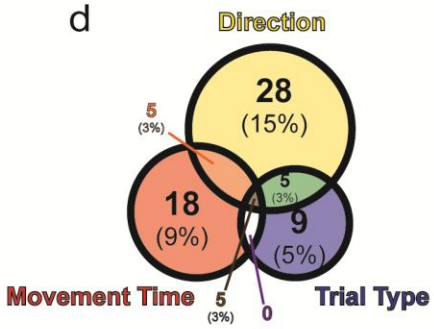

		Direction		Movement Time		Trial Type	
	β-valence	+	-	+	-	+	-
Decreasing Type	mDS	33	23	***22****	6	***12****	3
	lOFC	10	18	***25****	6	3	2
	mPFC^{CON}	28	16	22	12	16	6
	mPFC^{PNE}	***29****	14	21	11	9	8

The multiple regression procedure is a powerful way to tease apart the functions of individual neurons by selectively including variance in firing rate to specific task parameters. Decreasing-type cells, relative to increasing-type cells, tend to be selective to individual parts of the task to a lesser degree. That is, the percentages of decreasing-type neurons modulated by at least one task parameter are lower (Fig. 6.4; mDS = 46%; lOFC = 42%; mPFC control = 35%; mPFC PNE = 33%) when compared the increasing-type cells. Though these decreasing-type proportions of neurons are relatively similar, the region with the greatest percentage of modulated cells is mDS, similar to increasing-type cells.

Direction selectivity of individual decreasing-type neurons is highest in mDS where 34% of neurons are significantly correlated with response direction although oddly, the number of positive β-values is not different from negative β-values. This is surprising for a region tied to motor output and suggests that its function may be less directionally biased. The remaining brain regions show comparable direction-based firing (lOFC = 21%; mPFC control = 22%; mPFC PNE = 19%). Interestingly, PNE induces fewer direction selective neurons but of those, significantly more show a contralateral bias (positive β-value) relative to an ipsilateral bias (negative β-values). However, this effect is almost significant in control mPFC neurons as well.

The movement time variable produces interesting effects in the sense that a greater percentage of lOFC decreasing-type neurons are driven by the speed of responding relative to the other areas (Fig. 6.4; movement time; lOFC = 24%; mDS = 17%; mPFC control = 14%; mPFC PNE = 14%). It is fascinating that in mDS and lOFC, far larger counts of neurons fire more strongly during *slower* movement speeds (more

positive β-values) than faster movement speeds. This implies that greater activity of these neurons when animals are making their response is tied to more carefully executed trials.

When examining the proportion of neurons significantly activated during the contrast of STOP versus GO trials, there was a noticeably lower percentage of lOFC decreasing-type cells relative to the other regions (Fig. 6.4; trial type; lOFC = 4%; mDS = 9%; mPFC control = 9%; mPFC PNE = 7%). It can therefore be interpreted that lOFC decreasing-type cells are largely insensitive to whether a trial was a STOP or GO trial and further supports the aforementioned assertion that decreasing-type lOFC neurons play a role in modulating actions, possibly through local tuning of increasing-type cells. The low modulation of individual mPFC decreasing-type cells to the trial type parameter does not support an inhibitory function for this population but this does suggest that the *strength* of the directional signal (greater on STOP trials than GO trials in these neurons; Fig. 4.4) can be a powerful tool to measure activity in these neurons. Analyses regarding the interactive effects with the direction of a response are often neglected in single unit recording studies and in imaging research.

Overall, the proportions of decreasing-type cells that were modulated by individual task parameters were lower than their increasing-type counter-parts. The standout results from the decreasing-type cells are the relatively high direction-correlated neurons in mDS, the low fraction of movement time and high fraction of trial type correlated neurons in lOFC, and the modest reduction of significant mPFC PNE cells relative to mPFC control cells across each task variable.

Figure 6.5 replicates the population histogram analyses of decreasing-type neurons originally completed for mDS (Fig. 6.5 *top*), lOFC (Fig. 6.5 *middle*), and mPFC control (Fig. 6.5 *bottom*). Unlike increasing-type mDS neurons (Fig. 6.2a), decreasing-type mDS cells encode the direction elicited by the GO cue inconsistently prior to port exit (Fig. 6.5a). This effect is similar across each of the decreasing-type populations (Fig. 6.5 *middle*, *bottom*). However, the timing of the correct encoding of direction on STOP trials varies dramatically across the three populations. That is, there is significant encoding of the correct direction on STOP trials before (mPFC; Fig. 6.5h), slightly after (mDS; 6.5b), and well after (OFC; Fig. 6.5f) the SCRT. Because of this, mPFC decreasing-type cells appear to be useful for immediate redirecting of a response via informing the downstream mDS of the correct direction so that the appropriate movement can be programmed prior to an errant response. Additionally, mPFC decreasing-type neurons exhibit *greater* directional signaling under correct STOP trials (Fig. 6.5g) and comparable firing between the two trial types of similar response times/mechanics (GO trials and STOP errors; Fig. 6.5i). These mPFC results are in contrast to decreasing-type lOFC cells which only appear to minimally signal *any* direction-based response (Fig. 6.5e) and a directional signal that does not distinguish between STOP and GO trials. Interestingly, mDS decreasing-type cells clearly do not play a directionally conflicting role similar to mDS increasing-type cells. Instead, activity is similar during GO trials and STOP errors (Fig. 6.5c), and higher when a movement is inhibited/redirected (correct STOP trials; Fig. 6.5d). Because the directional signal on correct STOP trials (Fig. 6.5b) is not resolved prior to the SCRT, I conclude that this population offers a motor refinement signal that appropriates the correct resources to change an initiated response

either by local striatal tuning, or projection to the indirect pathway (Fig. 1.1) which possesses the capacity to broadly inhibit a movement.

Figure 6.5: **Comparison of population firing in decreasing-type cells across brain regions. Top)** A replication of figure 2.4A which shows average firing of decreasing-type mDS cells. **Middle)** A replication of figure 3.4A which shows average firing of decreasing-type lOFC cells. **Bottom)** A replication of figure 4.4A which shows average firing of decreasing-type mPFC cells.

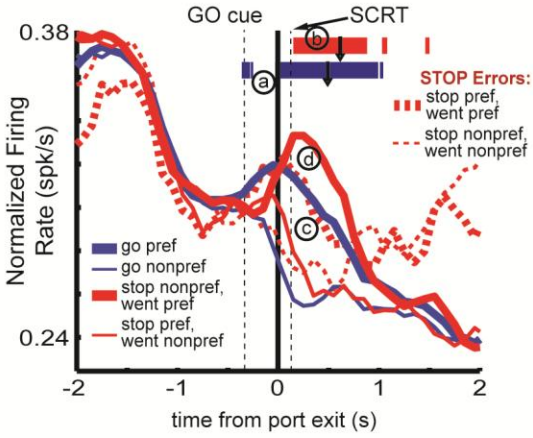

mDS: MOTOR REFINEMENT

Signals to afferents to reorient a movement in space

a) Inconsistent GO trial directional signalling prior to response initiation.

b) The correct direction is signalled after the SCRT on correct STOP trials.

c) STOP error firing mirrors correct GO firing.

d) Heightened activity when a movement is inhibited/redirected. Signals a pause/ reorientation of movement.

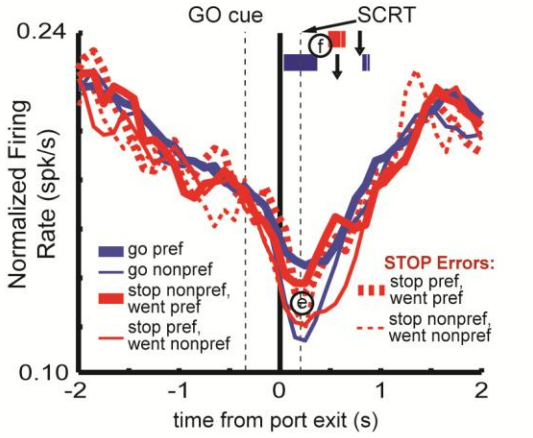

lOFC: RESPONSE DIRECTION

Minimal direction signalling

e) Direction is marignally encoded during the response.

f) STOP trial direction signalled far after SCRT.

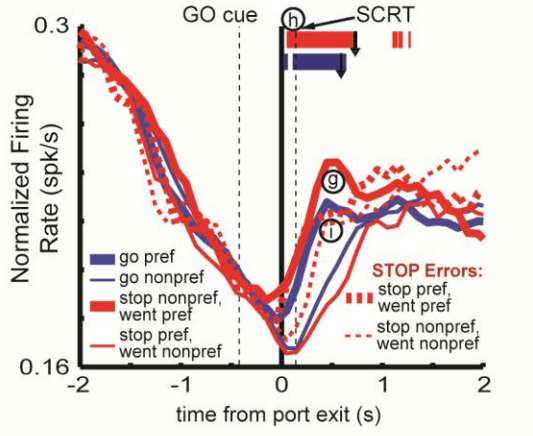

mPFC: RESPONSE REFINEMENT

A region important for refining a response when direction is conflicted

g) Directional signal on correct STOP trials is stronger than GO trials.

h) Directionally distinct prior to the SCRT.

i) GO trials and STOP errors exhibit comparable firing.

To gain perspective on how prior conflict impacts firing across decreasing-type populations, I again replicated the population histograms for mDS (Fig. 6.6 *top*), lOFC (Fig. 6.6 *middle*), and mPFC control (Fig. 6.6 *bottom*). Despite changes in firing in increasing-type cells regarding the degree of prior conflict, splitting STOP trials into the trial that preceded them in the decreasing-type populations altered firing very little. For instance, the directional signal for both types of STOP trials (higher and lower conflict, gS and sS) became distinct after the SCRT in mDS (Fig. 6.6a) and lOFC (Fig. 6.6) while it became distinct around the SCRT in mPFC (Fig. 6.6d). In fact, directional firing in decreasing-type lOFC neurons was so weak on sS trials that zero 100ms epochs were significant for the preferred over nonpreferred directions (i.e. no orange ticks). Although previous conflict did not appear to impact decreasing-type firing, this lack of an effect actually solidifies the roles for these populations that I proposed previously. For instance, in mDS decreasing-type cells, activity on both types of STOP trials does not vary from one another but *does* vary in reference to GO trials (Fig. 6.6b). Therefore, a function of motor refinement holds in the sense that it is only when a motor response needs to be altered from its initial trajectory that activity changes in mDS decreasing-type cells. Likewise, prior conflict does not drive firing in mPFC decreasing-type cells during the entirety of the response (Fig. 6.6e). However, there is greater activity on sS trials prior to movement initiation that highlights the role of this population in refining a response. That is, when the animal anticipates redirecting their behavior, activity is higher prior to movement initiation.

Figure 6.6: **Comparison of population firing based on prior conflict in decreasing-type cells across brain regions. Top)** A replication of figure 2.6A which shows average firing of decreasing-type mDS cells. **Middle)** A replication of figure 3.6A which shows average firing of decreasing-type lOFC cells. **Bottom)** A replication of figure 4.6A which shows average firing of decreasing-type mPFC cells.

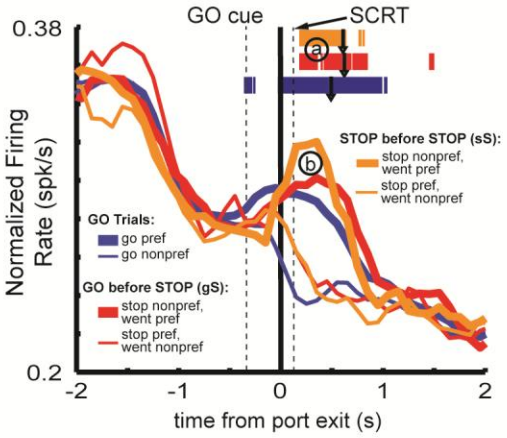

mDS: MOTOR REFINEMENT

A region insensitive to prior conflict

a) Regardless of preparation to inhibit/reorient, directional signal not distinct prior to SCRT.

b) Differences between STOP and GO trial activity only occur when movement trajectory is altered.

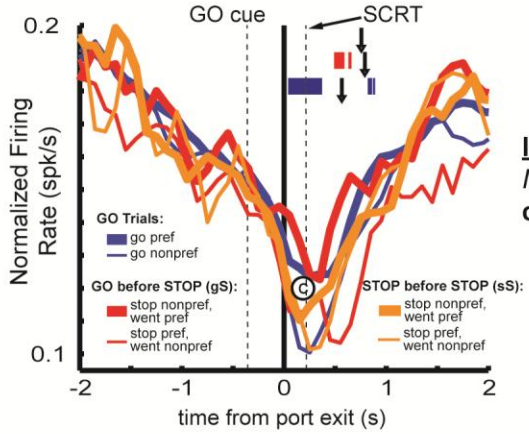

lOFC: RESPONSE DIRECTION

Minimal direction signalling

c) Sparse direction encoding on STOP trials.

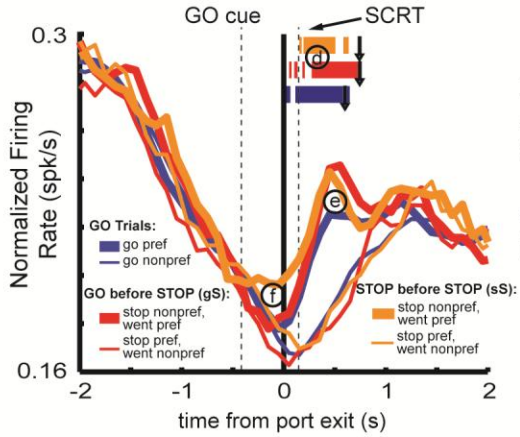

mPFC: RESPONSE REFINEMENT

A population indifferent to the degree of prior conflict

d) Directionally distinct around the SCRT on all STOP trials.

e) Prior conflict does not modulate STOP trial firing.

f) Earlier promotion of response reorientation under greater preparation.

Summary: Placing the explored brain regions in functional context

With the wealth of structural and functional data that have been gathered regarding executive functions including response inhibition (Fig. 1.1), it comes as no surprise that frontal regions are likely providing functionally distinct, but comparably complex inputs to the basal ganglia where appropriate actions can be placed in context and acted upon in a swift manner. The data that I have collected shows for the first time that lOFC directional signals exhibit the temporal precision to encode the correct response prior to inhibitory behavior that may fill the role in redirecting responding that mDS lacks. Additionally, under a recent history of conflict, mPFC neurons can track the degree of experienced conflict and presumably recruit attentional resources that give rise to the behavioral conflict adaptation effect. As a result, lOFC neurons can more reliably encode the correct direction and resolve the mitigated conflict in a faster manner. Given that all mammals are designed to take maximal advantage of their surroundings in foraging and/or predator avoidance contexts, it is unsurprising that the gathering of neural resources during times of maximal conflict can produce more accurate behavior, particularly under changing circumstances.

As described above, the impact that lOFC and mPFC ultimately have on behavior is via mDS. That is, conflict adaptation and monitoring function might govern behavior by modulating directional signals in mDS. But how do these executive control signals in cortex develop in the first place? Theories as to neurophysiological basis of this behavioral control vary, but two plausible ones stand out. The first involves the linking of midbrain dopamine to reward and cognitive control. Whereas dopamine phasically responses to reward related (*217*) or motivationally salient cues (*92*), tonic dopamine

release from the midbrain sustains motivation for a cognitive task (*218*). Midbrain dopamine neurons project strongly to the cortex causing a range of resultant changes in firing from increasing signal-to-noise ratio (*219*) to sharpening cortical tuning (*220*). It is therefore not unreasonable that top-down executive signals can impact behavior on the current trial in my task via connections to the basal ganglia while dopamine from the ventral tegmental area or substantia nigra pars compacta (neighbor of the SNr) updates the cortex based on recent responding to produce sufficient behavioral control. The second theory involves the anterior cingulate cortex (ACC) as the hub of control processing over the rest of the prefrontal cortex. Among numerous functions, ACC has been implicated in the updating of reward-based contingencies (*221*), triggering compensatory adjustments in cognitive control (*222*), conflict detection (*223*, *224*), and conflict monitoring (*225*). Due to this heterogeneity of cingulate function, it has been proposed that ACC can compute an "expected value of control" where resources are allocated to neighboring regions to produce appropriate behaviors given recent context (*222*). This is supported by the loss of conflict adaptation following cingulotomy (*224*).

Importantly, theories regarding the updating of control via dopamine and ACC are not mutually exclusive. The updating signals from the dopamine system after performance on a given trial likely alter firing throughout the cortex including mPFC, lOFC, and ACC. In fact, the error related negativity (ERN) deemed critical for the modification of performance has been hypothesized to be generated from changes in dopamine firing altering ACC activity (*226*). Albeit a speculative interpretation, I hypothesize that mPFC, along with other neighboring structures including ACC, are able to calculate the degree of conflict recently experienced in my task based on updating

from dopaminergic signals. This conflict information can then be used to appropriate cognitive resources to improve behavior under the most difficult circumstances.

Chapter 10: Detailed methodology

Subjects: Male Long-Evans rats were obtained at 175-200g from Charles River Labs. Rats were tested at the University of Maryland in accordance with NIH and IACUC guidelines.

Surgical procedures and histology: Surgical procedures followed guidelines for aseptic technique. Electrodes were manufactured and implanted as in prior recording experiments (*1, 2, 42, 221, 227-229*). Rats had a drivable bundle of ten 25µm diameter FeNiCr wires (Stablohm 675, California Fine Wire, Grover Beach, CA) chronically implanted in the left or right hemisphere dorsal to medial dorsal striatum (n = 8 rats; 0.4mm posterior to bregma, 2.4mm left [n = 4] or right [n = 4] of the midline, and 3.5mm ventral to the brain surface), lateral OFC (n = 5 rats; 3mm anterior to bregma, 3.2mm left [n = 2] or right [n = 3] of the midline, and 4mm ventral to the brain surface) or medial PFC (n = 16 rats; 3.3mm anterior to bregma, 0.6mm left [n = 8] or right [n = 8] of the midline, and 2mm ventral to the brain surface). Immediately prior to implantation, these wires were freshly cut with surgical scissors to extend ~1mm beyond the cannula and electroplated with platinum (H_2PtCl_6, Aldrich, Milwaukee, WI) to an impedance of ~300kOhms. Cephalexin (15mg/kg p.o.) was administered twice daily for two weeks post-operatively to prevent infection.

Behavioral task: Recording was conducted in aluminum chambers approximately 18" on each side with downward sloping walls narrowing to an area of 12" x 12" at the bottom. On one wall, a central odor port was located above two adjacent fluid wells. Directional lights were located next to the fluid wells. House lights were

located above the panel. Task control was implemented via computer. Port entry, licking, and well entry were monitored by disruption of photobeams.

The basic design of a trial is illustrated in figure 1.1A,B. Each trial began by illumination of house lights that instructed the rat to nose poke into the central port. Nose poking initiated a 1000ms pre-cue delay period. At the end of this delay, a directional light to the animal's left or right was flashed for 100ms. The trial was aborted if a rat exited the port at any time prior to offset of the directional cue light. On 80% of trials, presentation of either the left or right light signaled the direction in which the animal could respond in order to obtain sucrose reward in the fluid well below. On 20% of trials, *simultaneous* with the rat exiting the nose poke port, the light opposite to the location of the originally cued direction turned on and remained illuminated until the behavioral response was made. These trials will be referred to as STOP trials and were randomly interleaved with GO trials. Rats were required to stop the movement signaled by the first light and respond in the direction of the second light. After correct responses, rats were required to remain in the fluid well for a variable period between 800 and 1000ms (pre-fluid delay) before reward delivery (10% sucrose solution). Trials were presented in a pseudorandom sequence such that left and right trials were presented in equal numbers (+/-1 over 250 trials). The inter-trial interval (ITI) was a rigid 3 and 4s for correct and incorrect trials, respectively. The time necessary to stop and redirect behavior (SCRT) on STOP trials was computed by the difference between movement times on correct STOP and GO trials.

Single-unit recording: Procedures were the same as described previously (*42*). Wires were screened for activity daily; if no activity was detected, the rat was removed,

and the electrode assembly was advanced 40 or 80μm. Otherwise active wires were selected to be recorded, a session was conducted, and the electrode was advanced at the end of the session in order to gather new cells each session. Neural activity was recorded using four identical Plexon Multichannel Acquisition Processor systems (Dallas, TX), interfaced with odor discrimination training chambers. Signals from the electrode wires were amplified 20X by an op-amp headstage, located on the electrode array. Immediately outside the training chamber, the signals were passed through a differential pre-amplifier (Plexon Inc, PBX2/16sp-r-G50/16fp-G50) where single unit signals were amplified 50X and filtered at 150-9000 Hz. The single unit signals were then sent to the Multichannel Acquisition Processor box, where they were further filtered at 250-8000 Hz, digitized at 40 kHz and amplified at 1-32X. Waveforms (>2.5:1 signal-to-noise) were extracted from active channels and recorded to disk by an associated workstation with event timestamps from the behavior computer. Waveforms were not inverted before data analysis.

Data analysis: Units were sorted using Offline Sorter software from Plexon Inc (Dallas, TX), using a template matching algorithm. Sorted files were then processed in Neuroexplorer to extract unit timestamps and relevant event markers. These data were subsequently analyzed in Matlab (Natick, MA). Baseline firing was taken during a 1s epoch starting 2s prior to trial initiation (nose-poke). This baseline epoch was chosen as a period where rats are relatively stationary, yet prepared to initiate the upcoming trial. For the majority of the analyses, activity was examined during the period between nose poke exit and well entry (termed 'response epoch'), while the movement was being made and/or cancelled. Activity in population histograms was normalized by dividing by the

maximal firing rate of each neuron. All statistical procedures were executed using raw firing rates. Wilcoxon tests were used to measure significant shifts from zero in distribution plots ($p < 0.05$). T-tests were used to measure within cell differences in firing rates and behavioral data where indicated ($p < 0.05$). Significant direction signaling, as a function of time, was determined using a sliding window analysis. For STOP and GO trials independently, activity between the preferred and nonpreferred directions was compared in 100ms epochs which slid 10ms after each iteration. To complement these analyses I used least-squares multiple regression as a means to determine the number of cells where firing rate was significantly correlated with either the trial type (STOP/GO), movement time, and/or response direction parameters when variance for the two remaining factors was accounted for. To achieve this, I ran the following multiple model for each individual cell:

$$Y = \beta_0 + \beta_1 MovementTime + \beta_2 TrialType + \beta_3 Direction$$

where Y = firing rate (spikes/s) during the response epoch, *MovementTime* = latency between unpoke and well entry, *Direction* = coded as (-1 = ipsilateral) (1 = contralateral), and *TrialType* = coded as (-1 = GO) (1 = STOP).

To determine the significance for each predictor as a function of firing rate during the response epoch, I computed the unique variance of each individual parameter and divided it by the variance unaccounted for when each respective parameter was not included in the model (partial r^2). Significance of each partial r^2 was recorded along with the valence of the associated β-value. Counts of positively and negatively correlated cells were compared via binomial sign test ($p < 0.05$). For clarity, it was possible that a single

cell could show a significant partial r^2 for all three parameters. Each parameter was calculated in the same manner regardless of whether a neuron was an increasing- or decreasing-type cell. Absolute value of the firing rate was never used.

To capture activity that differentiated based on the previous trial, I examined firing on STOP and GO trials after either STOP or GO trials. The analysis allows for examination of trials that had the most 'conflict' or competition between two responses (i.e. GO vs. STOP). Abbreviations for trials that are differentiated by the trial type preceding it are labeled as lowercase ('g' or 's'; GO, STOP) which indicates the trial type before the trial marked by the uppercase letter ('G' or 'S'; GO, STOP). Wilcoxon tests were used to measure significant shifts from zero in distribution plots ($p < 0.05$).

Correlations between firing rate and behavioral measures (percent correct, movement time; Fig. 5.4) were calculated using Pearson's r after averaging values within each session. Correlation coefficients were determined to be statistically different via Student's t-test after Fisher's z-transformation for correlation coefficients.

Prenatal nicotine exposure: Procedures were similar to those described by Schneider and colleagues (*182*). In a subset (n = 5) of nulliparous female rats, nicotine was added to their only source of drinking water while the control mothers (n = 5) were provided with unadulterated drinking water. Nicotine bitartrate (Sigma, St Louis, MO) was dissolved in water. To acclimate the nicotine exposed dams to the taste of nicotine, the dosage was increased weekly over the course of three weeks (0.02mg/ml, 0.04mg/ml, and 0.06mg/ml). The range of nicotine between 1 and 6mg/kg/day has been shown to produce plasma nicotine levels in the range of 10-50ng/ml in habitual smokers (*230*).

Additionally, experiments that have administered nicotine via drinking water at doses comparable to ours have found plasma nicotine levels between 21 and 60ng/ml (*182, 231*). The mothers I used consumed an average of 5.93mg/kg/day of nicotine during pregnancy, which is within the range shown to produce behavioral deficits in offspring without causing physical impairments (*182, 231*). Nicotine exposed mothers in the present experiment consumed significantly less water than controls during pregnancy (98.89ml/kg/day; 131ml/kg/day; t-test; $p < 0.01$) and gained weight at a slower rate prior to pregnancy (0.21% gain per day; 0.68% gain per day; t-test; $p < 0.01$), characteristics that have been observed before by Schneider and colleagues (*182*). Pregnancy duration and fluid consumption comparisons are detailed in table 5.1.

All pups were cross-fostered to control mothers in order to isolate the effects of nicotine exposure prenatally and minimize unique rearing practices by nicotine exposed mothers. Pups were not exposed to nicotine in any manner after birth. Cross-fostering was performed on postnatal day 3 to ensure that any handling of pups by experimenters did not cause maternal rejection (*173*). Pups from the same litter were cross-fostered to the same control dam. As a result, all cross-fostering was successful and I obtained 39 PNE pups (mean litter size = 13.0; sex ratio = 56.6) and 45 control pups (mean litter size = 12.3; sex ratio = 49.0) from three nicotine exposed mothers and four control mothers. The pups were weaned on postnatal day 21. I used male pups in all recording experiments because PNE has been shown to have more dramatic behavioral effects on males than females and ADHD-like diagnoses are more prevalent in males (*205, 207, 232, 233*). Control and PNE pup weights were not significantly different from each other during first day of training (postnatal day 49; nicotine = 271g; control = 259g; t-test; p =

0.56). Eight male pups per group were randomly selected from three control (dam C1, n = 3; dam C3, n = 2; dam C5, n = 3) and three nicotine exposed mothers (dam N3, n = 3; dam N4, n = 3; dam N5, n = 2) to undergo training and electrode surgery (see above).

References

1. Bryden, D. W., Burton, A. C., Kashtelyan, V., Barnett, B. R., and Roesch, M. R. (2012) Response inhibition signals and miscoding of direction in dorsomedial striatum, *Front Integr Neurosci 6*, 69.
2. Bryden, D. W., and Roesch, M. R. (2015) Executive control signals in orbitofrontal cortex during response inhibition, *J Neurosci 35*, 3903-3914.
3. Kalanithi, P. S., Zheng, W., Kataoka, Y., DiFiglia, M., Grantz, H., Saper, C. B., Schwartz, M. L., Leckman, J. F., and Vaccarino, F. M. (2005) Altered parvalbumin-positive neuron distribution in basal ganglia of individuals with Tourette syndrome, *Proc Natl Acad Sci U S A 102*, 13307-13312.
4. Kataoka, Y., Kalanithi, P. S., Grantz, H., Schwartz, M. L., Saper, C., Leckman, J. F., and Vaccarino, F. M. (2010) Decreased number of parvalbumin and cholinergic interneurons in the striatum of individuals with Tourette syndrome, *J Comp Neurol 518*, 277-291.
5. Eagle, D. M., and Baunez, C. (2010) Is there an inhibitory-response-control system in the rat? Evidence from anatomical and pharmacological studies of behavioral inhibition, *Neurosci Biobehav Rev 34*, 50-72.

6. Aron, A. R., and Poldrack, R. A. (2005) The cognitive neuroscience of response inhibition: relevance for genetic research in attention-deficit/hyperactivity disorder, *Biol Psychiatry 57*, 1285-1292.

7. Bellgrove, M. A., Chambers, C. D., Vance, A., Hall, N., Karamitsios, M., and Bradshaw, J. L. (2006) Lateralized deficit of response inhibition in early-onset schizophrenia, *Psychol Med 36*, 495-505.

8. Durston, S., de Zeeuw, P., and Staal, W. G. (2009) Imaging genetics in ADHD: a focus on cognitive control, *Neurosci Biobehav Rev 33*, 674-689.

9. Fillmore, M. T., and Rush, C. R. (2002) Impaired inhibitory control of behavior in chronic cocaine users, *Drug Alcohol Depend 66*, 265-273.

10. Fillmore, M. T., Rush, C. R., and Hays, L. (2006) Acute effects of cocaine in two models of inhibitory control: implications of non-linear dose effects, *Addiction 101*, 1323-1332.

11. Gauggel, S., Rieger, M., and Feghoff, T. A. (2004) Inhibition of ongoing responses in patients with Parkinson's disease, *J Neurol Neurosurg Psychiatry 75*, 539-544.

12. Monterosso, J. R., Aron, A. R., Cordova, X., Xu, J., and London, E. D. (2005) Deficits in response inhibition associated with chronic methamphetamine abuse, *Drug Alcohol Depend 79*, 273-277.

13. Nigg, J. T., Silk, K. R., Stavro, G., and Miller, T. (2005) Disinhibition and borderline personality disorder, *Dev Psychopathol 17*, 1129-1149.

14. Oosterlaan, J., and Sergeant, J. A. (1998) Response inhibition and response re-engagement in attention-deficit/hyperactivity disorder, disruptive, anxious and normal children, *Behav Brain Res 94*, 33-43.

15. Oosterlaan, J., Logan, G. D., and Sergeant, J. A. (1998) Response inhibition in AD/HD, CD, comorbid AD/HD + CD, anxious, and control children: a meta-analysis of studies with the stop task, *J Child Psychol Psychiatry 39*, 411-425.

16. Rubia, K., Oosterlaan, J., Sergeant, J. A., Brandeis, D., and v Leeuwen, T. (1998) Inhibitory dysfunction in hyperactive boys, *Behav Brain Res 94*, 25-32.

17. Rubia, K., Smith, A., and Taylor, E. (2007) Performance of children with attention deficit hyperactivity disorder (ADHD) on a test battery of impulsiveness, *Child Neuropsychol 13*, 276-304.

18. Rubia, K., Smith, A. B., Brammer, M. J., Toone, B., and Taylor, E. (2005) Abnormal brain activation during inhibition and error detection in medication-naive adolescents with ADHD, *Am J Psychiatry 162*, 1067-1075.

19. Schachar, R., Logan, G. D., Robaey, P., Chen, S., Ickowicz, A., and Barr, C. (2007) Restraint and cancellation: multiple inhibition deficits in attention deficit hyperactivity disorder, *J Abnorm Child Psychol 35*, 229-238.

20. Schachar, R., Tannock, R., Marriott, M., and Logan, G. (1995) Deficient inhibitory control in attention deficit hyperactivity disorder, *J Abnorm Child Psychol 23*, 411-437.

21. Leventhal, D. K., Gage, G. J., Schmidt, R., Pettibone, J. R., Case, A. C., and Berke, J. D. (2012) Basal ganglia beta oscillations accompany cue utilization, *Neuron 73*, 523-536.

22. Polanczyk, G., de Lima, M. S., Horta, B. L., Biederman, J., and Rohde, L. A. (2007) The worldwide prevalence of ADHD: a systematic review and metaregression analysis, *Am J Psychiatry 164*, 942-948.

23. Aron, A. R. (2007) The neural basis of inhibition in cognitive control, *Neuroscientist 13*, 214-228.

24. Barkley, R. A. (1997) Behavioral inhibition, sustained attention, and executive functions: constructing a unifying theory of ADHD, *Psychol Bull 121*, 65-94.

25. Merkt, J., Singmann, H., Bodenburg, S., Goossens-Merkt, H., Kappes, A., Wendt, M., and Gawrilow, C. (2013) Flanker performance in female college students with ADHD: a diffusion model analysis, *Atten Defic Hyperact Disord 5*, 321-341.

26. Liu, Y., Gehring, W. J., Weissman, D. H., Taylor, S. F., and Fitzgerald, K. D. (2012) Trial-by-Trial Adjustments of Cognitive Control Following Errors and Response Conflict are Altered in Pediatric Obsessive Compulsive Disorder, *Front Psychiatry 3*, 41.

27. Pliszka, S. R., Glahn, D. C., Semrud-Clikeman, M., Franklin, C., Perez, R., 3rd, Xiong, J., and Liotti, M. (2006) Neuroimaging of inhibitory control areas in children with attention deficit hyperactivity disorder who were treatment naive or in long-term treatment, *Am J Psychiatry 163*, 1052-1060.

28. Sergeant, J. A., and van der Meere, J. (1988) What happens after a hyperactive child commits an error?, *Psychiatry Res 24*, 157-164.

29. Sesack, S. R., Deutch, A. Y., Roth, R. H., and Bunney, B. S. (1989) Topographical organization of the efferent projections of the medial prefrontal

cortex in the rat: an anterograde tract-tracing study with Phaseolus vulgaris leucoagglutinin, *J Comp Neurol 290*, 213-242.

30. Schilman, E. A., Uylings, H. B., Galis-de Graaf, Y., Joel, D., and Groenewegen, H. J. (2008) The orbital cortex in rats topographically projects to central parts of the caudate-putamen complex, *Neurosci Lett 432*, 40-45.

31. Wager, T. D., Sylvester, C. Y., Lacey, S. C., Nee, D. E., Franklin, M., and Jonides, J. (2005) Common and unique components of response inhibition revealed by fMRI, *Neuroimage 27*, 323-340.

32. Gabbott, P. L., Warner, T. A., Jays, P. R., Salway, P., and Busby, S. J. (2005) Prefrontal cortex in the rat: projections to subcortical autonomic, motor, and limbic centers, *J Comp Neurol 492*, 145-177.

33. Wall, N. R., De La Parra, M., Callaway, E. M., and Kreitzer, A. C. (2013) Differential innervation of direct- and indirect-pathway striatal projection neurons, *Neuron 79*, 347-360.

34. Jarbo, K., and Verstynen, T. D. (2015) Converging structural and functional connectivity of orbitofrontal, dorsolateral prefrontal, and posterior parietal cortex in the human striatum, *J Neurosci 35*, 3865-3878.

35. Price, J. L. (2007) Definition of the orbital cortex in relation to specific connections with limbic and visceral structures and other cortical regions, *Ann N Y Acad Sci 1121*, 54-71.

36. Vertes, R. P. (2004) Differential projections of the infralimbic and prelimbic cortex in the rat, *Synapse 51*, 32-58.

37. Christakou, A., Robbins, T. W., and Everitt, B. J. (2004) Prefrontal cortical-ventral striatal interactions involved in affective modulation of attentional performance: implications for corticostriatal circuit function, *J Neurosci 24*, 773-780.

38. Rogers, R. D., Baunez, C., Everitt, B. J., and Robbins, T. W. (2001) Lesions of the medial and lateral striatum in the rat produce differential deficits in attentional performance, *Behav Neurosci 115*, 799-811.

39. Brown, V. J., and Robbins, T. W. (1989) Elementary processes of response selection mediated by distinct regions of the striatum, *J Neurosci 9*, 3760-3765.

40. Hauber, W., and Schmidt, W. J. (1994) Differential effects of lesions of the dorsomedial and dorsolateral caudate-putamen on reaction time performance in rats, *Behav Brain Res 60*, 211-215.

41. Schmidt, R., Leventhal, D. K., Mallet, N., Chen, F., and Berke, J. D. (2013) Canceling actions involves a race between basal ganglia pathways, *Nat Neurosci 16*, 1118-1124.

42. Bryden, D. W., Johnson, E. E., Diao, X., and Roesch, M. R. (2011) Impact of expected value on neural activity in rat substantia nigra pars reticulata, *Eur J Neurosci 33*, 2308-2317.

43. Sato, M., and Hikosaka, O. (2002) Role of primate substantia nigra pars reticulata in reward-oriented saccadic eye movement, *J Neurosci 22*, 2363-2373.

44. Steegmann, A. T. (1962) Dr. Harlow's famous case: the "impossible" accident of Phineas P. Gage, *Surgery 52*, 952-958.

45. Lavallee, C. F., Herrmann, C. S., Weerda, R., and Huster, R. J. (2014) Stimulus-response mappings shape inhibition processes: a combined EEG-fMRI study of contextual stopping, *PLoS One 9*, e96159.

46. Jimura, K., Hirose, S., Kunimatsu, A., Ohtomo, K., Koike, Y., and Konishi, S. (2014) Late enhancement of brain-behavior correlations during response inhibition, *Neuroscience 274C*, 383-392.

47. Lovstad, M., Funderud, I., Meling, T., Kramer, U. M., Voytek, B., Due-Tonnessen, P., Endestad, T., Lindgren, M., Knight, R. T., and Solbakk, A. K. (2012) Anterior cingulate cortex and cognitive control: neuropsychological and electrophysiological findings in two patients with lesions to dorsomedial prefrontal cortex, *Brain Cogn 80*, 237-249.

48. Boccardi, E., Della Sala, S., Motto, C., and Spinnler, H. (2002) Utilisation behaviour consequent to bilateral SMA softening, *Cortex 38*, 289-308.

49. Volkow, N. D., Wang, G. J., Tomasi, D., Kollins, S. H., Wigal, T. L., Newcorn, J. H., Telang, F. W., Fowler, J. S., Logan, J., Wong, C. T., and Swanson, J. M. (2012) Methylphenidate-elicited dopamine increases in ventral striatum are associated with long-term symptom improvement in adults with attention deficit hyperactivity disorder, *J Neurosci 32*, 841-849.

50. Ye, Z., Altena, E., Nombela, C., Housden, C. R., Maxwell, H., Rittman, T., Huddleston, C., Rae, C. L., Regenthal, R., Sahakian, B. J., Barker, R. A., Robbins, T. W., and Rowe, J. B. (2014) Selective serotonin reuptake inhibition modulates response inhibition in Parkinson's disease, *Brain 137*, 1145-1155.

51. McEnaney, K. W., and Butter, C. M. (1969) Perseveration of responding and nonresponding in monkeys with orbital frontal ablations, *J Comp Physiol Psychol 68*, 558-561.

52. Iversen, S. D., and Mishkin, M. (1970) Perseverative interference in monkeys following selective lesions of the inferior prefrontal convexity, *Exp Brain Res 11*, 376-386.

53. Kheramin, S., Body, S., Ho, M., Velazquez-Martinez, D. N., Bradshaw, C. M., Szabadi, E., Deakin, J. F., and Anderson, I. M. (2003) Role of the orbital prefrontal cortex in choice between delayed and uncertain reinforcers: a quantitative analysis, *Behav Processes 64*, 239-250.

54. Schoenbaum, G., Nugent, S. L., Saddoris, M. P., and Setlow, B. (2002) Orbitofrontal lesions in rats impair reversal but not acquisition of go, no-go odor discriminations, *Neuroreport 13*, 885-890.

55. Albin, R. L., Young, A. B., and Penney, J. B. (1989) The functional anatomy of basal ganglia disorders, *Trends Neurosci 12*, 366-375.

56. Hanes, D. P., and Schall, J. D. (1996) Neural control of voluntary movement initiation, *Science 274*, 427-430.

57. Hanes, D. P., Patterson, W. F., 2nd, and Schall, J. D. (1998) Role of frontal eye fields in countermanding saccades: visual, movement, and fixation activity, *J Neurophysiol 79*, 817-834.

58. Eagle, D. M., and Robbins, T. W. (2003) Inhibitory control in rats performing a stop-signal reaction-time task: effects of lesions of the medial striatum and d-amphetamine, *Behav Neurosci 117*, 1302-1317.

59. Eagle, D. M., Wong, J. C., Allan, M. E., Mar, A. C., Theobald, D. E., and Robbins, T. W. (2011) Contrasting roles for dopamine D1 and D2 receptor subtypes in the dorsomedial striatum but not the nucleus accumbens core during behavioral inhibition in the stop-signal task in rats, *J Neurosci 31*, 7349-7356.

60. Mayse, J. D., Nelson, G. M., Park, P., Gallagher, M., and Lin, S. C. (2014) Proactive and reactive inhibitory control in rats, *Front Neurosci 8*, 104.

61. Bari, A., Mar, A. C., Theobald, D. E., Elands, S. A., Oganya, K. C., Eagle, D. M., and Robbins, T. W. (2011) Prefrontal and monoaminergic contributions to stop-signal task performance in rats, *J Neurosci 31*, 9254-9263.

62. Roesch, M. R., Taylor, A. R., and Schoenbaum, G. (2006) Encoding of time-discounted rewards in orbitofrontal cortex is independent of value representation, *Neuron 51*, 509-520.

63. Feierstein, C. E., Quirk, M. C., Uchida, N., Sosulski, D. L., and Mainen, Z. F. (2006) Representation of spatial goals in rat orbitofrontal cortex, *Neuron 51*, 495-507.

64. Stalnaker, T. A., Calhoon, G. G., Ogawa, M., Roesch, M. R., and Schoenbaum, G. (2012) Reward prediction error signaling in posterior dorsomedial striatum is action specific, *J Neurosci 32*, 10296-10305.

65. Furuyashiki, T., Holland, P. C., and Gallagher, M. (2008) Rat orbitofrontal cortex separately encodes response and outcome information during performance of goal-directed behavior, *J Neurosci 28*, 5127-5138.

66. Carter, C. S., and van Veen, V. (2007) Anterior cingulate cortex and conflict detection: an update of theory and data, *Cogn Affect Behav Neurosci 7*, 367-379.

67. Botvinick, M. M., Braver, T. S., Barch, D. M., Carter, C. S., and Cohen, J. D. (2001) Conflict monitoring and cognitive control, *Psychol Rev 108*, 624-652.

68. Mayr, U., Awh, E., and Laurey, P. (2003) Conflict adaptation effects in the absence of executive control, *Nat Neurosci 6*, 450-452.

69. Mansouri, F. A., Buckley, M. J., and Tanaka, K. (2014) The essential role of primate orbitofrontal cortex in conflict-induced executive control adjustment, *J Neurosci 34*, 11016-11031.

70. Gratton, G., Coles, M. G., and Donchin, E. (1992) Optimizing the use of information: strategic control of activation of responses, *J Exp Psychol Gen 121*, 480-506.

71. Miyachi, S., Hikosaka, O., Miyashita, K., Karadi, Z., and Rand, M. K. (1997) Differential roles of monkey striatum in learning of sequential hand movement, *Exp Brain Res 115*, 1-5.

72. Jog, M. S., Kubota, Y., Connolly, C. I., Hillegaart, V., and Graybiel, A. M. (1999) Building neural representations of habits, *Science 286*, 1745-1749.

73. Matsumoto, N., Hanakawa, T., Maki, S., Graybiel, A. M., and Kimura, M. (1999) Role of [corrected] nigrostriatal dopamine system in learning to perform sequential motor tasks in a predictive manner, *J Neurophysiol 82*, 978-998.

74. Graybiel, A. M. (2000) The basal ganglia, *Curr Biol 10*, R509-511.

75. Bailey, K. R., and Mair, R. G. (2006) The role of striatum in initiation and execution of learned action sequences in rats, *J Neurosci 26*, 1016-1025.

76. Yin, H. H., and Knowlton, B. J. (2006) The role of the basal ganglia in habit formation, *Nat Rev Neurosci 7*, 464-476.

77. Schmitzer-Torbert, N. C., and Redish, A. D. (2008) Task-dependent encoding of space and events by striatal neurons is dependent on neural subtype, *Neuroscience 153*, 349-360.

78. Wang, K. S., McClure, J. P., Jr., Alselehdar, S. K., and Kanta, V. (2015) Direct and indirect pathways of the basal ganglia: opponents or collaborators?, *Front Neuroanat 9*, 20.

79. Balleine, B. W., Delgado, M. R., and Hikosaka, O. (2007) The role of the dorsal striatum in reward and decision-making, *J Neurosci 27*, 8161-8165.

80. Ma, L., Hyman, J. M., Phillips, A. G., and Seamans, J. K. (2014) Tracking progress toward a goal in corticostriatal ensembles, *J Neurosci 34*, 2244-2253.

81. Taira, M., and Georgopoulos, A. P. (1993) Cortical cell types from spike trains, *Neurosci Res 17*, 39-45.

82. Vigneswaran, G., Kraskov, A., and Lemon, R. N. (2011) Large identified pyramidal cells in macaque motor and premotor cortex exhibit "thin spikes": implications for cell type classification, *J Neurosci 31*, 14235-14242.

83. Gage, G. J., Stoetzner, C. R., Wiltschko, A. B., and Berke, J. D. (2010) Selective activation of striatal fast-spiking interneurons during choice execution, *Neuron 67*, 466-479.

84. Wiltschko, A. B., Pettibone, J. R., and Berke, J. D. (2010) Opposite effects of stimulant and antipsychotic drugs on striatal fast-spiking interneurons, *Neuropsychopharmacology 35*, 1261-1270.

85. Berke, J. D. (2008) Uncoordinated firing rate changes of striatal fast-spiking interneurons during behavioral task performance, *J Neurosci 28*, 10075-10080.

86. Kawaguchi, Y., Wilson, C. J., Augood, S. J., and Emson, P. C. (1995) Striatal interneurones: chemical, physiological and morphological characterization, *Trends Neurosci 18*, 527-535.

87. Mallet, N., Le Moine, C., Charpier, S., and Gonon, F. (2005) Feedforward inhibition of projection neurons by fast-spiking GABA interneurons in the rat striatum in vivo, *J Neurosci 25*, 3857-3869.

88. Emeric, E. E., Brown, J. W., Leslie, M., Pouget, P., Stuphorn, V., and Schall, J. D. (2008) Performance monitoring local field potentials in the medial frontal cortex of primates: anterior cingulate cortex, *J Neurophysiol 99*, 759-772.

89. Stuphorn, V., and Schall, J. D. (2006) Executive control of countermanding saccades by the supplementary eye field, *Nat Neurosci 9*, 925-931.

90. Ito, S., Stuphorn, V., Brown, J. W., and Schall, J. D. (2003) Performance monitoring by the anterior cingulate cortex during saccade countermanding, *Science 302*, 120-122.

91. Stuphorn, V., Taylor, T. L., and Schall, J. D. (2000) Performance monitoring by the supplementary eye field, *Nature 408*, 857-860.

92. Bromberg-Martin, E. S., Matsumoto, M., and Hikosaka, O. (2010) Dopamine in motivational control: rewarding, aversive, and alerting, *Neuron 68*, 815-834.

93. Maia, T. V., and Frank, M. J. (2011) From reinforcement learning models to psychiatric and neurological disorders, *Nat Neurosci 14*, 154-162.

94. Kolomiets, B. P., Deniau, J. M., Glowinski, J., and Thierry, A. M. (2003) Basal ganglia and processing of cortical information: functional interactions between

trans-striatal and trans-subthalamic circuits in the substantia nigra pars reticulata, *Neuroscience 117*, 931-938.

95. Alexander, G. E., and Crutcher, M. D. (1990) Functional architecture of basal ganglia circuits: neural substrates of parallel processing, *Trends Neurosci 13*, 266-271.

96. Mink, J. W., and Thach, W. T. (1993) Basal ganglia intrinsic circuits and their role in behavior, *Curr Opin Neurobiol 3*, 950-957.

97. Maurice, N., Deniau, J. M., Glowinski, J., and Thierry, A. M. (1999) Relationships between the prefrontal cortex and the basal ganglia in the rat: physiology of the cortico-nigral circuits, *J Neurosci 19*, 4674-4681.

98. Felsen, G., and Mainen, Z. F. (2008) Neural substrates of sensory-guided locomotor decisions in the rat superior colliculus, *Neuron 60*, 137-148.

99. Schroll, H., Beste, C., and Hamker, F. H. (2015) Combined lesions of direct and indirect basal ganglia pathways but not changes in dopamine levels explain learning deficits in patients with Huntington's disease, *Eur J Neurosci*.

100. Parthasarathy, H. B., and Graybiel, A. M. (1997) Cortically driven immediate-early gene expression reflects modular influence of sensorimotor cortex on identified striatal neurons in the squirrel monkey, *J Neurosci 17*, 2477-2491.

101. Hikosaka, O., Nakamura, K., and Nakahara, H. (2006) Basal ganglia orient eyes to reward, *J Neurophysiol 95*, 567-584.

102. Deniau, J. M., Mailly, P., Maurice, N., and Charpier, S. (2007) The pars reticulata of the substantia nigra: a window to basal ganglia output, *Prog Brain Res 160*, 151-172.

103. Redgrave, P., Prescott, T. J., and Gurney, K. (1999) The basal ganglia: a vertebrate solution to the selection problem?, *Neuroscience 89*, 1009-1023.

104. Gurney, K., Prescott, T. J., and Redgrave, P. (2001) A computational model of action selection in the basal ganglia. I. A new functional anatomy, *Biol Cybern 84*, 401-410.

105. Schall, J. D., Hanes, D. P., and Taylor, T. L. (2000) Neural control of behavior: countermanding eye movements, *Psychol Res 63*, 299-307.

106. Schall, J. D. (2001) Neural basis of deciding, choosing and acting, *Nat Rev Neurosci 2*, 33-42.

107. Logan, G. D., Cowan, W. B., and Davis, K. A. (1984) On the ability to inhibit simple and choice reaction time responses: a model and a method, *J Exp Psychol Hum Percept Perform 10*, 276-291.

108. Kravitz, A. V., Tye, L. D., and Kreitzer, A. C. (2012) Distinct roles for direct and indirect pathway striatal neurons in reinforcement, *Nat Neurosci 15*, 816-818.

109. Freeze, B. S., Kravitz, A. V., Hammack, N., Berke, J. D., and Kreitzer, A. C. (2013) Control of basal ganglia output by direct and indirect pathway projection neurons, *J Neurosci 33*, 18531-18539.

110. Schoenbaum, G., Roesch, M. R., Stalnaker, T. A., and Takahashi, Y. K. (2009) A new perspective on the role of the orbitofrontal cortex in adaptive behaviour, *Nat Rev Neurosci 10*, 885-892.

111. McDannald, M. A., Jones, J. L., Takahashi, Y. K., and Schoenbaum, G. (2014) Learning theory: a driving force in understanding orbitofrontal function, *Neurobiol Learn Mem 108*, 22-27.

112. Wilson, R. C., Takahashi, Y. K., Schoenbaum, G., and Niv, Y. (2014) Orbitofrontal cortex as a cognitive map of task space, *Neuron 81*, 267-279.

113. Charles, M. B. (1969) Perseveration in Extinction and in Discrimination Reversal Tasks Following Selective Frontal Ablations in Macaca Mulatta, *Physiology and Behavior 4*, 9.

114. Jones, B., and Mishkin, M. (1972) Limbic lesions and the problem of stimulus--reinforcement associations, *Exp Neurol 36*, 362-377.

115. Rolls, E. T., Hornak, J., Wade, D., and McGrath, J. (1994) Emotion-related learning in patients with social and emotional changes associated with frontal lobe damage, *J Neurol Neurosurg Psychiatry 57*, 1518-1524.

116. Meunier, M., Bachevalier, J., and Mishkin, M. (1997) Effects of orbital frontal and anterior cingulate lesions on object and spatial memory in rhesus monkeys, *Neuropsychologia 35*, 999-1015.

117. McAlonan, K., and Brown, V. J. (2003) Orbital prefrontal cortex mediates reversal learning and not attentional set shifting in the rat, *Behav Brain Res 146*, 97-103.

118. Bissonette, G. B., Martins, G. J., Franz, T. M., Harper, E. S., Schoenbaum, G., and Powell, E. M. (2008) Double dissociation of the effects of medial and orbital prefrontal cortical lesions on attentional and affective shifts in mice, *J Neurosci 28*, 11124-11130.

119. Izquierdo, A., Suda, R. K., and Murray, E. A. (2004) Bilateral orbital prefrontal cortex lesions in rhesus monkeys disrupt choices guided by both reward value and reward contingency, *J Neurosci 24*, 7540-7548.

120. Chudasama, Y., and Robbins, T. W. (2003) Dissociable contributions of the orbitofrontal and infralimbic cortex to pavlovian autoshaping and discrimination reversal learning: further evidence for the functional heterogeneity of the rodent frontal cortex, *J Neurosci 23*, 8771-8780.

121. Fellows, L. K., and Farah, M. J. (2003) Ventromedial frontal cortex mediates affective shifting in humans: evidence from a reversal learning paradigm, *Brain 126*, 1830-1837.

122. Hornak, J., O'Doherty, J., Bramham, J., Rolls, E. T., Morris, R. G., Bullock, P. R., and Polkey, C. E. (2004) Reward-related reversal learning after surgical excisions in orbito-frontal or dorsolateral prefrontal cortex in humans, *J Cogn Neurosci 16*, 463-478.

123. Schoenbaum, G., Setlow, B., Nugent, S. L., Saddoris, M. P., and Gallagher, M. (2003) Lesions of orbitofrontal cortex and basolateral amygdala complex disrupt acquisition of odor-guided discriminations and reversals, *Learn Mem 10*, 129-140.

124. Mobini, S., Body, S., Ho, M. Y., Bradshaw, C. M., Szabadi, E., Deakin, J. F., and Anderson, I. M. (2002) Effects of lesions of the orbitofrontal cortex on sensitivity to delayed and probabilistic reinforcement, *Psychopharmacology (Berl) 160*, 290-298.

125. Eagle, D. M., Baunez, C., Hutcheson, D. M., Lehmann, O., Shah, A. P., and Robbins, T. W. (2008) Stop-signal reaction-time task performance: role of prefrontal cortex and subthalamic nucleus, *Cereb Cortex 18*, 178-188.

126. Majid, D. S., Cai, W., Corey-Bloom, J., and Aron, A. R. (2013) Proactive selective response suppression is implemented via the basal ganglia, *J Neurosci 33*, 13259-13269.

127. Bechara, A., Damasio, H., Damasio, A. R., and Lee, G. P. (1999) Different contributions of the human amygdala and ventromedial prefrontal cortex to decision-making, *J Neurosci 19*, 5473-5481.

128. Zeeb, F. D., and Winstanley, C. A. (2011) Lesions of the basolateral amygdala and orbitofrontal cortex differentially affect acquisition and performance of a rodent gambling task, *J Neurosci 31*, 2197-2204.

129. Casey, B. J., Trainor, R. J., Orendi, J. L., Schubert, A. B., Nystrom, L. E., Giedd, J. N., Castellanos, F. X., Haxby, J. V., Noll, D. C., Cohen, J. D., Forman, S. D., Dahl, R. E., and Rapoport, J. L. (1997) A Developmental Functional MRI Study of Prefrontal Activation during Performance of a Go-No-Go Task, *J Cogn Neurosci 9*, 835-847.

130. Chikazoe, J., Jimura, K., Hirose, S., Yamashita, K., Miyashita, Y., and Konishi, S. (2009) Preparation to inhibit a response complements response inhibition during performance of a stop-signal task, *J Neurosci 29*, 15870-15877.

131. Horn, N. R., Dolan, M., Elliott, R., Deakin, J. F., and Woodruff, P. W. (2003) Response inhibition and impulsivity: an fMRI study, *Neuropsychologia 41*, 1959-1966.

132. Hoover, W. B., and Vertes, R. P. (2011) Projections of the medial orbital and ventral orbital cortex in the rat, *J Comp Neurol 519*, 3766-3801.

133. Chudasama, Y., Kralik, J. D., and Murray, E. A. (2007) Rhesus monkeys with orbital prefrontal cortex lesions can learn to inhibit prepotent responses in the reversed reward contingency task, *Cereb Cortex 17*, 1154-1159.

134. Winstanley, C. A., Theobald, D. E., Cardinal, R. N., and Robbins, T. W. (2004) Contrasting roles of basolateral amygdala and orbitofrontal cortex in impulsive choice, *J Neurosci 24*, 4718-4722.

135. Swick, D., Ashley, V., and Turken, A. U. (2008) Left inferior frontal gyrus is critical for response inhibition, *BMC Neurosci 9*, 102.

136. Ghods-Sharifi, S., Haluk, D. M., and Floresco, S. B. (2008) Differential effects of inactivation of the orbitofrontal cortex on strategy set-shifting and reversal learning, *Neurobiology of learning and memory 89*, 567-573.

137. Roberts, A. C., and Wallis, J. D. (2000) Inhibitory control and affective processing in the prefrontal cortex: neuropsychological studies in the common marmoset, *Cereb Cortex 10*, 252-262.

138. Schmidt, R., Leventhal, D. K., Mallet, N., Chen, F., and Berke, J. D. (2013) Canceling actions involves a race between basal ganglia pathways, *Nat Neurosci 16*, 1118-1124.

139. Hyafil, A., Summerfield, C., and Koechlin, E. (2009) Two mechanisms for task switching in the prefrontal cortex, *J Neurosci 29*, 5135-5142.

140. Butter, C. M. (1969) Perseveration in Extinction and in Discrimination Reversal Tasks Following Selective Frontal Ablations in Macaca Mulatta, *Physiology & Behavior 4*, 163-&.

141. Bouton, M. E. (2004) Context and behavioral processes in extinction, *Learn Mem 11*, 485-494.

142. Mishkin, M., Vest, B., Waxler, M., and Rosvold, H. E. (1969) A Re-Examination of Effects of Frontal Lesions on Object Alternation, *Neuropsychologia 7*, 357-&.

143. Pickens, C. L., Saddoris, M. P., Setlow, B., Gallagher, M., Holland, P. C., and Schoenbaum, G. (2003) Different roles for orbitofrontal cortex and basolateral amygdala in a reinforcer devaluation task, *J Neurosci 23*, 11078-11084.

144. Haggard, P. (2011) Decision time for free will, *Neuron 69*, 404-406.

145. Roitman, J. D., and Roitman, M. F. (2010) Risk-preference differentiates orbitofrontal cortex responses to freely chosen reward outcomes, *Eur J Neurosci 31*, 1492-1500.

146. Weeks, R. A., Turjanski, N., and Brooks, D. J. (1996) Tourette's syndrome: a disorder of cingulate and orbitofrontal function?, *QJM 89*, 401-408.

147. Makris, N., Biederman, J., Valera, E. M., Bush, G., Kaiser, J., Kennedy, D. N., Caviness, V. S., Faraone, S. V., and Seidman, L. J. (2007) Cortical thinning of the attention and executive function networks in adults with attention-deficit/hyperactivity disorder, *Cereb Cortex 17*, 1364-1375.

148. Burguiere, E., Monteiro, P., Feng, G., and Graybiel, A. M. (2013) Optogenetic stimulation of lateral orbitofronto-striatal pathway suppresses compulsive behaviors, *Science 340*, 1243-1246.

149. Aron, A. R., Robbins, T. W., and Poldrack, R. A. (2014) Inhibition and the right inferior frontal cortex: one decade on, *Trends Cogn Sci 18*, 177-185.

150. Banca, P., Voon, V., Vestergaard, M. D., Philipiak, G., Almeida, I., Pocinho, F., Relvas, J., and Castelo-Branco, M. (2015) Imbalance in habitual versus goal directed neural systems during symptom provocation in obsessive-compulsive disorder, *Brain*.

151. Moorman, D. E., and Aston-Jones, G. (2014) Orbitofrontal cortical neurons encode expectation-driven initiation of reward-seeking, *J Neurosci 34*, 10234-10246.

152. Schoenbaum, G., Roesch, M. R., Stalnaker, T. A., and Takahashi, Y. K. (2009) A new perspective on the role of the orbitofrontal cortex in adaptive behaviour, *Nature reviews. Neuroscience 10*, 885-892.

153. Padoa-Schioppa, C. (2011) Neurobiology of economic choice: a good-based model, *Annual review of neuroscience 34*, 333-359.

154. Wallis, J. D. (2007) Neuronal mechanisms in prefrontal cortex underlying adaptive choice behavior, *Ann N Y Acad Sci 1121*, 447-460.

155. Schultz, W., Tremblay, L., and Hollerman, J. R. (2000) Reward processing in primate orbitofrontal cortex and basal ganglia, *Cerebral cortex 10*, 272-284.

156. Nakamura, K., Roesch, M. R., and Olson, C. R. (2005) Neuronal activity in macaque SEF and ACC during performance of tasks involving conflict, *J Neurophysiol 93*, 884-908.

157. Risterucci, C., Terramorsi, D., Nieoullon, A., and Amalric, M. (2003) Excitotoxic lesions of the prelimbic-infralimbic areas of the rodent prefrontal cortex disrupt motor preparatory processes, *Eur J Neurosci 17*, 1498-1508.

158. Euston, D. R., Gruber, A. J., and McNaughton, B. L. (2012) The role of medial prefrontal cortex in memory and decision making, *Neuron 76*, 1057-1070.

159. Hauser, T. U., Iannaccone, R., Ball, J., Mathys, C., Brandeis, D., Walitza, S., and Brem, S. (2014) Role of the medial prefrontal cortex in impaired decision making in juvenile attention-deficit/hyperactivity disorder, *JAMA Psychiatry 71*, 1165-1173.

160. Christakou, A., Robbins, T. W., and Everitt, B. J. (2001) Functional disconnection of a prefrontal cortical-dorsal striatal system disrupts choice reaction time performance: implications for attentional function, *Behav Neurosci 115*, 812-825.

161. Sul, J. H., Kim, H., Huh, N., Lee, D., and Jung, M. W. (2010) Distinct roles of rodent orbitofrontal and medial prefrontal cortex in decision making, *Neuron 66*, 449-460.

162. Oualian, C., and Gisquet-Verrier, P. (2010) The differential involvement of the prelimbic and infralimbic cortices in response conflict affects behavioral flexibility in rats trained in a new automated strategy-switching task, *Learn Mem 17*, 654-668.

163. Pezze, M., McGarrity, S., Mason, R., Fone, K. C., and Bast, T. (2014) Too little and too much: hypoactivation and disinhibition of medial prefrontal cortex cause attentional deficits, *J Neurosci 34*, 7931-7946.

164. Eagle, D. M., and Robbins, T. W. (2003) Lesions of the medial prefrontal cortex or nucleus accumbens core do not impair inhibitory control in rats performing a stop-signal reaction time task, *Behav Brain Res 146*, 131-144.

165. Wickstrom, R. (2007) Effects of nicotine during pregnancy: human and experimental evidence, *Curr Neuropharmacol 5*, 213-222.

166. Milberger, S., Biederman, J., Faraone, S. V., Chen, L., and Jones, J. (1996) Is maternal smoking during pregnancy a risk factor for attention deficit hyperactivity disorder in children?, *Am J Psychiatry 153*, 1138-1142.

167. Milberger, S., Biederman, J., Faraone, S. V., and Jones, J. (1998) Further evidence of an association between maternal smoking during pregnancy and attention deficit hyperactivity disorder: findings from a high-risk sample of siblings, *J Clin Child Psychol 27*, 352-358.

168. Ernst, M., Moolchan, E. T., and Robinson, M. L. (2001) Behavioral and neural consequences of prenatal exposure to nicotine, *J Am Acad Child Adolesc Psychiatry 40*, 630-641.

169. Fried, P. A., and Watkinson, B. (2001) Differential effects on facets of attention in adolescents prenatally exposed to cigarettes and marihuana, *Neurotoxicol Teratol 23*, 421-430.

170. Cornelius, M. D., and Day, N. L. (2009) Developmental consequences of prenatal tobacco exposure, *Curr Opin Neurol 22*, 121-125.

171. Morgan, A. B., and Lilienfeld, S. O. (2000) A meta-analytic review of the relation between antisocial behavior and neuropsychological measures of executive function, *Clin Psychol Rev 20*, 113-136.

172. Mick, E., Biederman, J., Faraone, S. V., Sayer, J., and Kleinman, S. (2002) Case-control study of attention-deficit hyperactivity disorder and maternal smoking,

alcohol use, and drug use during pregnancy, *J Am Acad Child Adolesc Psychiatry 41*, 378-385.

173. Zhu, J., Zhang, X., Xu, Y., Spencer, T. J., Biederman, J., and Bhide, P. G. (2012) Prenatal nicotine exposure mouse model showing hyperactivity, reduced cingulate cortex volume, reduced dopamine turnover, and responsiveness to oral methylphenidate treatment, *J Neurosci 32*, 9410-9418.

174. Schneider, T., Ilott, N., Brolese, G., Bizarro, L., Asherson, P. J., and Stolerman, I. P. (2011) Prenatal exposure to nicotine impairs performance of the 5-choice serial reaction time task in adult rats, *Neuropsychopharmacology 36*, 1114-1125.

175. Slotkin, T. A. (1998) Fetal nicotine or cocaine exposure: which one is worse?, *J Pharmacol Exp Ther 285*, 931-945.

176. Navarro, H. A., Mills, E., Seidler, F. J., Baker, F. E., Lappi, S. E., Tayyeb, M. I., Spencer, J. R., and Slotkin, T. A. (1990) Prenatal nicotine exposure impairs beta-adrenergic function: persistent chronotropic subsensitivity despite recovery from deficits in receptor binding, *Brain Res Bull 25*, 233-237.

177. Seidler, F. J., Levin, E. D., Lappi, S. E., and Slotkin, T. A. (1992) Fetal nicotine exposure ablates the ability of postnatal nicotine challenge to release norepinephrine from rat brain regions, *Brain Res Dev Brain Res 69*, 288-291.

178. Muneoka, K., Ogawa, T., Kamei, K., Muraoka, S., Tomiyoshi, R., Mimura, Y., Kato, H., Suzuki, M. R., and Takigawa, M. (1997) Prenatal nicotine exposure affects the development of the central serotonergic system as well as the dopaminergic system in rat offspring: involvement of route of drug administrations, *Brain Res Dev Brain Res 102*, 117-126.

179. Muhammad, A., Mychasiuk, R., Nakahashi, A., Hossain, S. R., Gibb, R., and Kolb, B. (2012) Prenatal nicotine exposure alters neuroanatomical organization of the developing brain, *Synapse 66*, 950-954.

180. Mychasiuk, R., Muhammad, A., Gibb, R., and Kolb, B. (2013) Long-term alterations to dendritic morphology and spine density associated with prenatal exposure to nicotine, *Brain research 1499*, 53-60.

181. Schall, J. D., and Boucher, L. (2007) Executive control of gaze by the frontal lobes, *Cogn Affect Behav Neurosci 7*, 396-412.

182. Schneider, T., Bizarro, L., Asherson, P. J., and Stolerman, I. P. (2010) Gestational exposure to nicotine in drinking water: teratogenic effects and methodological issues, *Behav Pharmacol 21*, 206-216.

183. Andreasen, N. C., Rezai, K., Alliger, R., Swayze, V. W., 2nd, Flaum, M., Kirchner, P., Cohen, G., and O'Leary, D. S. (1992) Hypofrontality in neuroleptic-naive patients and in patients with chronic schizophrenia. Assessment with xenon 133 single-photon emission computed tomography and the Tower of London, *Arch Gen Psychiatry 49*, 943-958.

184. Rubia, K., Overmeyer, S., Taylor, E., Brammer, M., Williams, S. C., Simmons, A., and Bullmore, E. T. (1999) Hypofrontality in attention deficit hyperactivity disorder during higher-order motor control: a study with functional MRI, *Am J Psychiatry 156*, 891-896.

185. Berman, K. F., Torrey, E. F., Daniel, D. G., and Weinberger, D. R. (1992) Regional cerebral blood flow in monozygotic twins discordant and concordant for schizophrenia, *Arch Gen Psychiatry 49*, 927-934.

186. Volkow, N. D., Fowler, J. S., Wang, G. J., and Swanson, J. M. (2004) Dopamine in drug abuse and addiction: results from imaging studies and treatment implications, *Mol Psychiatry 9*, 557-569.

187. Carter, C. S., Perlstein, W., Ganguli, R., Brar, J., Mintun, M., and Cohen, J. D. (1998) Functional hypofrontality and working memory dysfunction in schizophrenia, *Am J Psychiatry 155*, 1285-1287.

188. Dickstein, S. G., Bannon, K., Castellanos, F. X., and Milham, M. P. (2006) The neural correlates of attention deficit hyperactivity disorder: an ALE meta-analysis, *J Child Psychol Psychiatry 47*, 1051-1062.

189. Robinson, E. S., Eagle, D. M., Mar, A. C., Bari, A., Banerjee, G., Jiang, X., Dalley, J. W., and Robbins, T. W. (2008) Similar effects of the selective noradrenaline reuptake inhibitor atomoxetine on three distinct forms of impulsivity in the rat, *Neuropsychopharmacology 33*, 1028-1037.

190. Bari, A., Eagle, D. M., Mar, A. C., Robinson, E. S., and Robbins, T. W. (2009) Dissociable effects of noradrenaline, dopamine, and serotonin uptake blockade on stop task performance in rats, *Psychopharmacology (Berl) 205*, 273-283.

191. Aron, A. R., Dowson, J. H., Sahakian, B. J., and Robbins, T. W. (2003) Methylphenidate improves response inhibition in adults with attention-deficit/hyperactivity disorder, *Biol Psychiatry 54*, 1465-1468.

192. DeVito, E. E., Blackwell, A. D., Clark, L., Kent, L., Dezsery, A. M., Turner, D. C., Aitken, M. R., and Sahakian, B. J. (2009) Methylphenidate improves response inhibition but not reflection-impulsivity in children with attention deficit hyperactivity disorder (ADHD), *Psychopharmacology (Berl) 202*, 531-539.

193. Bedard, A. C., Ickowicz, A., Logan, G. D., Hogg-Johnson, S., Schachar, R., and Tannock, R. (2003) Selective inhibition in children with attention-deficit hyperactivity disorder off and on stimulant medication, *J Abnorm Child Psychol 31*, 315-327.

194. Tannock, R., Schachar, R. J., Carr, R. P., Chajczyk, D., and Logan, G. D. (1989) Effects of methylphenidate on inhibitory control in hyperactive children, *J Abnorm Child Psychol 17*, 473-491.

195. Chamberlain, S. R., Hampshire, A., Muller, U., Rubia, K., Del Campo, N., Craig, K., Regenthal, R., Suckling, J., Roiser, J. P., Grant, J. E., Bullmore, E. T., Robbins, T. W., and Sahakian, B. J. (2009) Atomoxetine modulates right inferior frontal activation during inhibitory control: a pharmacological functional magnetic resonance imaging study, *Biol Psychiatry 65*, 550-555.

196. Vaidya, C. J., Austin, G., Kirkorian, G., Ridlehuber, H. W., Desmond, J. E., Glover, G. H., and Gabrieli, J. D. (1998) Selective effects of methylphenidate in attention deficit hyperactivity disorder: a functional magnetic resonance study, *Proc Natl Acad Sci U S A 95*, 14494-14499.

197. Bymaster, F. P., Katner, J. S., Nelson, D. L., Hemrick-Luecke, S. K., Threlkeld, P. G., Heiligenstein, J. H., Morin, S. M., Gehlert, D. R., and Perry, K. W. (2002) Atomoxetine increases extracellular levels of norepinephrine and dopamine in prefrontal cortex of rat: a potential mechanism for efficacy in attention deficit/hyperactivity disorder, *Neuropsychopharmacology 27*, 699-711.

198. Blood-Siegfried, J., and Rende, E. K. (2010) The long-term effects of prenatal nicotine exposure on neurologic development, *J Midwifery Womens Health 55*, 143-152.

199. Pauly, J. R., and Slotkin, T. A. (2008) Maternal tobacco smoking, nicotine replacement and neurobehavioural development, *Acta Paediatr 97*, 1331-1337.

200. Schmitz, M., Denardin, D., Laufer Silva, T., Pianca, T., Hutz, M. H., Faraone, S., and Rohde, L. A. (2006) Smoking during pregnancy and attention-deficit/hyperactivity disorder, predominantly inattentive type: a case-control study, *J Am Acad Child Adolesc Psychiatry 45*, 1338-1345.

201. Tong, S., and McMichael, A. J. (1992) Maternal smoking and neuropsychological development in childhood: a review of the evidence, *Dev Med Child Neurol 34*, 191-197.

202. Thapar, A., Fowler, T., Rice, F., Scourfield, J., van den Bree, M., Thomas, H., Harold, G., and Hay, D. (2003) Maternal smoking during pregnancy and attention deficit hyperactivity disorder symptoms in offspring, *Am J Psychiatry 160*, 1985-1989.

203. Jacobsen, L. K., Slotkin, T. A., Mencl, W. E., Frost, S. J., and Pugh, K. R. (2007) Gender-specific effects of prenatal and adolescent exposure to tobacco smoke on auditory and visual attention, *Neuropsychopharmacology 32*, 2453-2464.

204. Button, T. M., Maughan, B., and McGuffin, P. (2007) The relationship of maternal smoking to psychological problems in the offspring, *Early Hum Dev 83*, 727-732.

205. Peters, D. A., and Tang, S. (1982) Sex-dependent biological changes following prenatal nicotine exposure in the rat, *Pharmacol Biochem Behav 17*, 1077-1082.

206. Peters, D. A., Taub, H., and Tang, S. (1979) Postnatal effects of maternal nicotine exposure, *Neurobehav Toxicol 1*, 221-225.

207. Pauly, J. R., Sparks, J. A., Hauser, K. F., and Pauly, T. H. (2004) In utero nicotine exposure causes persistent, gender-dependant changes in locomotor activity and sensitivity to nicotine in C57Bl/6 mice, *Int J Dev Neurosci 22*, 329-337.

208. Zhu, J., Lee, K. P., Spencer, T. J., Biederman, J., and Bhide, P. G. (2014) Transgenerational transmission of hyperactivity in a mouse model of ADHD, *J Neurosci 34*, 2768-2773.

209. Chen, B. T., Yau, H. J., Hatch, C., Kusumoto-Yoshida, I., Cho, S. L., Hopf, F. W., and Bonci, A. (2013) Rescuing cocaine-induced prefrontal cortex hypoactivity prevents compulsive cocaine seeking, *Nature 496*, 359-362.

210. Jentsch, J. D., and Taylor, J. R. (1999) Impulsivity resulting from frontostriatal dysfunction in drug abuse: implications for the control of behavior by reward-related stimuli, *Psychopharmacology (Berl) 146*, 373-390.

211. Dalley, J. W., Everitt, B. J., and Robbins, T. W. (2011) Impulsivity, compulsivity, and top-down cognitive control, *Neuron 69*, 680-694.

212. Blokland, A. (1998) Reaction time responding in rats, *Neurosci Biobehav Rev 22*, 847-864.

213. Padoa-Schioppa, C. (2011) Neurobiology of economic choice: a good-based model, *Annu Rev Neurosci 34*, 333-359.

214. Cai, X., and Padoa-Schioppa, C. (2014) Contributions of orbitofrontal and lateral prefrontal cortices to economic choice and the good-to-action transformation, *Neuron 81*, 1140-1151.

215. Carter, C. S., Braver, T. S., Barch, D. M., Botvinick, M. M., Noll, D., and Cohen, J. D. (1998) Anterior cingulate cortex, error detection, and the online monitoring of performance, *Science 280*, 747-749.

216. Stalnaker, T. A., Cooch, N. K., McDannald, M. A., Liu, T. L., Wied, H., and Schoenbaum, G. (2014) Orbitofrontal neurons infer the value and identity of predicted outcomes, *Nat Commun 5*, 3926.

217. Schultz, W. (1998) Predictive reward signal of dopamine neurons, *J Neurophysiol 80*, 1-27.

218. Howe, M. W., Tierney, P. L., Sandberg, S. G., Phillips, P. E., and Graybiel, A. M. (2013) Prolonged dopamine signalling in striatum signals proximity and value of distant rewards, *Nature 500*, 575-579.

219. Durstewitz, D., and Seamans, J. K. (2008) The dual-state theory of prefrontal cortex dopamine function with relevance to catechol-o-methyltransferase genotypes and schizophrenia, *Biol Psychiatry 64*, 739-749.

220. Gamo, N. J., and Arnsten, A. F. (2011) Molecular modulation of prefrontal cortex: rational development of treatments for psychiatric disorders, *Behav Neurosci 125*, 282-296.

221. Bryden, D. W., Johnson, E. E., Tobia, S. C., Kashtelyan, V., and Roesch, M. R. (2011) Attention for learning signals in anterior cingulate cortex, *J Neurosci 31*, 18266-18274.

222. Shenhav, A., Botvinick, M. M., and Cohen, J. D. (2013) The expected value of control: an integrative theory of anterior cingulate cortex function, *Neuron 79*, 217-240.

223. Nee, D. E., Kastner, S., and Brown, J. W. (2011) Functional heterogeneity of conflict, error, task-switching, and unexpectedness effects within medial prefrontal cortex, *Neuroimage 54*, 528-540.

224. Sheth, S. A., Mian, M. K., Patel, S. R., Asaad, W. F., Williams, Z. M., Dougherty, D. D., Bush, G., and Eskandar, E. N. (2012) Human dorsal anterior cingulate cortex neurons mediate ongoing behavioural adaptation, *Nature 488*, 218-221.

225. Glascher, J., Adolphs, R., Damasio, H., Bechara, A., Rudrauf, D., Calamia, M., Paul, L. K., and Tranel, D. (2012) Lesion mapping of cognitive control and value-based decision making in the prefrontal cortex, *Proc Natl Acad Sci U S A 109*, 14681-14686.

226. Holroyd, C. B., and Coles, M. G. (2002) The neural basis of human error processing: reinforcement learning, dopamine, and the error-related negativity, *Psychol Rev 109*, 679-709.

227. Burton, A. C., Kashtelyan, V., Bryden, D. W., and Roesch, M. R. (2014) Increased firing to cues that predict low-value reward in the medial orbitofrontal cortex, *Cereb Cortex 24*, 3310-3321.

228. Roesch, M. R., Esber, G. R., Bryden, D. W., Cerri, D. H., Haney, Z. R., and Schoenbaum, G. (2012) Normal aging alters learning and attention-related teaching signals in basolateral amygdala, *J Neurosci 32*, 13137-13144.

229. Kashtelyan, V., Tobia, S. C., Burton, A. C., Bryden, D. W., and Roesch, M. R. (2012) Basolateral amygdala encodes upcoming errors but not response conflict, *Eur J Neurosci 35*, 952-959.

230. Benowitz, N., and Jacob, P., III. (1987) Metabolism, Pharmacokinetics and Pharmacodynamics of Nicotine in Man, In *Tobacco Smoking and Nicotine* (Martin, W., Van Loon, G., Iwamoto, E., and Davis, L., Eds.), pp 357-373, Springer US.

231. Paz, R., Barsness, B., Martenson, T., Tanner, D., and Allan, A. M. (2007) Behavioral teratogenicity induced by nonforced maternal nicotine consumption, *Neuropsychopharmacology 32*, 693-699.

232. Romero, R. D., and Chen, W. J. (2004) Gender-related response in open-field activity following developmental nicotine exposure in rats, *Pharmacol Biochem Behav 78*, 675-681.

233. Vaglenova, J., Birru, S., Pandiella, N. M., and Breese, C. R. (2004) An assessment of the long-term developmental and behavioral teratogenicity of prenatal nicotine exposure, *Behav Brain Res 150*, 159-170.